The Regulation of Respiration on Plant Growth and Development of *Fallopia japonica*, Japanese knotweed

Julia Shearman

September 2015

Submitted in partial fulfilment towards the requirements for the degree of Doctor of philosophy (DPhil)

I hereby declare that this thesis has not been and will not be submitted in whole or in part to another university for the award of any other degree

Signature

……..

University of Sussex

Julia Shearman

Submitted for the degree of Doctor of philosophy

The Regulation of Respiration on Plant Growth and Development of *Fallopia japonica*, Japanese knotweed

Summary

Fallopia japonica, or Japanese knotweed is a rhizomatous perennial herb native to East Asia; most notably Japan, China and Korea. Upon discovery of this species and subsequent import to Europe in the 1840's, it was considered an esteemed ornamental plant – winning the medal for the 'most interesting new plant of the year' in 1847.

F. japonica soon became known as a menace rather than a champion, when it began to spread throughout its new environment, spreading to gardens and nurseries and regenerating from discarded plant fragments. The species ability to cause environmental damage has earnt it a place in the 'top 100 world's worst most invasive alien species' list.

Commercially available herbicides have proven have little effect on *F. japonica*, and to be successful require many repeat applications. The plant can grow up to 10 cm per day during the early budding and shoot stage and can easily dominate an environment when left unchecked. A key objective of this research was to determine the biochemical pathways of energy generation particularly during the rapid phase of growth with the longer term goal of identifying potential inhibitors of this process which may have commercial opportunities.

Very little research is available regarding the biochemistry of growth of *F. japonica,* thus detailed protocols were required to be established and optimised prior to biochemical investigations.

Mitochondrial isolations and following respiratory activity measurements were performed on *F. japonica* prepared from naturalised plants. Such mitochondrial samples were found to have a very low respiratory rates when compared to mitochondria isolated from other species such as *Arum maculatum*. This was confirmed following an analysis of the respiratory complexes via electrophoresis, which revealed that all complexes were of low abundance in comparison with other plant species. Transmission electron microscopy also revealed that the numbers and volumes of mitochondria in budding tissue were considerably fewer and larger than those observed in other rapidly expanding plant tissues - providing further confirmation of the respiratory measurements.

In an attempt to overcome the small yield associated with mitochondrial isolations, research is also presented on the generation, optimisation and characterisation of suspension cultures from *F. japonica* explants. Suspension cultures were shown to have almost identical characteristics in terms of mitochondrial protein complement and respiratory capacity as observed in bud and shoot isolations. Preliminary mass spectroscopy data indicated a large proportion of ATP synthase subunits were present in the isolated mitochondrial fractions from leaf, bud, shoot and suspension cultures. Glycolytic analysis of fractions isolated from suspension cultures were also undertaken the outcome of which are discussed in terms of the energy generation pathways within *F. japonica* and the implications of how such pathways may be controlled.

Contents

Abbreviations used

AA	Antimycin A
ADP	Adenosine diphosphate
APS	Ammonium Persulfate
ATP	Adenosine triphosphate
BN-PAGE	Blue-native polyacrylamide gel electrophoresis
BSA	Bovine serum albumin
DAB	Diaminobenzidine
DDM	n-Dodecyl β-D-maltoside
DTT	1,4-Dithiothreitol
EDTA	Ethylenediaminetetraacetic acid
FADH	Flavin adenine dinucleotide
NADH	Nicotinamide adenine dinucleotide
PDA	Potato dextrose agar
PGR	Plant growth regulator
PMS	Phenazine methosulphate
PMSF	Phenylmethylsulfonyl
PVDF	Polyvinylidene fluoride
TEM	Transmission electron microscopy
TEMED	Tetramethylethylenediamine
TTC	2,3,5-Triphenyl tetrazolium chloride

Acknowledgements

First and foremost I would like to thank Professor Anthony Moore, Dr David Whitehouse, Dr Paul Beckett, Richard Schofield and the environmental consultancy firm Phlorum for giving me the opportunity to undertake this PhD CASE studentship. I have immensely enjoyed my time working on this project and am extremely grateful for all of the support and supervision provided throughout.

Secondly I would like to thank Dr Mary Albury, Dr Catherine Elliott & Dr Luke Young for their teaching and guidance in the laboratory, as well as my fellow PhD students Benjamin May and James Misselbrook for keeping me (slightly) sane over the last four years.

Thirdly, huge thanks to Dr Martyn Stenning for his help with safely growing Japanese knotweed in the greenhouses, Dr Julian Thorpe for all his help using the TEM, Dr John Bailey of the University of Leicester for providing me with the initial *Fallopia japonica* plants and the many other people who have helped and inspired me along the way.

Last and definitely not least, my thanks to my family and friends who have supported me throughout not just my PhD but my entire university education. My Mum and sister for all the laughter/moving help/tears/wine, my Dad and Loveday for all of your support, I would never have been able to do it without all of you. To Luke, Flora, Daire, Amanda, Charlotte and too many others to name (you all know who you are), thank you so much for being with me through the highs and the lows.

1 Introduction

1.1 Discovery of Fallopia japonica

Japanese knotweed, or *Fallopia japonica*, is referred to by several names in the literature, partially due to its discovery (ies) and subsequent import to Europe and the USA. The plant was first described by Houttuyn in 1777 as *Reynoutria japonica*, after Carl Peter Thunberg, a Swedish botanist, returned to Amsterdam with samples obtained from Nagasaki on the island of Kyushu in Japan [1]. Philip Franz von Siebold, a German physician, visited the same island in 1822, and also collected specimens which he sent back to Leiden, The Netherlands [2]. In 1846, after returning to his specimens in Leiden, Siebold and his colleague Joseph Gerhard Zuccarini named the plant *Polygonum cuspidatum* [3]. It was propagated and sold by the horticultural company Von Siebold & Co from Leiden under the name *Polygonum sieboldii* [3]. It was not until 1901, when Japanese botanist Tomitaro Makino published an article in the Botanical Magazine Tokyo, combining the two previous names into *Polygonum Reynoutria*, that the species discovered by Houttuyn and Siebold were found to be the same [4].

Ronse Decraene & Akeroyd brought about the reclassification of several species, including Japanese knotweed, from the genus *Polygonum* to *Fallopia*, [5] which was supported by Stace in 1991 [6] and Bailey & Stace in 1992 [7]. The nomenclature has not reached international agreement. The most commonly used name for Japanese knotweed in the United Kingdom is *Fallopia japonica* (Houtt.) Ronse Decraene which is the name used throughout this project. In the United States and much of the Japanese literature it is referred to as *Polygonum cuspidatum* Sieb. & Zucc. [8, 9].

1.1.1 Introduction to the UK

The introduction of *F. japonica var. japonica* to the British Isles has also been heavily researched, as the dates cited in the literature are conflicting. Conolly (1977) [10] quotes a date of introduction to the Horticultural Society of London, Chiswick as 1825, obtained from the 'Royal Horticultural Society Supplement to the Dictionary of Gardening' by Synge in 1956 [11]. However, this plant was later discovered to have been *F. japonica* of Chinese accession, which differs morphologically from the Siebold clone of *F. japonica var. japonica* spread throughout the U.K. [3]

Figure 1-1 *Fallopia japonica* spring growth. May 2013

F. japonica was awarded a gold medal in 1847 by the Society of Agriculture & Horticulture at Utrecht for the most interesting new plant of the year (Bailey & Conolly (2000) [3] ex. Siebold (1948) [12]). *F. japonica* was first made commercially available in 1848 from Von Siebold & Company of Lieden, The Netherlands – in the sales catalogue, the plant is recommended for use as fodder for cattle, a sandbank stabilizer and praised for its ornamental features, amongst other benefits [12]. Figure 1-1 shows an image of spring growth of naturalised *F. japonica* in Brighton, UK. Bailey & Conolly (2000) [3] note that the Royal Botanical Gardens, Kew has a record of receiving '*Polygonum sieboldii*' along with a range of plants from Siebold of Lieden on the 9th of August 1850 – and potentially then provided samples of these plants to a nursery in Kingston.

One of the earliest known records of the plant becoming naturalized in the UK was produced in 1886 by John Storrie [13], where he remarks that it is growing in abundance around cinder tips in Glamorgan, South Wales. In 1887 there is a report of *Fallopia japonica* in Alexandra park, Oldham in South Lancashire [14], a report from 1900 in Ledbury; Hereford, Southport, South Lancashire in 1907, Swindon, North Wiltshire in 1910 and also accounts of the plant in Scotland and Ireland in the early 1900's [10]. These areas are thought to have acted as centres for garden escapes, with plant material either spreading via vegetative means, or from cuttings establishing themselves on waste heaps to form new stands. By 1905, the Journal of the Royal Horticultural Society began to advise against planting Japanese knotweed (*P. cuspidatum*) unless it was 'most carefully kept in check' [15].

By 1909, areas in south-west Britain, specifically Glamorganshire, Exeter and Cornwall were reporting the plant as abundant, with one comment from Davey (1909) regarding Cornwall's *F. japonica* population as 'perfectly naturalized' [16]. Up until approximately 1950 there were comparatively few accounts of *F. japonica* in eastern regions. Conolly (1977) suggests that this may be due to an increase of reports of the plant, rather than the lack of plant material present before this time [10]. In 1996, *F. japonica* was recorded in over 55% of the 2862 10 km squares representing the UK by the Biological Records Centre; in the year 2000 the amount

of Japanese knotweed in the area of Swansea alone was approximately 100 hectares [17]. In 2006, Kurose et al state that *F. japonica* is present in "virtually every corner of the country" [18] and this is visualised in Figure 1-2. The majority of the plant present throughout the UK is *Fallopia japonica var. japonica* and, for simplicity, will be referred to as *F. japonica* throughout this project.

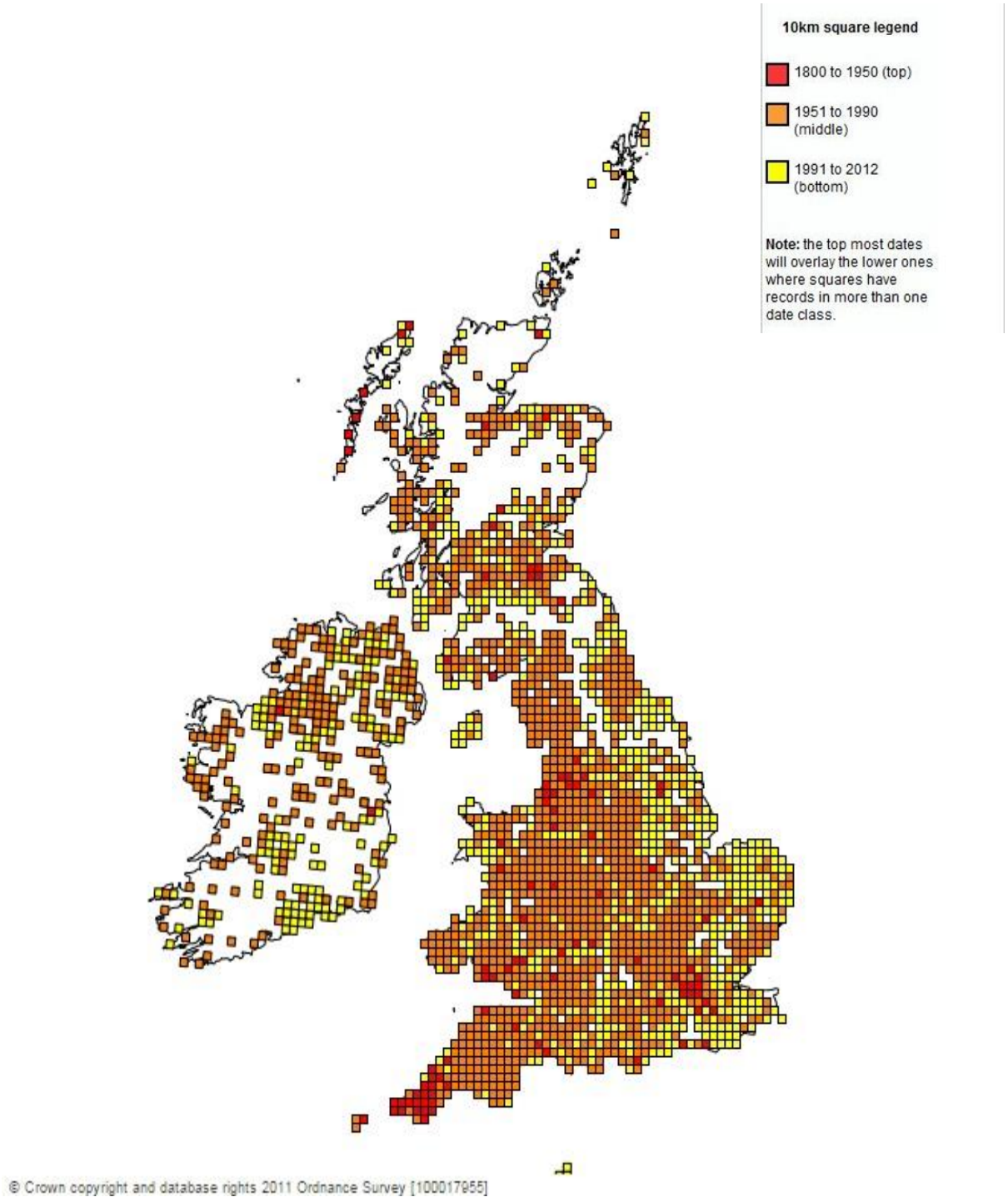

Figure 1-2 Map showing the distribution of *Fallopia japonica* in the U.K. - generated with data provided by the National Biodiversity Network [19]. Dates range from 1800 – 2012 which represent the most recent available data. White areas represent areas where *F. japonica* is not known to be present.

1.1.2 Current spread throughout the UK and Europe

The spread of *F. japonica* throughout the UK has become a huge issue. Regional councils, especially in the south west of the UK use their websites to provide information on the plant for both the general public and developers [19, 20]. This is an attempt to promote best practice of control of *F. japonica* and to try and prevent any further spread of the plant around the country, as well as providing legal information and forums for the public. It became illegal in 1981 when the Wildlife and Countryside Act was passed into law [21] to 'plant, or otherwise cause the species (*F.japonica*) to grow in the wild'. The Environmental Protection Act of 1990 also mentions *F. japonica*, classifying it as 'controlled waste' and specifying disposal regulations. Soil containing rhizome material is regarded as contaminated and if taken away from a site, must be buried to a depth of at least five meters [22].

The issue of controlling Japanese knotweed influenced the formation of the Japanese knotweed Alliance in 2001. The members of this alliance include the Centre for Agricultural Biosciences International (CABI), the Department for Environment, Food and Rural Affairs (Defra), The Environment Agency, local councils and Network Rail [23]. The aim of this project management board is to oversee a scientific research programme which examined the potential for biological or natural control of *F. japonica* in Great Britain. The alliance stated in 2003 that an estimate of the cost of controlling Japanese knotweed to the U.K economy is £165 million, with a potential cost of £1.56 billion if eradication were to be attempted countrywide [23]. A more recent report concurs with these estimates, noting that management costs will increase the figure by several hundreds of thousands of pounds [24].

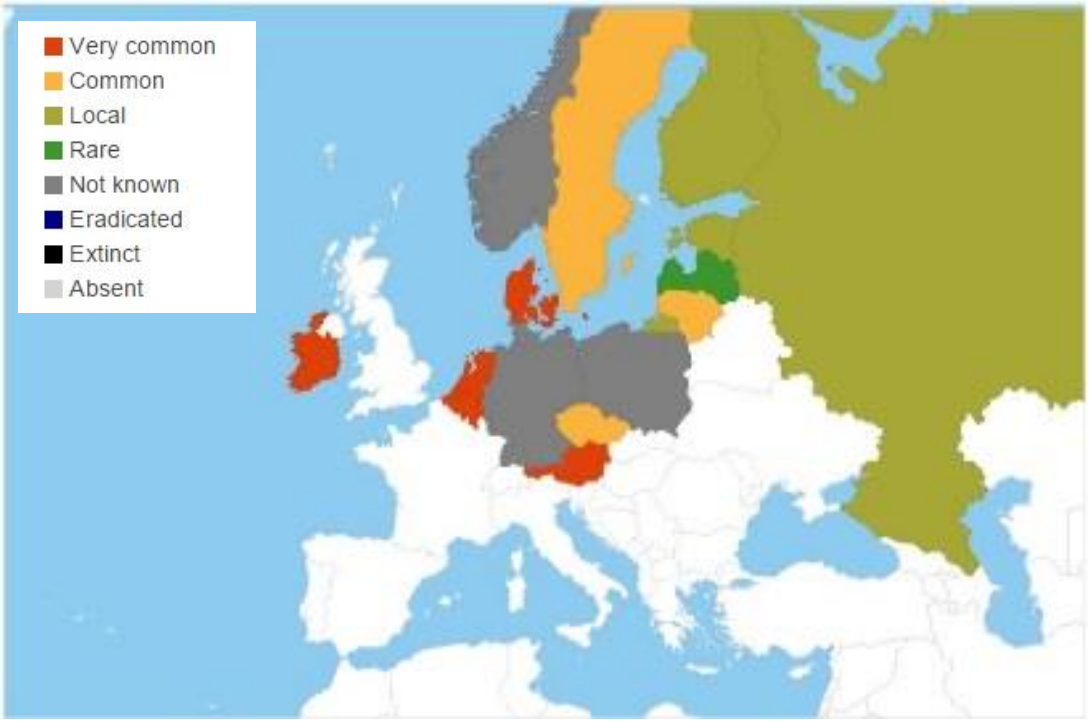

Figure 1-3 Frequency map *F. japonica* in Europe – Image from NOBANIS, European Network of Invasive Alien Species [25]. White colour indicates countries from which no information was gathered.

F. japonica is also an increasing issue in Europe, where its presence is noted in many different habitats, from the arctic geographical regions in northern Scandinavia to the Mediterranean regions in northern Italy [26, 27]. Although *F. japonica* tends to thrive in more temperate climes such as the UK and Ireland, the presence of the species throughout Europe is testament to its hardiness and ability to invade a wide variety of environments. Figure 1-3 is a data map indicating the frequency of *F. japonica* across central and northern Europe from NOBANIS, a database of information on a variety of invasive species. All of the countries from which data are collected are coloured on the map - this dataset does not include information from the UK or any southern European countries. Denmark, Ireland, Belgium, Austria and the Netherlands all note *F. japonica* as very common, with no information submitted from either Germany or Poland.

Figure 1-4 Invasiveness map for *F. japonica* in Northern and central Europe - Image from NOBANIS [25]. White colour indicates countries from which no information was gathered.

Figure 1-4 shows an invasiveness map for the dataset of countries shown in Figure 1-3. Invasiveness is a measure of the ability of the species to spread from one area to another, with the risk level of a given species ranked as not invasive, potentially invasive or invasive [28]. With the data gathered from the countries marked in these figures, all of the countries which are known to have introduced *F. japonica* have a risk level of either potentially invasive or invasive. These data, amongst other invasive risk listings, have contributed to *F. japonica* becoming known as one of the most invasive species on Earth [9].

1.1.3 Hybridisation

In Britain, almost all of the stands of *F. japonica var. japonica* are morphologically identical, octaploid (2n=88), male sterile & possess truncate leaf bases [9]. In 2000, Hollingsworth & Bailey assessed 150 samples of *F.japonica* from around the UK and 16 samples from the Czech Republic, Germany, France and the USA using a Random Amplified Polymorphic DNA (RAPD) technique. All samples were shown to give an identical multi-primer RAPD profile [17]. This led Bailey

(2007) to suggest that all of the plants in Britain are clones of the original plant which was introduced by Siebold [29]. Although no plant material has been found in the native range which precisely matches the introduced *F. japonica var. japonica* [17], the closest match found during molecular characterisation studies originated from Nagasaki prefecture. This area is at the southern tip of the island of Kyushu, which is the region where Phillip von Siebold was based in the early 19th century [18].

This *F. japonica var. japonica* is one of three species of *Fallopia* present in Europe and is known as the 'true' invasive knotweed [30]. *Fallopia japonica var. compacta* is a dwarf variant of the plant, which rarely exceeds 1.5 m in height (this is in comparison to the approximate 3 m reached by *var. japonica*). This variant also does not frequently become naturalised, and for these reasons is not considered as pestilent as *F. japonica var. japonica* [29]. This dwarf variant is not recognised within the native range, as continuous morphological variation between *F .japonica var. japonica* and *F. japonica var. compacta* is observed [31]. The third species is *Fallopia sachalinensis* or Giant knotweed. As the name suggests, this is a larger plant than *F. japonica var. japonica* which has larger leaves, and although it is widely distributed around Europe, it is much less common than *F. japonica var. japonica* [29]. As previously mentioned in this review, the *Fallopia japonica var. japonica* species in Europe is present only as a single male sterile clone. Both *F. japonica var. compacta* and *F. sachlinensis* are present in Europe as hermaphrodite and female individuals, which have led to extensive hybridisations with the *Fallopia japonica var. japonica* male sterile clone though-out Europe [32]. These hybrids, along with the original parental species and backcrosses have been designated as Japanese knotweed *sensu lato* (*s.l*) by Bailey in 2007 [29].

1.2 Characteristics of *F. Japonica*

1.2.1 Growth characteristics, native range - Japan

Many studies of the growth pattern and mineral acquisition of *F. japonica* have been undertaken on Mt. Fuji at approximately 1500-2400 m above sea level

[33-39]. Fuji volcano is on the border of Honshu and Mariana arcs in central Japan. The most recent known eruption was the Hoei eruption in 1707 [40], which left the South East slope of the volcano devoid of vegetation and covered in a scoriaceous layer approximately 5 m thick which is too unstable and infertile for many plant species to establish themselves [37]. These studies recognise *F. japonica* as a dominant coloniser at an early stage of primary succession on the slopes of Mt. Fuji, demonstrating the hardiness of this species.

The development of these primary communities of *F. japonica* in the area of Mt. Fuji is by seedling establishment. The seedling survival in this type of soil is very low, as less than 2% survive overwinter after being scattered on the scoria surface at the beginning of the summer [39]. The intrinsically high root growth rate of the seedlings even in low nutrient level areas plays a crucial role in its establishment, as it helps the plant cope with the disturbances due to unstable surface of Mt. Fuji [36]. If a seedling does become established, it develops several rhizomes. From each of these rhizomes, the apical bud develops into an aerial shoot. These shoots are annual, as they die back during late autumn and produce winter buds at the base of the shoot area. One or more of these buds develop into a shoot the following spring – this forms a cluster of shoots, a 'shoot clump' or 'crown' [41]. Adachi et al (1996) suggest that each crown has a definitive life span of approximately 5 years [34]. The rhizomes also produce lateral buds, which remain dormant for the approximate 5 year term in which the crown is producing shoots, which suggests apical bud dominance [34]. Once the crown dies, the lateral buds branch away from the mother rhizome. In the study by Adachi et al (1996), this branching angle was found to be approximately 30-50° [34].

This pattern of rhizome growth causes a patch of clonal plant to form, which eventually shows decreasing shoot biomass in the centre of the patch - this is referred to as 'central die-back' [36]. Due to an increasing gradient of water content and organic minerals found from the peripheries to the centre of the patch [37], this central region provides a nutrient rich area which has potential to be colonised by other herbaceous species. An example of this is *Miscanthus oligostachyus* (Flame

grass) which would otherwise find it difficult to survive in the surrounding poor quality soils [33]. The central die-back is not thought to be a product of inter-specific or intra-specific competition, rather a function of the systemic growth pattern of the rhizomes [33]. Suzuki (1994) suggests that there is a regulatory mechanism for shoot growth within clonal plant species, which would minimise intra-specific competition by controlling the allocation of remobilized resources from the rhizome to the shoot buds. This would cause emergence of shoots at or around the same time in the crowns, preventing over-production of shoots in one area and mutual shading [38].

1.2.2 Growth characteristics in the UK

The information gained from the Japanese studies regarding the growth patterns of *Fallopia japonica* does not wholly describe the patterns of growth and invasiveness seen in its non-native range. Firstly, all of the individual plants of *Fallopia japonica var. japonica* in the UK studied to date are known to be male sterile - meaning that the plant must rely solely on vegetative growth [17]. This is in comparison to the Japanese studies, where seedling establishment formed the base of new communities and the genetic diversity between plants of different clonal colonies (ramets) is high [42]. Another comparison is that the plants studied in Japan were all at a high altitude, between 1500 & 2500 meters above sea level. Beerling et al (1994) describe the limitation of *F. japonica* to lowland areas, rarely established above 200m [43]. The altitude on Mt. Fuji is a determination factor of the length of the growing season, which decreases with increasing altitude [42]. The plant studied in Japan actually bares a stronger resemblance to the dwarf alpine variant, *F.japonica var. compacta* [34], whereas the most common variant in the UK is *var. japonica*.

In the UK, the plant mostly grows in habitats strongly influenced by man - for example, waste ground, quarries, road verges and railways. It is also common along river banks and woodland, characteristically growing in nutrient rich areas [43]. This is in contrast to the environmental conditions seen on Mt. Fuji, where the nutrient levels are low and the plant occurs on mountainsides - where the habitat is unlikely to have been influenced by man. A factor that makes the conditions harsher

for the *F. japonica* plants in their native environment is the presence of natural predators. Invertebrates such as chrysomelid beetles, stem boring larvae and Japanese Swift moth larvae (*Endoclita excrescens*) attack the leaves, stem and rhizome of the plants [42]. Natural predation is not an issue for the introduced *F. japonica* in the UK, although some research towards biological control involves introducing one of the plants natural predators, which will be discussed in further detail later in this chapter.

The central die-back phenomenon witnessed by Adachi *et al*. (1996) in Japan has not been recorded in communities of the plant in the UK [33, 34, 44]. Clonal crowns in the UK have a lifespan which far exceeds the 5 year limit witnessed in plants on Mt. Fuji, which may contribute to the reason that central die-back is not observed. The rhizome branching angle is also much sharper in the UK in comparison to the Japanese results, at 5-15° (compared to 30-50°) which will also cause a difference in the patch growth pattern of the ramets, introducing an element of intraspecific competition within patches [44]. The differences mentioned between the Japanese and UK plants led Smith et al (2007) to construct a 3D Correlated Random Walk (CRW) model to predict the behaviour of development of rhizome networks of *F. japonica var. japonica* in the UK [44] which compares with Adachi *et al*. (1996) 2D stochastic model for the development of rhizomes on Mt. Fuji [34]. In conclusion, these factors taken as a whole indicate that the *F. japonica* is able to take full advantage of the favourable conditions in the UK. The extent of the invasion across the country has led Bailey (2003) to remark that Japanese knotweed is "actually much more 'at home' abroad!" [42].

1.3 Issues associated with *F. Japonica*

Gardeners discovered early in *F. japonica*'s invasion of the UK that the plant was difficult to control and became notorious as a pest due to dominance of, and escapes from gardens. As the original nurseries which stocked the plant were located in the south west of the UK, this area has the greatest frequency of well-established stands [10]. This problem was exacerbated by the removal of plant material where it

had become established, and the dumping of plant waste. *F. japonica* is able to regenerate from rhizome fragments as small as 1cm, or 0.7g [45] and it is also able to regenerate from cut stem fragments [46]. When plant material is removed from an area, it must be done with great care, as any remaining pieces of rhizome or stem are capable of regenerating with growth rates of up to 10cm a day [47]. Dumping of the plant waste leads to the regeneration of the plant in new areas, where it can potentially become established.

The main problems caused by *F. japonica* in its adventive range are:

- Reduction of natural floral diversity. This is due to the extremely fast growth rate exhibited by the plant, which therefore can out-compete native plants primarily with respect to light availability [48]. There is also some evidence to suggest that leaf extracts from the *Fallopia* taxa exhibit phytotoxic effects on native species [49], which would cause difficulties for any plants trying to grow in or around the leaf litter from *F. japonica*. Reduction of native plants can also lead to the reduction in diversity of animals to which the out-competed native plants are linked.
- Disruption of the built environment. The rhizomes and stems of the plant are capable of growing through cracks in foundations and pavements [9, 50], as well as potentially causing flooding through damage to dams and blocking waterways [9]. Due to the plant being very difficult to eradicate completely from any given site, recurring costs for repair work and maintenance can run extremely high, and can add hundreds of thousands of pounds onto a developers budget [18]. One example is that of the Olympic park in London built for the 2012 games. Around 5% of the site contained established stands of *F. japonica*, which comprised around four hectares in total area, and cost around £70 million from the development budget [51]. The environmental agency provide a 'Knotweed Code of Practice' for developers, architects, landscapers and anyone involved in a site containing Japanese knotweed, in order to reduce costs and ensure that the plant material is managed within the law [52].

- Reduction in house prices and issues with mortgage lenders. Alongside the knotweed code of practice for housing developers with guidance on how to deal with the plant when present on brownfield sites, the Royal Institute of Chartered Surveyors (RICS) has released an information paper containing guidelines on the potential reduction in valuations on residential properties which *F. japonica* can cause [53]. This was put together in an attempt to dismiss some of the alarming claims fielded by some of the UK media [54] surrounding the damage and loss of value of properties which have *F. japonica* within their boundaries.
- Recreation and Landscape. The density of some stands of the plant causes access issues for pedestrians, and stands in urban areas are considered to be a sign of urban degradation [18, 55].

1.4 Current methods of control

1.4.1 Biological control

Unsurprisingly, Japanese knotweed control has become big business. There are companies which specialise in the treatment of the plant with several control/eradication options. Herbicide treatment, removal of the infected soil and disposal at an authorised site and root barriers are all common proposed treatments of areas which are infested – but all of these methods can prove to be extremely expensive and not always effective. Research into the control and eradication of knotweed is on-going; one current research trend focuses on Biological control.

CABI, as part of the Japanese knotweed Alliance performed surveys for natural enemies of knotweed across all four main islands of Japan at over 140 sites from 2002-2007 [56]. The surveys identified several insects and fungal pathogens, and these were brought back to the UK for testing by CABI under quarantine conditions. Initially, a hemibiotrophic leafspot fungus *Mycosphaerella polygoni-cuspidati* was thought to be the most interesting and potentially the most effective biocontrol agent brought back by the team. The fungus causes premature and massive defoliation of the knotweed, which could hinder the spread and impact of the weed by reducing the photosynthetic capacity [18]. However, according to the

Japanese knotweed alliance website, the fungus had proven to be much harder to work with than the potential insect agents, as it has a complex lifecycle & infection process [57].

These difficulties relating to the fungi have shifted the focus of biocontrol onto the insect agents. The psyllid, *Aphalara itadori*, is a sap sucking insect, which lays eggs on the leaves of the Japanese knotweed plants. The nymphs emerge and feed on the sap of the plants, which indicates that where the adult psyllids choose to lay their eggs is of importance [57]. A study by Shaw et al.(2009) to determine the host specificity of the psyllid concluded that "*Aphalara itadori* shows high fidelity to its normal host *Fallopia japonica* in the field in Japan and in the laboratory host range tests we have subjected it to" [56]. Despite questions raised about the selection of the insect control agent being based on host specificity alone rather than effectiveness of reducing growth in the plant [58], the psyllid was approved for release by Defra on the 9th of March 2010. The release and monitoring programme is currently underway, with the hope that the psyllid will be able to establish itself on a *F. japonica* population and inhibit growth of the plant [57]. An update from CABI in June 2013 reports successful overwintering of the psyllid at half of the release sites in low numbers, with limited numbers of adults present the following summer [59]. At the time of writing, a full report of the effectiveness of the biological control has yet to be released by CABI.

1.4.2 Herbicides

Chemical control of Japanese knotweed is the most popular and available course of action for most infestations. Recent research has sought to elucidate at which point during the year specific herbicides should be applied to knotweed in order to enhance effectiveness of chemical control [41]. This involves determining the relationship between the above ground organs of the plant and the storage organ (or rhizome), as translocation of the chemicals to the storage organs would be essential to wholly eradicate the plant. Bashtanova et al. (2009) proposed a programme of combined herbicidal applications which matches with phenological events, and also takes into account the physiology of the 'old' rhizomes – the areas

of the rhizome which are physiologically connected to the younger parts but have no aboveground shoots [41]. Summarised below are three of the main types of herbicide used to control Japanese knotweed.

1.4.2.1 Glyphosate

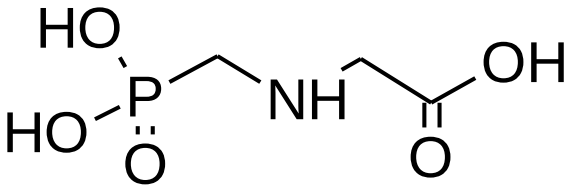

Figure 1-5 Chemical structure of glyphosate

Glyphosate inhibits aromatic amino acid synthesis, by inhibition of the enzyme 5-enolpyruvyl-shikimate-3-phosphate synthase (EPSPS) of the shikimate pathway [60]. This leads to reduction of protein synthesis and eventually death of the plant. Glyphosate is a non-persistent herbicide. Applications in the autumn would be effectively translocated to the rhizome, as at this time the rhizome is a very effective sink. However, the greatest amount of protein synthesis occurs in the rhizomes around the summer – meaning that the non-persistent glyphosate would have been degraded by the time it would have the greatest effect, and the damage to the rhizomes potentially would not be lethal [41]. An important plus point for this herbicide is the fact that it is non persistent. This reduces the damage which could be caused to any native flora in the surrounding environment and reduces the potential 'run off' of the herbicide into waterways, preventing pollution [61]. The chemical structure of glyphosate can be seen in Figure 1-5.

Glyphosate can be diluted via diversion as the herbicide is both xylem and phloem mobile. Therefore the presence of other sinks (e.g. growing shoots, leaves, flowers) will cause the chemical to be diverted from the underground organs, preventing the glyphosate from entering and effecting aromatic compound synthesis in the rhizome [41]. Glyphosate often fails to kill *F. japonica* [62]. Studies do show a reduction in shoot density post glyphosate treatment, especially when shoots and above ground organs are cut down and removed. However, Ahrens (1975) found that

for all cases of glyphosate treated *F. japonica* in their study, live roots were present in the soil which were able to produce viable shoots after the treatment was completed [63].

Glyphosate is also a non-selective herbicide [64], meaning it can potentially cause surrounding plants to be effected if application is achieved via spraying rather than a more specific targeted system, such as direct stem injection [65]. Transgenic crop plants are available containing glyphosate resistance genes, which allows general spraying of fields of crops with the herbicide to prevent any unwanted plant growth. The *CP4* gene found in *Agrobacterium* sp., when expressed in transgenic crops, produces a glyphosate resistant form of the EPSPS enzyme. This is a more environmentally focussed option of weed control, as it is less damaging to the soil due to decreased tilling and replaces more persistent herbicides [60].

1.4.2.2 Imazapyr

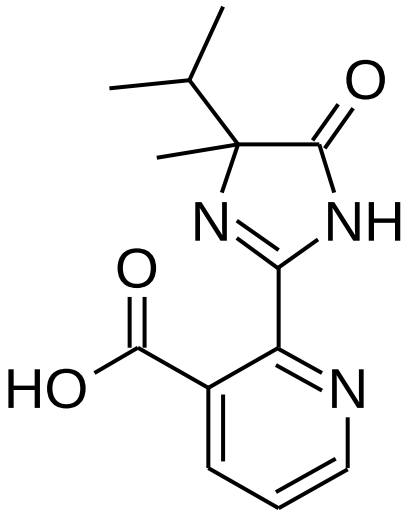

Figure 1-6 Chemical structure of imazapyr

Imazapyr is a non-selective herbicide, the chemical structure of which can be seen in Figure 1-6. Acetohydroxy acid synthase or acetolactate synthase (ALS) is the first enzyme in the branched chain amino acid biosynthetic pathway within plants [66]. This is the site of inhibition for imazapyr, therefore preventing the synthesis of

leucine, valine and isoleucine which are essential for plant cell growth and protein synthesis [67].

Imazapyr is similar to glyphosate in that it can also be diluted via diversion, as it is both phloem and xylem mobile and is also non-selective. This herbicide is thought to be more effective than glyphosate as it is a persistent herbicide and it also affects phloem transport [41]. A study by Figeroa (1989) showed that one year after application of imazapyr, shoot density of Japanese knotweed (stems/m^2) was reduced by 97% in comparison to glyphosate treated plants where the reduction was 56% [68]. Imazapyr is a slow acting herbicide and works particularly well for woody species of plants as it does not readily break down once taken into the roots [69]. Imazapyr has been reported to be excluded from roots of some species, causing no damage to the target plant and adverse effects to the surrounding vegetation [69].

1.4.2.3 Synthetic Auxins

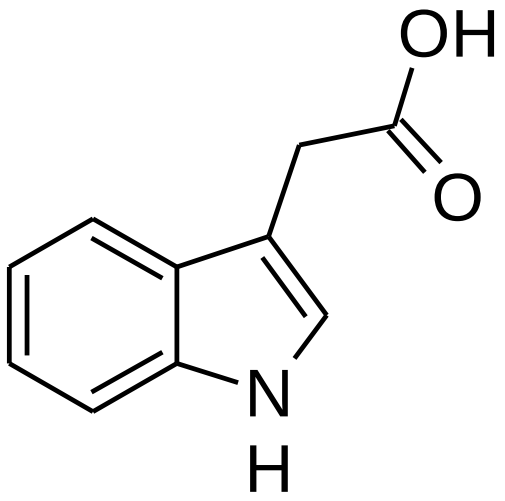

Figure 1-7 Chemical structure of Indole-3-acetic acid (IAA)

Synthetic auxins mimic the activity of natural plant auxin phytohormones. Figure 1-7 shows an image of a naturally occurring auxin, IAA. It is from this structure that the family of synthetic auxins are designed [70]. The damage is caused by disrupting the hormone balance, promoting signalling pathways which influence

the increase in RNA, DNA and protein synthesis. This results in disorganised growth of cells, preventing phloem transport due to swelling of surrounding cells [71].

Synthetic auxins can be diverted via dilution as it is both phloem and xylem mobile, which it has in common with the glyphosate and imazapyr herbicides. If applied in the spring or summer, auxins can actually promote growth of the storage organs, and enlargement of the rhizome [41]. Synthetic auxins are generally long lasting and are not easily broken down from within the plant [72].

1.5 Alternative strategies for control

Overall the applications of these herbicides often fail to completely kill the plant. This is mostly due to the fact that the application often does not coincide with the time when the herbicide would be most effective, either due to sink-source relations, persistency of the herbicide or diversion of the chemical due to mobility within the plant [41]. Bashtanova et al.(2009) offers some strategies to increase effectiveness of the current herbicides, including breaking dormancy of the rhizome buds by clipping apical shoots, ethanol application and ethylene precursor applications – which would all potentially increase translocation of herbicides into the rhizomes by breaking shoot apical dominance [41]. Also suggested is an integrated programme of herbicide application which would use combinations of herbicides at the time when the mode of action of each chemical would be most damaging to the plant.

Other strategies put forward in this paper include using regulators of sink-source relations to increase the import of phloem mobile herbicides into the rhizomes by application of phytohormones, sugars and light. As pointed out by the authors, these signals for potentially manipulating sink-source relations have not yet been investigated for *F. japonica*, so speculation of the results are based on knowledge of other plants [41].

- Phytohormones. Cytokinin and auxin application has been shown to activate starch synthesising capacity in potato at the initial stage of tuber formation [73],

which indicated that application of these phytohormones at the start of the growing season of Japanese knotweed may increase sink strength of the rhizome, which would allow earlier and more effective herbicide application [41].

- Sugars. Again in potato, it has been shown that application of exogenous sucrose induced tuberization and improved tuber weight [74]. Using this application of sucrose to Japanese knotweed may change the sink strength of the rhizome and help to translocate the herbicides to the rhizome more effectively [41].
- Light. In a study conducted on radishes, Drozdova et al. (2001) observed that light quality effected the concentration of hormones in plant tissues. Red light increased the sink strength of the petioles and stems, whereas blue light enhanced the development of the submerged hypocotyl and increased development [75]. Bashantova (2009) suggests that using far-red and blue photoselective covers may increase sink strength of the Japanese knotweed rhizome and therefore increase herbicide allocation [41].

1.6 Current biochemical knowledge

Very little is known of *F. japonica* biochemistry. Much of the research into *F. japonica* around the world has focussed upon population dynamics [76], ecology and biogeography [77], reproductive biology and regenetative capacity [78, 79] and nutrient cycling within soils where *F. japonica* is present [80]. A review by Bashtanova et al.(2009) mentioned previously in this chapter, provides linkage between the growth patterns and herbicidal chemical control, giving some ideas as to how to increase effectiveness and integrated applications by exploiting the sink-source relationship in the plant [41]. At the time of writing, to the best of my knowledge, there no reported studies in the literature relating to the biochemistry of growth of *F. japonica*.

1.6.1 Resveratrol

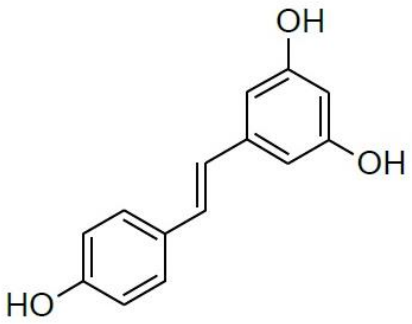

Figure 1-8 Chemical structure of resveratrol

F. japonica is a natural source of the stilbenoid resveratrol (3,5,4'-trihydroxy-*trans*-stilbene). Resveratrol is a natural polyphenol produced by over 70 different plant species, including: grapevines (*Vitis vinifera*), cranberries (*Vaccinium macrocarpon*), peanuts (*Arachis hypogaea*) [81], blueberries (*Vaccinium corymbosum)* [82] and also *F. japonica* [83]. The first study to highlight this compound linked it to the cardiovascular benefits of red wine, and subsequently concluded that resveratrol merited investigation as 'a potential cancer chemopreventitive agent in humans' [84]. From this pilot study, interest in this molecule has rapidly expanded; investigations as to the mechanism of action of resveratrol in many biochemical pathways have been undertaken. In plants, Resveratrol is a product of stilbene synthase. Stilbenes are secondary plant products with phytoalexin and antifungal properties, and the synthesis of stilbenes is induced upon either pathogenic attack or environmental stresses as part of the plants natural defence mechanism [85]. Resveratrol naturally occurs in both *cis* and *trans* isoforms, and also in a glucoside form known as piceid [86].

As recently as 4 years ago, resveratrol was primarily produced by growing 'field cultures' of *F. japonica* and harvesting the rhizomatous root system for isolation of the stilbenoid [87, 88]. Using keyword 'resveratrol' in the National Centre for Biotechnology Information (NCBI) search feature (available from: http://www.ncbi.nlm.nih.gov/pubmed), the results indicate 1221 publications from

the period of the 1st January 2014 to the 1st of January 2015 [89]. This is in itself is an indication as to the current level of interest in this compound.

The structure of resveratrol, as a polyphenol, lends itself to a function as a free radical scavenger, due to the potential for electron delocalisation across the chemical structure [90] as can be seen in Figure 1-8. Resveratrol also functions as an antioxidant via its ability to promote the activity of a variety of antioxidant enzymes, and increase levels of glutathione (which itself is a potent antioxidant), as shown on samples of human lymphocytes *in vitro* [91], and also on cultured rat aortic segments and endothelial cells [92].To date, no firm understanding of resveratrol's mechanistic effects, whether beneficial or adverse, has been achieved [93]. However, much effort is afforded to the production of this secondary plant metabolite, in which *F. japonica* has the primary role [94].

1.7 Energy generation in *F. japonica*

The processes of rapid growth, cell division, elongation and expansion require a large amount of energy. Replication of DNA, cytokinesis & synthesis of new macromolecules are all processes which have a high ATP demand [95]. It is known that mitochondria congregate around cellular areas with high energy requirements [96], and that there is a higher degree of invagination of the mitochondrial cristae in areas with high respiratory activity [97]. A study by Segui-Simarro et al. (2008) showed that shoot apical and meristematic cells contain numerous small discrete mitochondria in the cell periphery and a large mitochondrial mass in the perinuclear region in the model plant organism *A. thaliana* [96]. Large amounts of energy; in the form of ATP, is produced by the mitochondria via the respiratory chain in these rapidly dividing and expanding cells. A diagram showing the protein complexes making up the respiratory chain in plant mitochondria is shown in Figure 1-9 .

Most of the ATP generated by cells via aerobic respiration is done so by oxidative phosphorylation in the mitochondria, with proton (H^+) pumping providing

the reducing energy to convert ADP to ATP, conserving energy in the acid anhydride linkages within the ATP molecules [144]. The complexes of the electron transport chain are shown in Figure 1-9. The principle involves the oxidation of compounds for the generation of electrons - NADH as substrate for complex I and succinate as substrate at complex II. Oxidation of these compounds provides reducing power, in the form of electrons, to be passed through the mitochondrial inner membrane to the ubiquinone pool. This pool of ubiquinone is subsequently reduced and provides an electron 'shuttle' of sorts to complex III of the chain. Complex III transfers electrons to cytochrome *c*, which carries one electron at a time to complex IV of the chain, the terminal electron carrier [144].

The Chemiosmotic Theory states that coupling of electron transfer to ATP synthesis is indirect, via a H^+ electrochemical gradient [112]. Complexes I, III & IV of the electron transfer chain are involved with the non-spontaneous movement of H^+ ions from the matrix into the intermembrane space of the mitochondria [112]. The mechanisms by which electron transport is linked to H^+ transport across the mitochondrial membrane in complexes I and IV are not fully understood, although complex III participates in a H^+ translocation mechanism known as the Q cycle [144].

The overall payload of H^+ translocation through the mitochondrial membrane is the phosphorylation of ADP. The electrochemical gradient created diffuses back into the matrix via ATP synthase, complex V. ATP synthase is comprised of two major components, F_1 & F_O. F_O represents the integral membrane proteins which act as a proton channel, F_1 represents the proteins which extend as a 'stalk' into the mitochondrial matrix and contain the catalytic sites for ATP synthesis [112]. Approximately 10 H^+ are pumped through the mitochondrial membrane for each molecule of NADH oxidised by the electron transport chain, with at least 3 H^+ required for the formation of ATP when passing through the ATP synthase complex [144]. ATP is then used to drive metabolic reactions relating to growth, development and maintenance of cells.

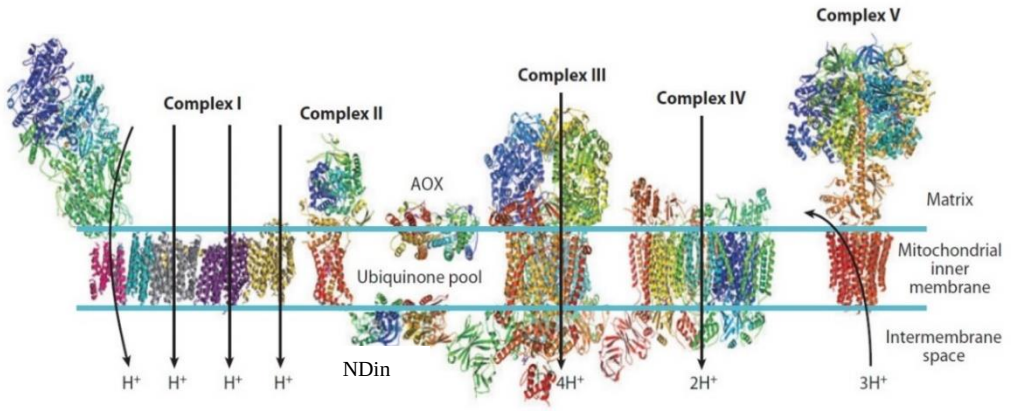

Figure 1-9 The electron transport chain of plant mitochondria shown with complexes shown as crystal structures where known. NADH:ubiquinone oxidoreductase (complex I), Succinate dehydrogenase (complex II), ubiquinol-cytochrome bc1 reductase (complex III), IV- cytochrome c oxidase (complex IV) and ATP synthase (complex V). Plant mitochondria specific enzymes: NDin – NAD(P)H dehydrogenase on the inner surface of the mitochondrial inner membrane. AOX – Alternative Oxidase. The ubiquinone pool is also represented in the mitochondrial inner membrane. Adapted from Moore et al. (2013).

1.8 Project aims

This project focusses on energy generation within *F. japonica* – the hypothesis being that large amounts of energy would be required for the huge growth rates demonstrated by this species.

Although energy generation involves several extremely complex systems within cells, the main emphasis throughout this project will be energy generation via oxidative phosphorylation through the ATP synthase within mitochondria. Areas which have high energy demand contain a higher concentration of mitochondria, with very active cells having up to 20% of the volume of cytoplasm occupied by mitochondria [144]. Considering this and the fantastic growth rate shown by *F. japonica*, investigation of the mitochondrial electron transport chain will be of paramount importance throughout this project. If, as hypothesised, the mitochondria are numerous within the areas of interest within the plant, it could change the approach to control and eradication of *F. japonica* by potentially highlighting new points of control with understanding of the biochemistry of energy generation within the species as a whole.

The overall aim of this project is to investigate the processes which control the rapid rate of cell division & expansion which occur at the beginning of the growth season of *F. japonica*. In cooperation with environmental consultancy firm Phlorum, this project sets out to elucidate the mechanisms that control the growth of *F. japonica*. Once characterised, the biochemistry of growth would give major insights into how the plant generates the energy to grow at a rate of up to 10 cm a day [47]. When the method of energy production is known, it gives the potential to produce novel targeted inhibitors for *F. japonica*, generation of which could increase the effects of herbicidal control, which in turn could have vast environmental and financial benefits.

2 Methods Chapter

2.1 Mitochondrial Isolation

In order to investigate respiration within a plant cell, protocols were followed and developed to isolate mitochondria from a variety of plant sources.

2.1.1 *Arum maculatum* spadix mitochondria isolation.

Collection of *Arum maculatum* spadices was performed predominantly during the months of April & May during the years 2011-2014 from the area surrounding the John Maynard Smith building at the University of Sussex. The spadices were removed from the plant when the spathe was fully open and purple colouration was observed. These factors indicate that the spadix is in its thermogenesis stage and will contain a large amount of active mitochondria.

A stock solution of mitochondrial isolation media was prepared with the constituents indicated in Table 2-1. The stock solution was adjusted to pH 7.5 (± 0.1) with 10 N potassium hydroxide (KOH) before use.

Component	**Molarity**	**Amount (g/4000ml)**
Mannitol	0.3 M	218.6
4-morpholinopropane sulfonic acid (MOPS)	20 mM	16.7
EDTA	2 mM	2.98

Table 2-1 Mitochondrial isolation stock solution composition

On the day of collection of *A. maculatum* spadices, 0.2% (w/v) Bovine Serum Albumen (BSA) was added to a volume of mitochondrial isolation stock

solution and allowed to dissolve fully at room temperature. The volume of stock solution used was dependent upon the amount of fresh plant material harvested. The solution was then re-adjusted to pH 7.5 (± 0.1) using 10 N KOH with care. BSA was added to the solution on the day of preparation to prevent any aggregation in solution. The resulting solution is henceforth referred to as wash media.

An amount of wash media was set aside and stored on ice, the volume of which was dependent upon the fresh weight of the plant material collected. To another smaller volume of wash media, 7 mM cysteine was added and allowed to dissolve fully without stirring at room temperature. This was referred to as 'grind media' and stored on ice. Cysteine is an antioxidant and was added to the buffer to prevent any oxidation of the mitochondrial proteins which can effect function [98].

In preparation for the isolation procedure, a JA20 and JA10 rotor were cooled along with centrifuge tubes to 4°C on ice. Once the *A. maculatum* spadices were collected, the fresh weight of plant material obtained was measured using electronic scales. The spadices were manually chopped into pieces measuring approximately 5 mm^2 before being placed into a large beaker containing cold grind buffer. The chopped spadix material in grind buffer was then homogenised using a Waring blender, 3 times four second bursts of high speed blending. This process was repeated until all of the spadix material had been homogenised.

The resulting homogenate was subsequently filtered through 2 layers of muslin, which had been wetted with wash media, to remove any remaining solid plant material. The filtrate was collected into a beaker on ice and divided into the pre-cooled centrifuge tubes. At all stages, where possible, the solutions and plant material were kept on ice to reduce any denaturation or enzymatic degradation of proteins during the isolation procedure caused either by heat or protease enzymes released from the damaged plant cells.

The filtrate was then centrifuged for 10 minutes at 3500 x*g*, either in large, 500ml centrifuge tubes in the JA10 rotor, or in smaller, 50ml centrifuge tubes in the

JA20 rotor, dependent upon the initial amount of plant material collected. This centrifugation step serves the purpose of removing cell debris and residual starch. The starch and debris pellet was discarded and the supernatant transferred into fresh centrifuge tubes to be taken forward to the second centrifugal stage.

The resulting supernatant was centrifuged for 10 minutes at 12000 x*g*, in JA10 or JA20 rotors. The pellet was resuspended in wash media using a soft bristled paintbrush before homogenisation using a Potter-Elvehjem glass homogeniser to ensure re-suspension and a constant consistency. This resuspended pellet was taken forward to the third centrifuge stage.

The third centrifugation step was carried out at 12000 x*g* for 10 minutes. The resulting supernatant was discarded and the pellet resuspended in a minimal amount of wash media using a soft bristled paintbrush. This fraction will contain mitochondria as well as some persistent contaminating fragments of organelles, such as cell wall & cell membrane fragments. At this point the samples were referred to as washed mitochondrial samples. These washed mitochondrial samples were analysed using oxygen electrode techniques (discussed later in this chapter section 2.9) to determine the level of mitochondrial activity in the sample. If the sample showed a reasonable respiratory rate (discussed later chapter 3.4) it was considered to be beneficial to take forward to the purification stage.

2.1.2 Percoll purification of mitochondria

Percoll consists of colloidal silica particles which have been coated in polyvinylpyrrolidone (PVP) and is a medium used for density gradient centrifugation of cells and subcellular particles. The premise is that of isopycnic separation, where the density of the molecule matches that of the surrounding media – in this case, Percoll. Percoll self-forms a gradient in a centrifuge tube, which is dependent upon the gravitational, or *g*, force. At speed, the particles at the bottom of the tube become enriched and therefore denser in comparison with the top of the gradient, which consists of more dispersed particles.

Percoll gradients were utilised to separate mitochondria from the washed mitochondrial samples obtained from the previously described centrifugation steps. The percoll isolation media described in Table 2-2 was freshly prepared on the day of isolation, approximately 300ml per 500g of fresh *A. maculatum* material was found to be sufficient for the following purification steps.

Component	**Amount**	**Action**
Percoll	21% (v/v)	Density separation of organelles
Sucrose	0.3 M	Maintenance of osmotic pressure
MOPS	5 mM	Buffering agent
Bovine Serum Albumin (BSA)	0.1% (v/v)	Stabilization of enzymes

Table 2-2 Percoll gradient preparation.

Resuspended pellets of washed mitochondria samples were carefully loaded onto percoll gradients contained in 50 ml centrifuge tubes, approximately 1 ml of the washed fraction was overlaid on top of the gradient, taking care not to disturb the percoll surface. The gradients were centrifuged at 23500 x*g* for 30 minutes in a JA20 rotor set to no deceleration.

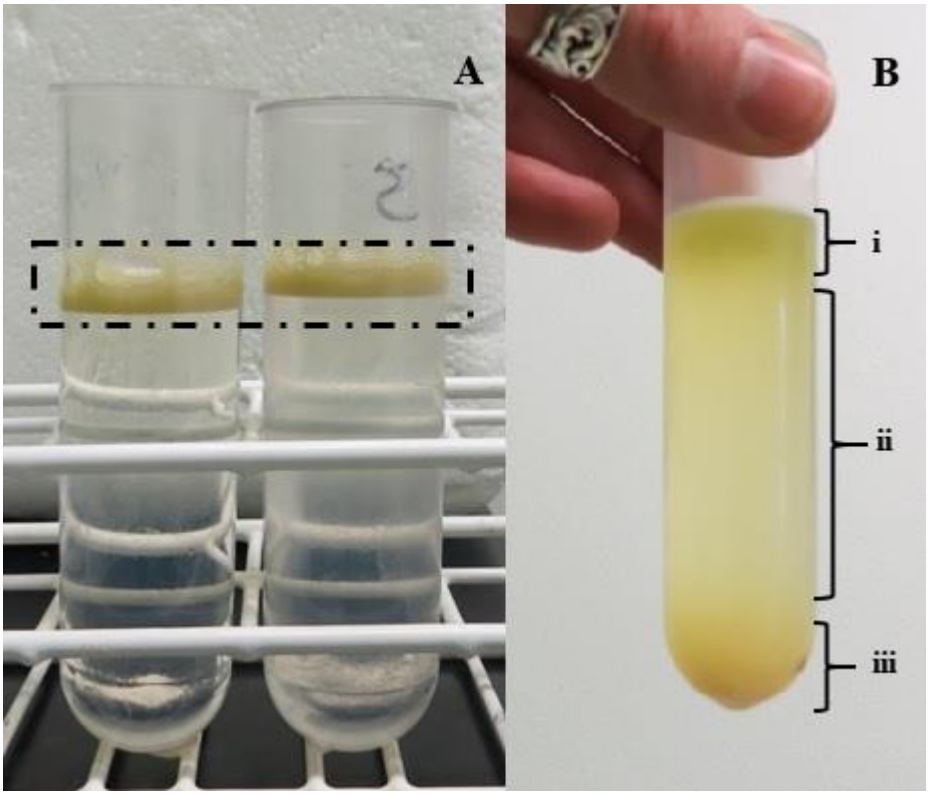

Figure 2-1 A (left image): An example of washed mitochondrial pellet overlaid on top of a percoll gradient. Boxed area indicates re-suspended washed mitochondrial pellet overlaid on a continuous percoll gradient 21% (v/v). Both centrifuge tubes contain identical gradients – washed mitochondrial sample is split over two gradients to ensure efficient separation. B (right image): An example of separated washed mitochondria sample following density gradient centrifugation on a percoll gradient. Highlighted sections i, ii and iii represent areas of interest, i – cell membranes and cell debris, ii – area estimated to contain mitochondria, iii – starch and peroxisomes.

Following centrifugation, the washed sample is further separated, as illustrated in Figure 2-1. A cloudy white area in the centre of the gradient contains the mitochondria and this area was aspirated from the rest of the gradient using a Pasteur pipette, taking great care not to disturb the rest of the gradient. These collected fractions were then transferred to clean 50 ml centrifuge tubes and centrifuged at 12000 x*g* for 10 minutes in a JA20 rotor.

The supernatant was discarded carefully, as the resulting pellet is sensitive to disturbance. This centrifugation step was repeated, using wash media to resuspend the mitochondrial pellet, in order to reduce the contamination of percoll in the

sample. Once this step has been repeated the pellets were resuspended in wash, pooled into one tube and placed on ice before gentle homogenisation via agitation with a soft bristled paintbrush. The resulting purified mitochondrial sample was aliquoted into smaller volumes and either used for analysis directly (as described in chapter 3) or snap frozen in liquid nitrogen and stored at -80°C.

2.1.3 Mitochondrial Isolation & Purification from Spinach leaves.

Mitochondria were also isolated from spinach leaves in order to draw comparisons between mitochondrial respiratory characteristics, isolation yields and to further optimise isolation procedures for different plant tissues. This protocol was adapted from Keech *et.al.* (2005) [99] and the protocol developed in the Moore laboratory for the isolation of *A. maculatum* spadix mitochondria which was described in section 2.1.1.

Component	**Amount**
Sucrose	0.3 M
2-[(2-Hydroxy-1,1-bis(hydroxymethyl)ethyl)amino]ethanesulfonic acid, N-[Tris(hydroxymethyl)methyl]-2-aminoethanesulfonic acid (TES)	60 mM
Ethylenediaminetetraacetic acid (EDTA)	2 mM
Potassium dihydrogen phosphate (KH_2PO_4)	10 mM
Tetrasodium pyrophosphate	25 mM
Glycine	1 mM
PVP-40	1% (w/v)
BSA	1% (w/v)
Sodium Ascorbate	50 mM
Cysteine	20 mM

Table 2-3 Composition of mitochondrial isolation grinding buffer for spinach leaves

Component	Amount in M	Amount in g/500ml
Sucrose	0.3 M	51.34
TES	10 mM	1.1
KH_2PO_4	10 mM	0.68

Table 2-4 Wash Buffer components for mitochondrial isolation from spinach leaves.

Component	Amount in M/%	Amount in g/ml in 180ml
Percoll	50% (v/v)	90mls
Sucrose	0.3 M	18.48
TES	10 mM	0.411
EDTA	1 mM	0.0525
KH_2PO_4	10 mM	0.243
Glycine	1 mM	0.012

Table 2-5 Percoll purification buffer (50% v/v) for isolation of mitochondria from spinach leaves.

Spinach leaves were purchased from Waitrose for the purpose of mitochondrial isolation. Initially, the entire bag of leaves (500 g) were washed in distilled water and drained thoroughly. Leaves were then de-stemmed and de-ribbed manually using a scalpel, before chopping into approximately $1cm^2$ pieces and placed in grinding buffer. The components of grinding buffer were as described in Table 2-1. The leaf segments in the grinding buffer were then blended in an ice cold Waring blender and filtered through muslin exactly as described in section 2.1.1.

The resulting homogenate was centrifuged at 2500 x*g* for 5 minutes in a JA20 rotor to remove any large debris. The resulting supernatant is centrifuged at 15000 x*g* for 15 minutes again in a JA20 rotor to form a pellet containing the crude

mitochondrial fraction. This pellet is resuspended in a minimal amount of wash buffer (described in Table 2-4) adjusted to pH 7.5 (± 0.1) with KOH and gently homogenised in a Potter-Elvehjem glass homogeniser.

This resuspended pellet fraction was then taken forward to purification. The purification media for the spinach mitochondrial isolation is described in Table 2-5. The pH of the purification media was adjusted to 7.5 (± 0.1) with KOH before use and divided into 40 ml measures in pre-cooled 50 ml capacity centrifuge tubes. These were centrifuged at 39000 x*g* for 40 minutes in a JA20 rotor and subsequently stored at 4˚C, taking care not to disturb the gradient during transition from the rotor onto ice.

The crude mitochondrial fraction was gently layered onto the top of the percoll purification media without disrupting the surface. At this stage, the centrifuge tubes would be comparable to those in Figure 2-1 (A). The percoll gradients were then centrifuged at 15000 x*g* for 15 minutes in a JA20 rotor set to no deceleration. The mitochondria form a whitish band towards the bottom of the gradient and were aspirated from the centrifuge tubes as described in section 2.1.2. The mitochondrial fraction was thereafter diluted in wash buffer to at least a 20x dilution and split between 50 ml centrifuge tubes. The suspended mitochondria were then centrifuged at 15000 x*g* for 20 minutes in a JA20 rotor in order to form a soft pellet. This centrifugation step was repeated after re-suspension of the pellet in a minimal amount of wash media. This centrifugation stage serves a dual purpose, in way of concentrating the mitochondria and also washing away any residual percoll which may be present in the sample.

The supernatant is poured from the resulting pellet, which was resuspended in a minimum amount of wash media – normally 1 ml – with a soft bristled paint brush. Protease inhibitor cocktail was added to the resuspended mitochondrial pellet at 4% (v/v) in order to prevent the action of any protease enzymes present in the sample and therefore avoiding the degradation of mitochondria. The resulting sample

was further aliquoted into smaller volumes (100 µl-500 µl) and either snap frozen in liquid nitrogen for storage, or used for analysis immediately.

2.1.4 *Fallopia japonica* mitochondrial isolation

In order to investigate the role of mitochondria in the early growth stages of *F. japonica*, mitochondria were isolated from early buds and shoots of the plant in the spring months (predominantly April & May) of the years 2011 – 2014. The plant material was collected from a wild-growing patch near the Falmer campus of the University of Sussex.

F. japonica buds and shoots were collected and returned to the laboratory as quickly as possible to be washed in distilled water in order to remove any soil or other debris. Figure 2-2 shows an example of the varying sizes of the buds collected for mitochondrial isolation.

Figure 2-2 - Example of appearances and various sizes of *F. japonica* shoot buds collected for mitochondrial isolation.

These buds were then manually chopped into smaller pieces approximately 5 mm in length, before being placed into grind media (as described in section 2.1.1) and blended using a Waring blender, with 3 x 3 second full speed bursts. The subsequent stages in the isolation of mitochondria from the *F. japonica* buds are

identical to those of the *A. maculatum* spadix mitochondrial isolation, which is described in detail in section 2.1.1. One item of note was that once the chopped *F. japonica* buds were blended and filtered through muslin, the resulting liquid was very viscous and had a stringy texture. As with the *A. maculatum* isolation, samples were taken from each stage of the protocol and deep frozen at -70℃ for later analysis.

2.2 Transmission Electron Microscopy

2.2.1 Sample preparation for Transmission Electron Microscopy (TEM)

Samples were prepared from *A. maculatum* spadix material as well as from *F. japonica* callus, cell suspension and bud materials for imaging using a transmission electron microscope (TEM - Model - Hitachi-7100) under the direction of Dr. Julian Thorpe at the University of Sussex.

2.2.1.1 Preparation of *A. maculatum* spadix sections for TEM

A. maculatum spadices were collected on the day of preparation and sectioned for TEM as quickly as possible. Discs were cut from the spadix of approximately 2-3 mm in thickness. These were further sectioned into small cubes of approximately 2 mm^3. An example of the sectioning process for the spadices is shown in Figure 2-3.

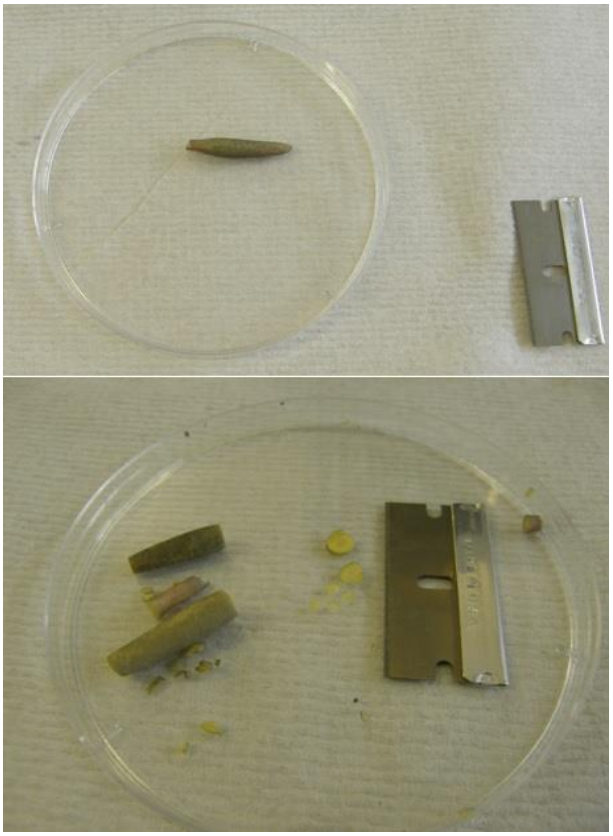

Figure 2-3 - Example of preparation of an *A. maculatum* spadix for TEM. The top image shows an *A. maculatum* spadix whole, the bottom image displays the discs and cubes into which the spadix is sectioned.

The prepared discs were carefully transferred into a fixative solution, containing 3% gluteraldehyde, and either 0.05 or 0.1 M sodium cacodylate at pH 7.4. The gluteraldehyde acts as a fixative, which kills the plant cells by rapidly cross-linking proteins, the cacodylate buffer contains arsenic and is used to prevent the growth of microorganisms and well as maintaining a steady pH environment for the plant cells. The sections are retained in the fixative solution with agitation at room temperature for 2 hours, before replacing the fixative solution and incubating the plant sections at 4℃ overnight for at least 8 hours.

2.2.1.2 Preparation of *F. japonica* material for TEM

When looking at the *F. japonica* buds, essentially the same sectioning and fixative process was undertaken as described for *A. maculatum* in section 2.2.1.1,

barring that with the *F. japonica* shoot buds, various sections were taken throughout the shoot bud - tip, middle and base - in order to compare the cellular composition of these three areas. An example of the areas investigated and their relation to the shoot buds is illustrated in Figure 2-4.

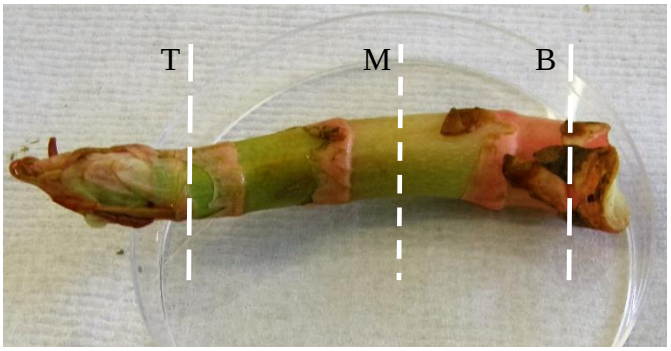

Figure 2-4 An example of the sectioning areas within the *F. japonica* shoot bud. T - Tip, M- Mid, B - Base

The *F. japonica* callus tissue was placed directly into the different fixative solutions, as the cells are readily accessible for the fixative in this state and further dissection is not necessary. Friable (callus which was deemed to be non-solid growth) callus were chosen as these cells are easier to separate from the main callus solid, would be the most viable and likely to be chosen to initiate suspension cultures.

Cell suspensions of *F. japonica* were prepared for TEM as follows; 1 ml samples were taken from cultures grown in the dark for 7 days, the cells collected by low-speed centrifugation (2000 x*g*), and resuspended in 500 µl of double strength suspension growth media. To the resuspended cells, 500 µl of fixative solution was added and the cells were incubated with agitation for 2 hours at room temperature before being transferred to a cold room to incubate at 4℃ overnight. Callus and cell suspension cultures of *F. japonica* are further discussed in chapter 5.

2.2.2 Post-fix, staining & dehydration of TEM samples

The following procedure is relevant to all samples. Post fixation, samples were washed in either 0.05 or 1 M sodium cacodylate buffer without gluteraldehyde

four times over an hour period with agitation. Samples were then transferred to fresh sodium cacodylate buffer containing 2% (v/v) osmium tetroxide and incubated with agitation at 4℃ overnight; a minimum of 8 hours. Osmium tetroxide is extremely toxic and should be handled with great care within a fume hood. The heavy metal lipid stain penetrates the samples and provides contrast in the resulting electron microscope images.

The osmium tetroxide staining was followed by 5 washes of each section with distilled water over a two hour period. This stage ensures complete removal of any osmium tetroxide from the surface of the samples and thus allows the samples to be handled outside of a fume hood. Following this, the samples were dehydrated using a series of increasing ethanol concentrations, ranging from 50-100% (v/v) ethanol, over a period of four hours. This stage is necessary to allow the resin to fully permeate the plant tissue. The samples were then introduced to propylene oxide in order to remove any residual ethanol; two twenty minute washes with agitation at room temperature.

The samples were subsequently transferred to a fresh vessel containing a 1:1 ratio of propylene oxide and resin. At this stage, the samples are incubated at room temperature for at least eight hours or overnight to allow full penetration of the resin into the plant tissue. Two to three changes of pure resin are performed – each incubated with agitation for 24 hours at room temperature. The samples were then extracted from the vessels containing resin and placed in a small receptacle with a label indicating the buffer molarity and identifying the section & tissue from which the samples were taken. This was filled with resin and placed in an oven for polymerisation for at least 8 hours.

Once the polymerisation of samples into the resin is complete, sections were taken from each block using a microtome, after carefully removing excess resin using a glass block so as to prevent damage to the diamond blade of the microtome. The microtome can be adjusted to give sections of various thicknesses – for the purposes of this project, 80 nm thick sections were cut from the samples. These

sections were then placed onto a support grid and allowed to dry. They were then stained with 0.2 μM uranium acetate by placing the grids sample-side-down onto a drop of the heavy metal and incubating at room temperature for one hour. Each grid was washed 5 times with distilled water over 15 minutes in the same fashion. Lead citrate staining was performed by placing the grid sample-side-down onto a drop of lead citrate in a petri dish for an hour at room temperature. A sodium hydroxide pellet was placed inside the petri dish to absorb any carbon dioxide present during the process which can have a detrimental effect on the staining. The grids were then washed with distilled water 5 times over twenty minutes, allowed to dry and were ready for visualisation using the TEM.

2.3 Growth of *Fallopia japonica* and generation of callus culture

F.japonica plants were kindly provided by Dr. John Bailey from the University of Leicester. These were then cultivated in glass greenhouses at the University of Sussex under the following conditions – 16 hour light, 8 hour darkness at 20℃, grown with all-purpose grade soil available from Sinclair via Fargro with the addition of Miracle-Gro all-purpose plant fertiliser at four week intervals.

2.3.1 Generation of callus culture from leaf explants of *F. japonica*

In order to have a continual supply of *F. japonica* plant material throughout the winter senescence months, as well as creating a basis for comparison of *F. japonica* bud cells and mitochondria, cell culture was initiated using leaves from the *F. japonica* plants grown in the greenhouse the University of Sussex. As there was no protocol available specifically for cell culture of *F. japonica* plants, several protocols which were available in the literature which had general instructions for initiation and maintenance of cell culture were adapted and optimised for use with *F. japonica* - [100-102].

To begin the process of creating a cell culture from *F. japonica* plant material, leaves which had fully unfurled yet not fully mature were selected from healthy, growing plants. Examples of the leaves chosen for beginning the cultures are shown

in Figure 2-5. These leaves were washed thoroughly in distilled water for a minimum of 20 minutes. The washed leaves were then briefly completely submerged in ethanol and transferred to sterile conditions in a flow hood, where all of the following stages were performed.

Figure 2-5 - Stages of maturity of *F. japonica* leaves chosen to initiate cell culture.

The ethanol-submerged leaves were washed in a solution of 10% (v/v) household bleach with 0.1% (v/v) tween and placed on an orbital shaker set to 120 rpm for 5 minutes. At this stage the leaves were considered to be sterile. To ensure complete removal of bleach and surfactant from the leaves, they were washed with 3 changes of sterile (autoclaved) water for 5 minutes each.

Once washed, the edges of the leaves which had been in contact with the bleach solution, the stem of the leaf and any area showing browning were cut away with the aid of a sterilised scalpel and forceps. The remaining leaf tissue was cut into small sections of around $1cm^2$ and scored lightly with a scalpel to encourage callus growth through wounding. The resulting leaf explants are illustrated in Figure 2-6.

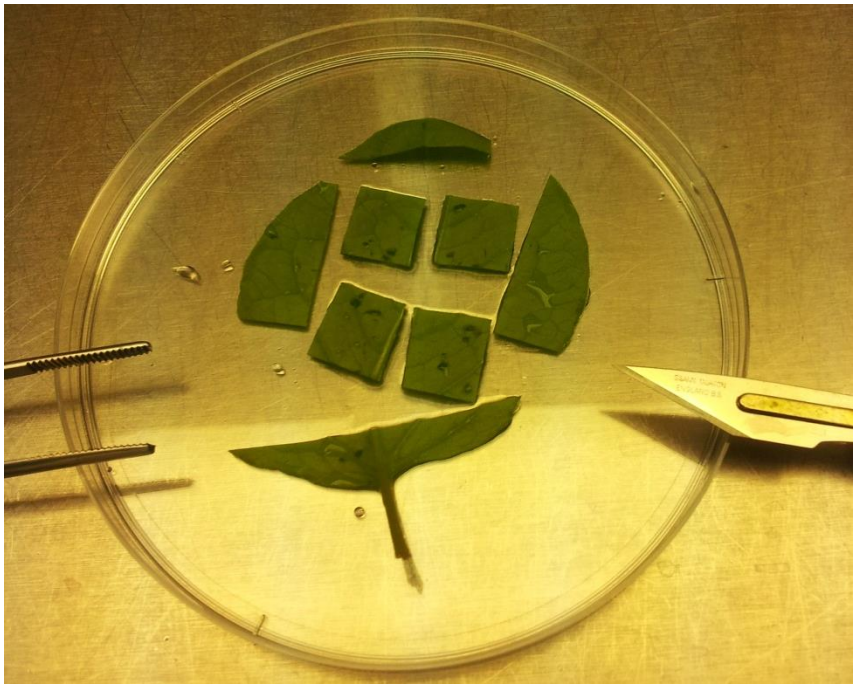

Figure 2-6 - Division of *F. japonica* leaves into explant sections for use in cell culture growth.

Initially, the leaf explants were grown on petri-dishes containing a gelling agent and Murashige and Skoog (MS) basal media. MS basal media contains essential nutrients for plant growth and was obtained from Sigma-Aldrich (catalogue number M5519). A list of the MS media components can be seen in Table 2-6. In order to prepare this media, 4.4 g/L of powdered MS was added to 90% of the total volume of distilled water while stirring. Once this had dissolved, 30 g/L sucrose was added to provide a carbon source for the plant cells. The pH of the media was adjusted to 5.4 (±0.1) using 0.1 M KOH before topping up the media to the final volume of 1L. This media was then dispensed into various sized vessels for autoclaving at 121℃ for 20 minutes. For solid media, a gelling agent in the form of plant culture tested agar (Sigma-Aldrich catalogue number A7921) was added at 0.6-1.0% (w/v) before autoclaving. Once cooled, autoclaved media was stored at 2-8℃ until use.

Component	Mg/L
Ammonium nitrate	1650
Boric acid	6.2
Calcium chloride (anhydrous)	332.2
Cobalt chloride hexahydrate	0.025
Cupric sulfate pentahydrate	0.025
Disodium EDTA dihydrate	37.26
Ferrous sulfate heptahydrate	27.8
Glycine	2
Magnesium sulfate (anhydrous)	180.7
Manganese sulfate monohydrate	16.9
myo-Inositol	100
Nicotinic acid	0.5
Potassium iodide	0.83
Potassium nitrate	1900
Potassium phosphate monobasic	170
Pyridoxine hydrochloride	0.5
Sodium molybdate dihydrate	0.25
Thiamine hydrochloride	0.1
Zinc sulfate heptahydrate	8.6

Table 2-6 Components of Murashige and Skoog basal media

2.3.1.1 Use of plant growth regulators in cell culture

Plant growth regulators (PGRs), or plant 'hormones' (phytohormones) are also required to initiate callus growth from tissue explants. PGRs can be divided into two categories – auxins and cytokinins – which work in tandem to control plant growth and development. Auxins stimulate cell division and differentiation, cytokinins effect apical dominance & promote plant cell growth. The concentration and choice of auxins and cytokinins is a crucial factor in plant cell culture and which combination and concentration is most effective can vary greatly from species to species. A further discussion of auxins and cytokinins can be found in chapter 5.

Name of growth regulator	**Type**	**Information**
Indole-3-acetic acid (IAA)	Auxin	Naturally occurring, potent plant auxin
α-Naphthalene acetic acid (α-NAA)	Synthetic auxin	Often used in rooting formulations for plant cuttings.
2,4-Dichlorophenoxyacetic acid (2,4-D)	Synthetic auxin	Utilised as an herbicide at high concentrations.
6-Benzylaminopurine (BAP)	Synthetic cytokinin	Inhibitor of respiratory kinases in plants, resulting in increased shelf life of vegetables.
Kinetin (Kin)	Cytokinin	Naturally occurring adenine-type cytokinin, used in conjunction with auxins to promote plant regeneration

Table 2-7 Plant growth regulators used for cell culture of *F.japonica*.

The available literature concerning plant cell culture has a wide range of concentration values recommended for use with various species of plants. Initially stock solutions were prepared of each PGR listed in Table 2-7 as follows; 1 mg/ml of

solid was added to a volume of 50-90% (v/v) ethanol and placed on a mechanical stirrer until fully dissolved. As PGRs are heat liable, filter sterilisation – using a sterile syringe complete with a Millipore 22 nm syringe driven filter unit - was completed as an alternative sterilisation process. The stock solutions were kept at 4-8℃ once prepared, and were used to supplement media with various concentrations and combinations of PGRs.

For the first set of explants which were produced from the *F. japonica* leaves, Indole-3-acetic acid (IAA) and 6-Benzylaminopurine (BAP) were used as an auxin and cytokinin source, respectively. Four different concentration combinations of auxin/cytokinin were used:

- 5 μM IAA + 5 μM BAP
- 25 μM IAA + 25 μM BAP
- 35 μM IAA + 35 μM BAP
- 50 μM IAA + 50 μM BAP

2.3.1.2 Growth of *F. japonica* callus

These concentrations of regulators were added to MS media containing agar once the media had been heated to liquid consistency and subsequently cooled to approximately 50℃. This was done in order to prevent the regulators from degradation or damage due to high temperature. The media was poured into sterile 9 cm diameter petri dishes and allowed to cool at room temperature until set. The scored leaf explants were then pressed gently into the surface of the agar, the lid replaced and the entire dish sealed using parafilm. The variation of PGR type, concentration and pH in the media are discussed in further detail in chapter 5.

The explant plates were subsequently incubated in a Weiss cabinet which provided constant illumination and temperature regulation at 22℃. The plates were checked regularly for contamination, both bacterial and fungal. Any plates found to be contaminated were disposed of via high temperature autoclaving to ensure complete sterilisation and safe disposal. Plates which were free from contamination

were kept in the Weiss cabinet for a minimum of two weeks before inspection for any signs of callus growth. For further discussion of callus tissue, refer to chapter 5. Any plates which had visible outgrowth from the original explant were taken back into a flow hood and the plant material was transferred onto a freshly made agar plate using sterile instruments, in order to ensure the callus cells had access to nutrients and glucose. This process was repeated every two weeks until the outgrowth from the leaf explant was considered to be large enough to separate from the original explant. This was normally achieved within six weeks - see chapter 5 for further details concerning callus 'status' and examples of callus stages.

2.3.2 Generation of cell suspension from *F. japonica* callus

Once the callus was separated from the original leaf explant and allowed to grow over several weeks it was considered for transfer into liquid media and the initiation of a suspension cell culture. The callus could be graded over several categories – colour, grain size and friability. To initiate cell suspension, 50-100 mg of the most friable callus was weighed under sterile conditions and transferred into a 250 ml conical flask containing 40 ml of sterile MS media containing the same concentration of PGRs which were present on the plate from which the callus was transferred. The flask was then passed through a flame to ensure sterility and sealed using either a foil cap or a foam stopper. The suspensions were then incubated at 25℃ on an orbital incubator set at 120 rpm in the dark. Figure 2-7 shows five flasks inoculated with friable *F. japonica* callus indicating the initial fresh weight of cells on each label.

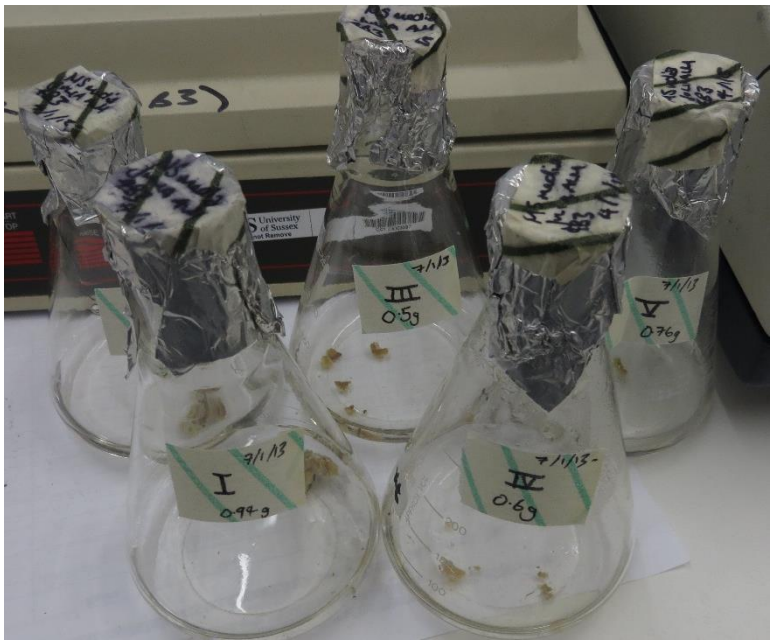

Figure 2-7 - Freshly inoculated flasks of liquid MS media with *F. japonica* callus. Corresponding initial weights of callus are indicated on each label.

After two weeks of incubation, the suspension cultures were visibly examined for signs of contamination, which would include browning of the culture indicating bacterial contamination, or spherical growths which would indicate fungal contamination. Any cultures which were found to be contaminated were disposed of via high temperature autoclaving. From each of the remaining cultures, 1 ml samples were extracted using a pipette with sterile disposable tips; 100 µl of this sample was plated onto L-Agar and another 100 µl onto a Potato Dextrose Agar (PDA) plate. This was performed to ensure that there was no contamination which was not visible to the human eye, bacterial or fungal, respectively. L-Agar plates were incubated at 37℃ and PDA plates at 25℃ for five days and examined for any growth after this period against a sterile water control. The corresponding culture to any plate which showed contamination growth was disposed of. This method of contamination testing was adapted from Torre *et al.* 2012 [103].

Suspension cultures which were free from any contamination were brought to a final volume of 60 ml with fresh medium plus corresponding PGRs under sterile conditions. These suspension cultures were incubated for a further two weeks at 25℃

on an orbital incubator set at 120 rpm in the dark. At the end of this period the contamination testing was repeated, and each culture was filtered using a sterile metal sieve (1 mm pore size) to remove any large aggregated cell clumps. At this time, if cell density was seen to have increased, 20-30 ml of culture was poured from the suspension and replaced with the corresponding amount of fresh media plus PGRs. This suspension was either kept at 4℃ until used for analysis (see sections 2.5 onwards for details of assays) or added to an equal amount of fresh media to create a new cell suspension. This process was repeated every two weeks to ensure continuation of the cell suspension.

2.3.3 Determination of fresh weight, dry weight, cell count, cell density & viability testing of cell suspensions.

In an attempt to investigate the relationship between fresh weights, dry weight, cell counts, viability and cell density, a two week experiment was set up which involved creating 18 separate suspensions from one original, established culture. Under sterile conditions, 45 ml of fresh media plus PGRs was added to 15 times 250 ml conical flasks, with 5 ml of established culture added to each. These were incubated as described in section 2.3.2, with one culture being taken each day and the following actions performed:

- 1.5 ml of each culture was extracted sterilely into a 2 ml Eppendorf.
- The remaining culture was filtered through 4 layers of Miracloth - pore size 22-25 µm (Merck Millipore catalogue number 475855) which had been previously weighed and the cells collected.
- The fresh weight was found by weighing the Miracloth plus the cells after all excess liquid had been squeezed from the cloth.
- The Miracloth containing the cells was then placed into a glass petri dish (90 mm diameter) and placed in an oven for 24 hours to ensure that all the moisture had been removed from the sample.
- The cloth was then re-weighed, minus the original weight to find the dry weight of the cells only.

- 200 µl of the sample taken from the culture was tested for contamination, via PDA and L-agar plates, as described in section 2.3.2, vs a sterile water control.
- 1 ml of the suspension was used to test viability of the cells; via the addition of 200 µl of 1% 2,3,5-Triphenyl tetrazolium chloride (TTC) solution. This solution, when reduced, gives a red colour – which enables it to be used as a respiration indicator. The following method was adapted from Steponkus *et al.* 1967 [104] & Torre *et al.* 2012 [103].
- The suspension/TTC solution was incubated at 37 ℃ for 2 hours, centrifuged at 12000 x*g* for 5 minutes and the resulting cell pellet resuspended in 95% ethanol and kept at room temperature overnight.
- The next day, without disturbing the cells at the bottom of the Eppendorf, 400 µl of the supernatant was taken and analysed using a spectrophotometer at 492 nm vs a 95% ethanol blank.
- The absorbance of the supernatant at 492 nm gave an indication of viability as the more intense red colouration would give a higher reading from the spectrophotometer.
- Cell counts were performed using a haemocytometer with a light microscope using x 50 magnification lens. 10 µl of suspension was used for each count and each count was repeated. The resulting numbers are an average of the two counts.

At the end of the two weeks, the results were collected and analysed in order to further optimise the suspension protocol and determine the rate of cell growth in the suspensions.

2.4 Growth of *Arabidopsis thaliana* callus culture and cell suspension

Arabidopsis thaliana is a model plant organism which has been intensely studied - it was the first plant to have its genome entirely sequenced in 2000 [105]. There is also a wealth of information regarding *A. thaliana* suspension grown cells including: synthesis of specific molecules [106] signal transduction in cultures [107] and monitoring of cell death [108]. Following this precedent, callus and suspension

cultures were initiated from leaf explants of *A. thaliana* in order to compare the growth and viability to that of the *F. japonica* cultures.

2.4.1 Growth of *A. thaliana*

Arabidopsis thaliana Columbia ecotype seeds were obtained from Dr. Jennifer Selinski at the University of Osnabrück, Germany. These were planted in all-purpose grade soil and grown in a Weiss cabinet for two weeks until leaves were evident. The leaves were then harvested and prepared for transfer onto solid media.

2.4.2 *Arabidopsis thaliana* callus culture

A. thaliana leaves were prepared as described in section 2.3.1 - exactly the same fashion as the *F. japonica* preparation. The same procedures were followed with the *A. thaliana* leaves as with the *F. japonica* leaf sections in the creation of callus culture in an attempt to directly compare the two species development during culture growth. Comparisons are drawn between the two cultures in chapter 7.

2.5 Protein Estimation Techniques

In order to determine the amount of protein in any given sample, a protein estimation was performed. The purpose of a protein estimation is gain an approximation as to the amount of protein present in a mixed sample in comparison to a set of known standards.

2.5.1 Bicinchoninic Acid (BCA) Detection

This estimation is based on a standard solution of bovine serum albumin protein (BSA) ranging from 2.0 – 0.1 mg/ml of protein. A standard 2 mg/ml solution is provided in a kit (Sigma catalogue number: BCA1-1KT), and diluted to form standards in a suitable range. The estimation is based on colorimetric detection of protein when mixed and incubated with solutions provided in the kit – solution A & B. The volumes used for the creation of the stock BCA standards can be seen in Table 2-8.

Standard Protein (mg/ml)	**BCA 2.0 mg/ml (µl)**	**H_2O (µl)**
1.0	500	500
0.8	400	600
0.6	300	700
0.4	200	800
0.2	100	900
0.1	50	950

Table 2-8 Creation of protein standards using 2 mg/ml BCA protein standard. Each standard is made up to 1 ml, 200 µl of each standard is required for one estimation.

All samples were diluted to a 1:50 ratio before use. Three repeats of each sample and two repeats of each standard were used to increase reliability of the technique – the average was taken once the samples have been analysed using the spectrophotometer. A total of 100 µl of each sample and standard repeat was added to a 1.5 ml plastic cuvette. The working reagent was made with reagents A & B mixed to a ratio of 50:1. 1 ml of the working reagent was added to each cuvette, and the components mixed by taking the mixture up and down in the pipette tip. The cuvettes were then incubated at 37℃ for 1 hour.

The detection of the amount of protein in the samples is achieved by a spectrophotometer set at 562 nm. The read out of the spectrophotometer gives an indication of the extent of the colour change in the sample which is proportional to the amount of protein in the sample. Using the standard repeat samples, a standard

curve can be created and the unknown samples protein content can be estimated using this curve.

2.6 Electrophoresis Techniques

Electrophoresis in general is a method applied to separating macromolecules – DNA, RNA and proteins - through a matrix according to their charge. Movement through a field is governed by the net charge and resistance. The resistance of the field through which the macromolecule is moving can be varied by alternating the size of the 'pores' in the matrix. In the case of polyacrylamide electrophoresis, the percentage of the crosslinking acrylamide determines the pore size, and therefore the resistance encountered by the macromolecule which is passing through.

2.6.1 Sodium dodecyl sulphate polyacrylamide gel electrophoresis (SDS-PAGE)

Samples containing proteins extracted from suspension cultures and samples from mitochondrial isolations were prepared for Sodium dodecyl sulphate polyacrylamide gel electrophoresis SDS-PAGE. SDS polyacrylamide gels consist of a resolving gel, which separates the peptides once they have entered the gel proper; and a stacking gel, in which wells are formed during the setting of the polyacrylamide and the samples are inserted at the beginning of electrophoresis. The stacking gel is of a lower percentage of acrylamide in comparison to the resolving gel, which causes the mix of peptides in the samples to enter the stacking gel readily when an electric current is passed through the apparatus. The mixture of sizes of the peptides then reach the resolving gel, which is of higher percentage acrylamide, and therefore smaller matrix pores. The peptides 'bunch up' at the junction of the two percentage gels and begin to enter the resolving gel and travel due to their size & charge.

Samples underwent a protein estimation as described in section 2.5 and this information was used to dilute each sample to a concentration of 1.5 µg/µl. 50 µl of the sample was taken and mixed with 50 µl of SDS containing loading dye which is described below:

- Loading dye :- 0.1 M TRIS-HCl, pH 6.8, 10 mM EDTA, 2% (w/v) SDS, 5% (w/v) glycerol, 0.05% (w/v) bromophenol blue

Each sample was then denatured on a hot-block set at 80-90℃ for 5 minutes. This was to ensure that the proteins were fully denatured and the sodium dodecyl sulphate (SDS) in the loading dye has had opportunity to bind to all of the charged areas of the peptides, which will modify their behaviour when run through a polyacrylamide gel. The samples were then ready to be loaded onto an SDS-PAGE gel.

2.6.1.1 Components of SDS-PAGE gels

To create the SDS polyacrylamide gels, the following solutions were used:

- 30% Acrylamide/bisacrylamide
- **Resolving Buffer** : 1.5 M tris(hydroxymethyl)aminomethane (Tris) pH 8.8 (RB)
- **Stacking Buffer**: 0.5 M Tris, pH 6.3 (SB)
- 10% SDS (w/v)
- 10% Ammonium persulfate (w/v)
- Distilled H_2O
- Tetramethylethylenediamine (TEMED)

These components form the resolving and stacking gels. Depending on the size of the peptides of interest, the acrylamide concentration was altered; higher percentage to form smaller pores and therefore effectively discern smaller peptides – lower percentage to form larger pores, allowing smaller peptides to 'run off' the end of the gel completely and allow a greater degree of distinction between larger peptides. An example of three resolving gel acrylamide percentages and the relative amounts of the components required to produce four SDS gels (total = 30 ml) of area 80 mm x 8 mm x 1 mm are shown in Table 2-9.

Final Acrylamide %	**H_2O**	**RB**	**SDS**	**Acrylamide**	**APS**	**TEMED**
7.5	14.38 ml	7.5 ml	300 µl	7.5 ml	300 µl	20 µl
10	11.88 ml	7.5 ml	300 µl	10.0 ml	300 µl	20 µl
12	9.88 ml	7.5 ml	300 µl	12.0 ml	300 µl	20 µl

Table 2-9 Table of components and volumes used to create the most commonly used percentage SDS-PAGE gels.

As previously mentioned, the stacking gel area of the SDS polyacrylamide gel is of lower acrylamide percentage to allow the entrance of the samples containing a variety of peptides to concentrate into thin bands before entering the resolving gel where they will begin to be separated[109]. The components required to produce stacking gels for four gels (total = 10 ml) of area 80 mm x 8 mm x 1 mm are shown in Table 2-10. In both of the referenced tables, APS and TEMED are underlined as they are added when all of the other components are mixed and are ready to be used.

H_2O	**SB**	**SDS**	**Acrylamide**	**APS**	**TEMED**
5.65 ml	2.5 ml	100 µl	**1.65 ml**	100 µl	7-10 µl

Table 2-10 Table of components and volumes used to create the stacking gel for SDS-PAGE gels

2.6.1.2 Creation and running of SDS-PAGE gels

SDS gels are formed by injecting or pouring the gel component mixture listed above in-between two glass slides. These slides are held apart by spacers which can be of varying thickness – the most commonly used are 1 mm thick by 10 mm x 80 mm. When APS and TEMED are added to the mixture, they begin the

polymerisation process. The solutions are then injected in-between the two glass plates to roughly three quarters the height of the glass plates and covered with a layer of propanol to exclude any bubbles from the surface of the gel in order to prevent contact with the air which would hinder polymerisation. The gels were then left at room temperature for approximately 30 minutes to allow the resolving gel to fully polymerise.

After this period, the propanol was removed from the top of the resolving gel and APS & TEMED were added to the stacking gel mixture to begin polymerisation. This stacking gel mixture was added to the top of the set resolving gel, up to the top of the glass plate assembly and plastic combs were inserted to form the sample wells. The gels were then left for a further 30 minutes to ensure full polymerisation. Once completely set, the gels were ready for use, or storage under running buffer, described below, at 4℃.

- **Running buffer** :- 0.1 M TRIS-HCl, pH 6.8, 10 mM EDTA, 2% (w/v) SDS, 5% (w/v) glycerol, 0.05% (w/v) bromophenol blue

Samples were prepared for electrophoresis as described in section 2.6.1. Prepared gels were inserted into gel holders and clipped into the electrophoresis housing which was inserted into a tank. The tank was filled to the level of the top of the glass plates with running buffer to ensure that the current, when switched on, will pass through the whole of the gel. The samples can be added to the wells in the gel either when the gels are emerged in the running buffer or 'dry' before the gels are immersed into the tank. The SDS polyacrylamide gels are then run at 150 V for approximately 1 hour, until the dye front has reached the bottom of the gel. The current is then turned off, the gels taken out of the tank and the stacking gel removed. The staining technique used to visualise the protein bands would depend on the objective of the gel.

2.6.1.3 Tricine SDS-PAGE

SDS-PAGE can be performed with glycine-Tris or tricine-Tris as the buffer system. The glycine-Tris buffer system, otherwise known as Laemmli SDS-PAGE,

is described in section 2.6.1.2. This system achieves the separation of proteins of 30 KDa or higher with consistent results, yet proteins of a smaller molecular weight are not well resolved. Tricine based buffer systems allow the separation of proteins in the range 1-100 KDa [109].

2.6.2 Polyacrylamide Gel Staining

2.6.2.1 Coomassie Staining

One method of staining SDS-PAGE gels is via the coomassie G-250 based product: gel code blue (Thermo Fisher Scientific – catalogue number: 24594). This staining technique requires washing of the run gels in distilled water for approximately 10 seconds before adding 20-25 ml gel code blue to the gel and incubating on an orbital shaker at 120 rpm at room temperature from 15 minutes to 1 hour – the longer incubation periods will provide increased sensitivity and therefore stain proteins which are present at lower levels. Following this, an overnight wash of the gel in distilled water removes any residual gel pieces and reduces the background staining to clearly identify the protein bands in the gel.

2.6.2.2 Silver Staining

Silver staining of SDS gels has approximately a hundred fold higher sensitivity in comparison to the coomassie based stains [110]. Here, a method of silver staining is described which is adapted from Schägger 2006 [111]. This method can be used following any coomassie based stain if increased protein detection sensitivity is desired.

The following reagents were required for this silver staining protocol:

- **Fixing solution:** 50% (v/v) methanol, 10% (v/v) acetic acid, 100 mM ammonium acetate.
- **Sensitizer solution:** 0.005% (w/v) sodium thiosulfate.
- **Silver Nitrate solution:** 0.1% (w/v) silver nitrate.
- **Developer:** 0.036% (w/v) formaldehyde, 2% (w/v) sodium carbonate.

- **Stop solution:** 50 mM Ethylenediaminetetraacetic acid (EDTA).
- **Coomassie destain:** 50% (v/v) methanol, 50 mM ammonium hydrogen carbonate.

To begin this protocol from a previously coomassie-stained gel, complete destain is required before silver staining can take place. The coomassie destain solution is applied to the gel for approximately 1 hour, or until the coomassie stain has been completely removed from the gel, which is followed by several washings in distilled water on an orbital shaker set at 120 rpm at room temperature.

If the gel is unstained and directly to be silver stained following electrophoresis, the fixing solution must be applied to the gel to fix the protein bands in place during the staining procedure. The duration of fixation is dependent upon the percentage of acrylamide forming the gel -15 minutes is required for 10% gels, ranging up to 30 minutes for 16% acrylamide gels. After this period, the gels are washed twice in distilled water, with each wash the same duration of the fixation step.

The sensitizer solution was then added to the gels for the same duration that the gels were in fixative. Addition of silver nitrate solution was made, with incubation for the same duration that the gels were in fixative. The gels were then washed with distilled water to remove excess silver nitrate and the developer solution added. The development takes place over a 1-5 minute period, during which the gels were watched closely as the staining can take place very rapidly. Once the gels were stained to a desirable degree, the stop solution was added, which chelates any remaining sliver ions and preventing further staining. Finally, the gels were washed several times in distilled water and can be stored in 5% (v/v) glycerol at 4℃ for several weeks.

2.6.3 Blue-Native PAGE

Blue-Native PAGE (BN-PAGE) was developed as a separation method for stable multiprotein complexes, most notably for membrane protein complexes; including respiratory chain complexes in mitochondria [112]. The following protocol is adapted from Wittig *et al.* 2006 [113].

2.6.3.1 Stock solutions and buffers for BN-PAGE

Table 2-11 shows stock solutions required to prepare the BN-PAGE gels and samples.

	Solutions	FW/Mw	Amount	Final Volume	Store	Remarks
A	1 M Imidazole	68.08	13.616 g	200 ml	7℃	
B	1 M Imidazole (pH 7.0)	68.08	3.404 g	50 ml	7℃	Adjust pH with concentrated HCl
C	20% (w/v) DDM	510.6	0.2 g	1 ml	-20℃	Divided into 100 µl aliquots
E	1 M Tricine	179.17	17.917 g	100 ml	7℃	
F	2 M 6-aminohexanoic acid (6-Aminocaproic acid)	103.1	10.31 g 26.36 g	50ml 100 ml	7℃	Not essential for BN-Page, but an efficient and inexpensive serine protease inhibitor
G	5% (w/v) Coomassie Blue G-250	854.04	0.5 g	10 ml	7℃	Suspended in 500 mM 6-amonihexanoic acid, known as Brilliant Blue G (Sigma)
H	AB-3 48% Acrylamide(A) 1.5%Bis-arylamide(B)		A: 48 g B: 1.5 g	100 ml	7℃	Crystallization occurs at 4℃
I	200 mM PMSF	174.19	0.0348 g	1 ml	7℃	Suspended in 90% Ethanol (freezer)
J	1 M Bis-Tris Propane	282.3	2.823 g	10 ml	7℃	
K	100 mM EDTA	372.24 (EDTA•2H_2O)	0.3722 g	10 ml	7℃	

Table 2-11 Reagents and stock solutions for preparation and running of BN-PAGE gels

	Cathode Buffer B (1L)	Stock solution required	Cathode Buffer B/10	Stock solution required
Tricine	50 mM	**E** 50 ml	50 mM	**E** 25 ml
Imidazole	7.5 mM	**A** 7.5 ml	7.5 mM	**A** 3.75 ml
Coomassie Blue G-250	0.02%	**G** 4 ml	0.002%	**G** 200 µl
pH	~7.0		~ 7.0	

Table 2-12 Cathode Buffer B & Cathode Buffer B/10 components. Cathode Buffer B should be stirred before use and stored at room temperature. Cathode Buffer B/10 should be stored at 4-7℃. Letters refer to stock solutions detailed in Table 2-11.

	Anode Buffer (1L)	Stock solution required	Gel Buffer 3x (50ml)	Stock solution required
Imidazole	25 mM	**A** 25 ml	75 mM	**A** 3.75 ml
6-aminohexanoic acid	----	----	1.5 M	**F** 37.5 ml
pH	7.0		7.0	

Table 2-13 Anode Buffer & Gel Buffer 3x components. pH should be adjusted with concentrated HCl and solutions stored at 7℃. Letters refer to stock solutions detailed in Table 2-11.

- **Fixing Solution -** 50% (v/v) Methanol, 10% (v/v) Acetic Acid, 100 mM Ammonium Acetate. Ammonium ions are added several hours before using the fixing solution to deactivate minor amounts of aldehyde contaminants.
- **Staining Solution –** 0.025% (w/v) Coomassie Blue G-250, 10% (v/v) Acetic Acid.
- **Destaining solution –** 10% (v/v) Acetic Acid. Store at 7℃.
- **Electroblotting buffer –** 50 mM Tricine [E], 7.5 mM Imidazole [A]. Store at 7℃.

Table 2-12 & Table 2-13 provides details as to the composition of anode and cathode buffers required for the creation and running of BN-PAGE gels. The use of the fixing, staining, destaining and electroblotting solutions are described later in this chapter.

2.6.3.2 Casting BN-PAGE gels

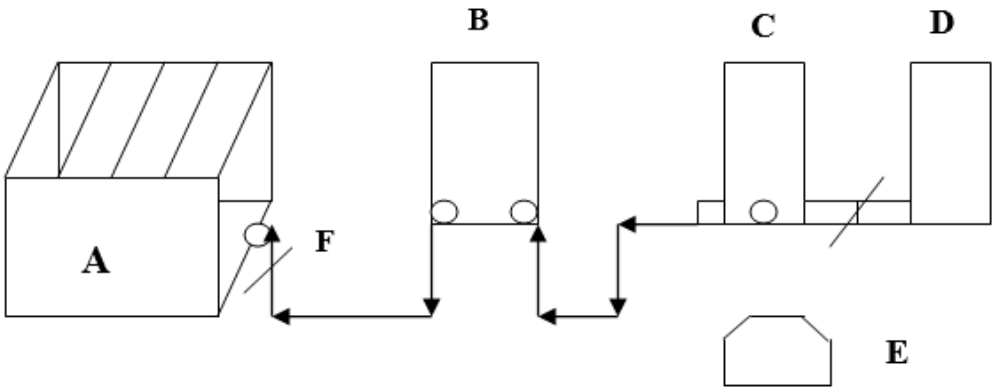

Figure 2-8 Equipment required for the casting of BN-PAGE gradient gels. A: Gel caster B: Peristaltic pump C: First chamber with stirrer, containing low percentage acrylamide solution D: Second chamber, contains high percentage acrylamide solution. E: Stirrer F: Clamp.

	Stacking Gel	Gradient Gel	
	3.5% Acrylamide	**4% Acrylamide**	**13% Acrylamide**
AB-3	0.44 ml	1.5 ml	3.9 ml
Gel Buffer 3x	2 ml	6 ml	5 ml
Glycerol	----	----	3 ml
H_2O	3.4 ml	10.4 ml	3 ml
10% (w/v) APS	75 µl	50 µl	50 µl
TEMED	7.5 µl	2 µl	2 µl

Table 2-14 Composition of BN-PAGE stacking and resolving gradient gels.

Table 2-14 gives the composition of the polyacrylamide mixtures needed to form the gradient gels on which the BN-PAGE technique is based. The gradient allows proteins and complexes in the range of 10 kDa – 10 MDa to be separated in one step [113]. In order to create the gradient, two different percentages of acrylamide solution (4% & 13%, as shown in Table 2-14) must be mixed using the apparatus shown in Figure 2-8. The gradient gels were cast at room temperature, with all solutions chilled on ice for at least 30 minutes beforehand. Approximately 5 ml of distilled H_2O is added to the bottom of the gel caster before any acrylamide solution is pumped into the apparatus to act as a barrier to air once the solutions have been mixed and to prevent untimely polymerisation of the acrylamide inside the apparatus.

APS and TEMED was first added to the 4% acrylamide solution and this was poured into the chamber C in Figure 2-8, which was placed on a magnetic stirrer to ensure adequate mixing and prevention of polymerisation in the chamber. The peristaltic pump was switched on at a rate of 1 ml/min and air was expelled from the tubing before connection was made to the casting apparatus. The clamp, F, was fastened and the connection was secured to the gel caster. The 13% acrylamide

solution then had APS and TEMED added to it and was poured into the second chamber, D, before the clamp was removed and the acrylamide solution was pumped into the gel caster. The connection between the chambers was only opened when the level of the 4% and 13% solutions were equal, to ensure no back-flow of the 4% solution into the other chamber. The 13% acrylamide solution contains glycerol to increase the density of the solution and aid the gradient formation.

The solutions were fully pumped into the gel caster after approximately 15 minutes, when the peristaltic pump was switched off and the gels were allowed to polymerise at room temperature for approximately 30 minutes. The amounts in Table 2-14 were sufficient to form 5 gradient gels. After the polymerisation period, the gel caster was dismantled and four gels are chosen to cast the stacking gel. This is performed as described as with SDS gels, described in section 2.6.1.2, with the solutions for stacking gels indicated in Table 2-14.

2.6.3.3 Sample preparation for BN-PAGE

Isolated or crude mitochondrial samples were diluted to a concentration of 10 µg/µl and divided into aliquots of 100 µl to be stored on ice. Each aliquot is centrifuged at 14 400 x*g* for 10 minutes at 4℃ using a benchtop centrifuge. Table 2-15 describes the components of the basic solubilisation buffer used for the solubilisation of mitochondrial membranes, without detergent. The detergent chosen for use was n-Dodecyl-β-D-maltopyranoside (DDM), which is a mild neutral detergent suited to the isolation of membrane proteins and complexes [113]. The detergent to protein ratio was optimised, and found to be most effective at either 1:1 or 1.5:1 on a gram to gram basis. This translated to using either 5 or 7.5 µl of 20% DDM, the results of which were both explored.

	Final concentration	Stock solution required
6-aminohexanoic acid	750 mM	**F** 3.75 µl
Phenylmethanesulfonylfluoride (PMSF)	1 mM	**I** 50 µl
Bis-Tris Propane	50 mM	**J** 500 µl
EDTA	0.5 mM	**H** 50 µl

Table 2-15 Components of Basic Solubilisation Buffer used for solubilisation of mitochondrial membranes

The centrifuged mitochondria were resuspended in 100 µl of solubilisation buffer with the addition of DDM whilst on ice. The resuspended mitochondria were centrifuged immediately at 16 100 x*g* for 40 minutes at 4℃. To each aliquot, 20 µl of coomassie blue solution (G) is added and mixed by inversion several times and kept on ice.

2.6.3.4 Running Blue-Native gels

BN-PAGE was performed using a mini-gel apparatus (Miniprotean Bio-Rad) at room temperature once all samples were loaded into the stacking gel sample wells. The gels were run at 100 V until the samples have entered the separating gel, approximately 30 minutes, after which the voltage was increased to 300 V. Cathode buffer B was used initially, with the addition of DDM, until the blue running front has moved approximately a third of the way down the gel, or after 30-45 minutes. At this point, the cathode buffer B was replaced with cathode buffer B/10 to reduce background staining of the gel. The gel was under electrophoresis conditions for a total of 2-3 hours, depending on the rate at which the samples travelled through the gel matrix.

2.6.3.5 Staining Blue-Native gels

Once the gels had been run, they were removed from the glass slides and the stacking gel removed. These were then incubated in fixing solution described in section 2.6.3.1 for at least 30 minutes, on an orbital shaker at 120rpm at room temperature. Gels were then stained using staining solution for at least 1 hour at room temperature. This stage was extended if inadequate staining was observed. Following this, two washes in destaining solution were performed, each lasting between 30-60 minutes. When the gels had been destained to a sufficient level, they were transferred to water and stored at 4℃. Gels were very fragile and were handled with great care.

2.7 Western Blotting

Western blotting, or protein immunoblot is a technique used to identify specific proteins from a mixture once separated on a polyacrylamide gel [114]. In short, proteins are transferred from the polyacrylamide matrix onto a solid support, either nitrocellulose or Polyvinylidene fluoride (PVDF) membrane. Antibodies targeted to a specific protein can then be used to probe the membrane and detected via chemiluminescence.

Following electrophoresis, the glass slides are dissembled and gels prepared for western transfer by transferring to a box containing transfer buffer.

- **10x Transfer buffer (TB)** – 1.92 M glycine, 13 mM TRIS pH 7.2
- 1 L total: 800 mls distilled water, 100 ml 10x Transfer Buffer, 100 ml Methanol. Stored at 4℃.

The transfer of the protein bands to either the nitrocellulose or PVDF is performed by setting up a ‘sandwich’:

- Initially, a sponge soaked with transfer buffer was placed on one side of a support.

- 3 mm paper was also soaked with transfer buffer and placed on top of the sponge.
- The gel was placed on top of the paper, having had a corner removed in order to aid orientation.
- The nitrocellulose of PVDF membrane was soaked in transfer buffer and placed on top of the gel, with a corner cut from it and in the same orientation of the gel.
- Another layer of transfer buffer soaked 3 mm paper was placed on top of this stack, and any air bubbles removed by gently rolling over with a test tube.
- Finally, a second soaked sponge was placed on top and the support is closed together to hold the layers of the 'sandwich' in place.

The support was slotted into a housing which was placed into an electrophoresis tank. The tank was filled with transfer buffer, complete with an ice pack and stirrer to prevent overheating. The tank was set upon a mechanical stirrer and connected to power, running at 100V for 1 hour. Halfway through the run, the ice pack was checked and replaced if melting has occurred. At this point the protein bands were expected to have transferred to the chosen membrane.

2.7.1 Detection

Once transfer was complete, the gel and paper which formed the 'sandwich' were discarded and the membrane retained. To confirm that the protein has been fully transferred from the gel, a ponceau stain was undertaken. To perform this, 5 ml of ponceau solution (Sigma – catalogue number P3504) was added to the membrane and agitated for ~ 30 seconds before washing with distilled water. Protein bands were visible as red bands and any marker protein positions marked onto the membrane in pencil – if this was confirmed, the dye can be washed from the membrane using Tris-buffered saline tween (TBST) buffer, as described below.

- **10 x TBST** (Tris-buffered saline tween). 140 mM NaCl, 20 mM Tris-HCl pH 7.6, 0.1% (v/v) Tween-20. Diluted to 1 x (working strength) with distilled water

When the ponceau stain was removed, a blocking solution, described below, was added to the membrane and left either at 4℃ overnight or for 2 hours at room temperature.

- **Block** - 2% (w/v) milk powder, 3%(w/v) BSA in 1x TBST

Following this period, 10 µl of the primary antibody was added to the block and membrane, agitated on an orbital shaker for 1 hour at room temperature. Three quick (~ 5 second) washes in 1x TBST of the membrane was followed by 6 x 5 minute washes in 1x TBST. At this point the membrane was placed in a second block wash, with 10 µl of the secondary antibody and agitated on an orbital shaker for 1 hour at room temperature. The membrane was then quickly washed and another 6 x 5 minute washes are performed. The membrane was then placed in BLOT rinse and was ready for detection.

- **10x BLOT rinse** – 10 mM TRIS pH 7.2, 5 mM EDTA. Diluted to 1x BLOT with distilled water.

Detection was performed in a dark room using an enhanced chemiluminescence (ECL) kit (Thermo Fisher – catalogue number 32106) following manufacturer's instructions. In short, the membrane was placed in an extremity case with x-ray film cut to size. Solutions from the ECL kit were added to the membrane and any excess blotted off with 3 mm paper. The x-ray film was then closed inside the case with the membrane and exposed to the chemiluminescence given off by the antibodies attached to the protein of interest on the membrane. The exposure was varied in accordance to the strength of the signal given off from the membrane. The film was fed into a developer and once processed, can be overlaid onto the membrane to mark on protein marker positions and relative size of the membrane.

2.8 In-Gel Activity Staining

According to Sabar et al. 2005 [115], in-gel histochemical activity staining is a powerful technique which combines the protein complex separating capability of

BN-PAGE with histochemical staining of active enzymes in-gel. This method is often used to determine the activity of mitochondrial respiration chain complexes. For example, dehydrogenase staining relies on the precipitation of formazan as blue-purple crystals derived from the reduction of nitro-blue tetrazolium (NBT). The dye is colourless and serves as a hydrogen acceptor during the oxidation of the reducing powers such as NADH-H^+ or FADH-H^+ by dehydrogenases. NBT accepts the hydrogen directly from NADH oxidising systems such as NADH dehydrogenase (complex I), whereas the reduction of the dye by succinate dehydrogenase is enhanced by the addition of an artificial electron carrier such as phenazine methosulphate (PMS). Cytochrome c oxidase can be analysed via in-gel activity staining making use of the oxidation of diaminobenzidine (DAB) by cytochrome c. This reaction forms a brown precipitate at the site of the enzymatic activity. In Table 2-16 the reagents, substrates and reagents are provided in detail.

Complex	**Buffer & pH**	**Substrate**	**Reagent [% (w/v)]**
NADH dehydrogenase (complex I)	0.1 M Tris-HCl pH 7.4	0.2 mM NADH	0.2 NBT
Succinate dehydrogenase (complex II)	50 mM KH_2PO_4, 0.1 mM ATP, 0.2 mM PMS, pH 7.4	10 mM Succinate	0.2 NBT
Cytochrome c oxidase (complex IV)	50 mM KH_2PO_4, pH 7.4	1 mg/ml^{-1} cytochrome c	0.1 DAB

Table 2-16 Buffers, substrates and reagents required for in-gel activity histochemical staining. KH_2PO_4 – monopotassium phosphate. ATP – adenosine triphosphate.

BN-PAGE was performed exactly as described in section 2.6.3, with the exception of increasing protein concentration in each sample lane to 100 µg. Once the gels have run, they were rinsed in distilled water briefly, then equilibrated for ten minutes in the reaction buffer corresponding to the enzyme of interest as described in Table 2-16, at room temperature. This is then replaced with fresh reaction buffer including the reagents and incubated for various times:

- 1-3 minutes NADH dehydrogenase
- 3-9 minutes Succinate dehydrogenase
- 10-12 minutes Cytochrome c oxidase

The reactions are stopped with the addition of 45% (v/v) methanol and 10% (v/v) in distilled water. The gels can be stored in this solution overnight and subsequently preserved in 10% (v/v) glycerol when kept at 4℃.

2.9 Oxygen Electrode Analysis

Oxygen electrodes are used to polarographically measure the amount of oxygen in a solution [116]. This is achieved by applying a voltage of -0.16 V across two electrodes, a platinum cathode and a silver anode, which are bridged with the electrolyte saturated potassium chloride. When assembled, the electrodes are in contact, via a membrane, with the contents of the chamber – to which various samples, substrates and inhibitors may be added. Figure 2-9 reveals the components in a diagrammatic fashion.

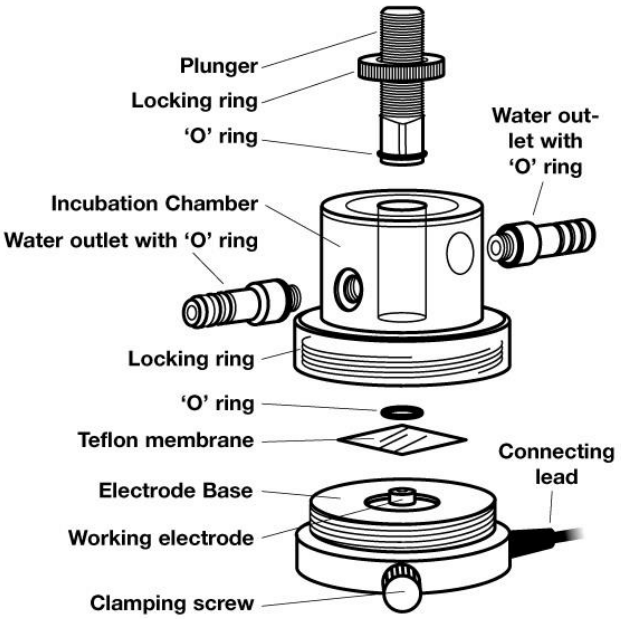

Figure 2-9 Diagrammatic representation of the components of a Clark-Rank Oxygen electrode[117].

Every oxygen molecule which reaches the platinum cathode is reduced to water via the following reaction;

- $O_2 + 2H_2O + 4e^- \rightarrow 4OH^-$

For every reduction reaction, a corresponding oxidation reaction takes place at the silver cathode;

- $4Ag + 4Cl^- \rightarrow 4AgCl + 4e^-$

The resulting current which flows between the two electrodes is converted to voltage, therefore allowing the amount of oxygen in the chamber to be constantly monitored. The oxygen electrode is calibrated by adding air saturated distilled water for 100%, and the addition of sodium dithionite

Additions can be made to the reaction in order to investigate – in real-time - effects of substrates or inhibitors on the samples in the chamber. This is an extremely useful tool as it allows mitochondrial samples to be analysed and to estimate the activity of each protein in the respiratory chain. A 400 µl chamber was used during analysis, the basic process involving the addition of plant medium A as a reaction buffer (composition shown below), followed by addition of a sample of interest and any further substrates or inhibitors for respiration as required. Details of substrates and inhibitors can be found in chapter 3.

- **Plant medium A** – 300 mM mannitol, 1 mM $MgCl_2$, 10 mM KCl, 5 mM K_2HPO_4, 20 mM MOPS, pH 7.2.

2.10 Mass Spectroscopy

Mass spectroscopy is a powerful technique that allows the identification of proteins in a given sample by analysis of their mass to charge ratio [118]. A charge is conferred to the sample via ionization and the sample then passed through an analyser instrument onto a detector. In order to reduce the amount of proteins in a

given sample, and therefore increase the specificity of the results, electrophoresis can be performed on a sample and a band or spot of interest can be excised and prepared for mass spectroscopy.

2.10.1 Preparation of SDS & BN-PAGE gels for mass spectroscopy – In-gel digestion

In order to identify proteins and peptides separated on a SDS or BN-PAGE gel, mass spectroscopy was used. This technique allowed samples to be separated into its constituents and each categorised and roughly quantitated. The first stage of preparation for mass spectroscopy was to photograph the gel and mark which bands were to be excised and analysed. The gel bands were the excised using a clean scalpel. When more than one band was being cut from the gel, the scalpel blade was rinsed in Industrial Methylated Spirits (IMS) to prevent cross contamination of peptides between bands of interest. Depending on the size of the excised piece of gel, it was divided into two or, for the larger bands, three pieces to improve surface area to volume ratio when adding solutions. The gel pieces were then transferred into an Eppendorf for further processing.

Solutions for the digestions were prepared freshly on each occasion. Initially, the coomassie stain had to be removed from the proteins in the gel matrix – this was achieved using an acetonitrile solvent which is described below.

- **PAGE destain:** 50% acetonitrile (MeCN), 50 mM ammonium bicarbonate (NH_4HCO_3)

Approximately 500 µl of PAGE destain was added to each Eppendorf, which was then placed in an orbital shaker incubator set at 37°C and 120 rpm for a 5 minute incubation. The solute was removed and the process repeated three times, by which point most of the coomassie stain had been separated from the proteins contained in the gel pieces. Following this, as much solute as possible was removed and the gel pieces were dehydrated using a vacuum concentrator (speed vac) for approximately 5 minutes without heating.

The gel pieces were then subjected to reduction, which aids unfolding of the proteins within the gel – consequentially increasing the number of sites available for enzymatic cleavage. Dithiothreitol (DTT) was used as the reducing agent, converting the disulphide bonds within cystine into cysteines free sulfhydryl groups [119]. The DTT solution is described below:

- 10 mM DTT, 25 mM NH_4HCO_3

Approximately 50 µl of the DTT solution was added to each Eppendorf containing gel pieces, and incubated at 50℃ for 45 minutes on a hot block to allow swelling of the gel pieces back to full size. After this period, the eppendorfs were removed from the hot block and allowed to return to room temperature and any remaining DTT solution was removed.

The next step in the preparation was alkylation of the proteins contained in the gel, in order to prevent reoxidation of the sulfhydryl groups and maintaining the unfolded status of the reduced proteins. This was achieved using an iodoacetamide solution, which is described below:

- 50 mM iodoacetamide, 25 mM NH_4HCO_3

Approximately 100 µl of iodoacetamide solution was added to each Eppendorf, or enough to fully cover the gel pieces, and incubated for 45 minutes at room temperature. This incubation was performed in the dark, as iodoacetamide is photolabile [120].

Following alkylation, excess liquid was removed from the Eppendorf. Two changes of PAGE destain with 5 minute shaking were made, after which as much liquid as possible was removed from each Eppendorf. At this point, the samples were centrifuged for 5 minutes using a vacuum concentrator. The lids of each of the Eppendorfs were pierced with a scalpel to aid the evaporation of any remaining solutions. Trypsin solution was prepared in ammonium carbonate solution:

- 12.5 ng/ul Trypsin, 25 mM NH_4HCO_3

Trypsin solution (described above) was added to cover the gel pieces in the eppendorfs and left to incubate on ice for 10 minutes. The gel pieces swell up as they are rehydrated by the trypsin solution and after the incubation period any remaining solution was removed. The gel pieces are then covered with ammonium carbonate solution and incubated at 37℃ for 4 hours or overnight.

- 25 mM NH_4HCO_3

When the incubation was complete, formic acid was added to the Eppendorfs at a final concentration of approximately 5% (v/v). The Eppendorf was then vortexed for 1 minute and the supernatant removed into a clean Eppendorf. This contained peptides and should be kept on ice at all times. In order to ensure that all peptides have eluted from the gel pieces, MeCN was added to cover the pieces. Incubation with shaking at room temperature for 5 minutes followed by centrifugation and removal of the supernatant was sufficient to remove remaining peptides. This stage may be repeated if the gel does not look dehydrated.

To concentrate the sample and remove some of the solvents from the solution of peptides the vacuum concentrator was utilized. At a low or medium heat setting the solvent was slowly removed by evaporation, with checking of the samples so as to not dry them out approximately every 15 minutes. The resulting peptide solution can be stored short term in a -20℃ freezer, or for a longer term (over one month) in an -80℃ freezer.

3 Mitochondrial Isolation from *Fallopia japonica*

3.1 Introduction

To investigate how *F. japonica* generates so much energy during early growth stages, buds were collected from naturalised plants in the area surrounding the University of Sussex during the years 2012 through to 2015 and attempts were made to isolate mitochondria from these plant tissues. Mitochondria are known to be the 'powerhouse' of eukaryotic cells (where mitochondria are present) – and although plants also generate energy via photosynthesis – early *F. japonica* buds do not photosynthesise immediately after emergence from the soil, yet still achieve extraordinary growth rates.

The emerging buds have a red or pink colouration, as can be seen in Figure 3-1, which is typical of anthocyanin accumulation within the buds [119]. In immature plant tissues, anthocyanins are thought to provide a 'sunscreen', or a photoprotective role – as they reduce the amount of visible light available for photosynthesis, as well as a visible signal to detract herbivores [120]. The stems of *F. japonica* retain this red/pink spotting upon reaching maturity. As the red pigments absorb visible light, this prevents the light from participating in photosynthesis. Overall, this decreases the amount of light available for chlorophyll excitation, which limits the potential of photosynthesis to be the dominant source of energy generation at the early stages of growth.

In light of this, preparations of mitochondrial samples from the naturalised plants were attempted. Many protocols exist in the literature describing the isolation of mitochondria from many different plant organs and species; including green leaf tissue from *Spinacia oleracea* (spinach) [121], woody stems from the *Bambuseae* (Bamboo) family [122], tubers of *Solanum tuberosum* (potato) [123] & specialised plant organs such as the thermogenic stamens of *A. maculatum* [124]. As there was no protocol available for the isolation of mitochondria from *F. japonica*, a combination of protocols in the literature were considered in the optimisation of the protocol for *F. japonica* mitochondrial isolation.

3.2 Plant material preparation

Fallopia japonica buds were chosen for the isolation of mitochondria as they were theorized to contain large numbers of this organelle. This hypothesis was deduced due to the rapid growth displayed at the early growth stages of the plant when it is seen to be naturalised. *F. japonica* buds were collected from an approximately 5 m^2 'wild' patch of naturalised plants in the early spring of the years 2012-2015. The exact dates varied throughout this period, as late snow and cold weather had a delaying effect on the emergence of the buds in the spring of these years. Typically, collection of plant material occurred during the months of April and May.

Figure 3-1 shows an image taken in early April 2013 of a rhizome crown developing buds in a particularly dense fashion, with prominent emerging buds highlighted. The buds were harvested by digging down around the emerging bud and excising the bud material from as close to the join with the rhizome as possible, with the aim of maximising the amount of material available for mitochondrial isolation.

3.3 Protocol development & purification

3.3.1 *F. japonica* bud & shoot material

Initially, the mitochondrial preparation protocol for *A. maculatum* spadices, which had been developed in the Moore laboratory, was used for the *F. japonica* bud material as there was no species-specific protocol available. This protocol is described in detail in chapter 2. Initially, starting plant material weight was used to determine the amount of buffer to be used throughout the procedure, as larger amounts of starting material required a larger volume of isolation buffer during the homogenisation process - the buffer volume to starting material weight ratio was optimised throughout the project.

One major difference in performing the mitochondrial isolation protocol for *A. maculatum* with *F. japonica* shoot material was made clear when the homogenised plant material was filtered through muslin in order to remove any large solids from the extract. At this point, the *F. japonica* extract had become very viscous and had a stringy quality where the *A. maculatum* extract was very much more fluid in consistency.

Several attempts were made to purify the crude extract using the Percoll density gradient separation method described in chapter 2. An example of the density gradients are shown in Figure 3-2, where the *F. japonica* mitochondrial sample is represented on the left and spinach extract on the right. Obvious differences can be seen between the two samples – there is clear delineation between the bands in the spinach sample gradient, of which the band representative of the mitochondria in Figure 3-2 was removed and tested using the oxygen electrode. This sample proved to have respirational activity and served to confirm the Percoll separation process of mitochondria was viable. The *F. japonica* sample is not so well separated and no clear mitochondrial band was visible [125]. This made it difficult to determine where the mitochondria were located in the gradient, resulting in large volume samples being taken from the area indicated in Figure 3-2.

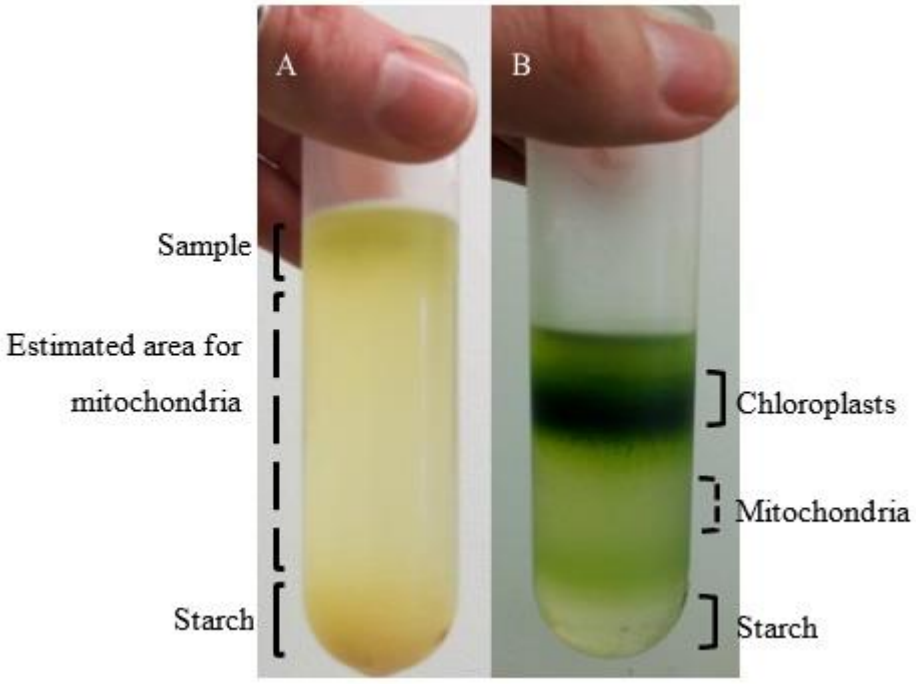

Figure 3-2 an example of continuous 21% Percoll purification gradients of *F. japonica* buds, A and spinach leaves, B.

After each attempt, the area of the gradient which was expected to contain the mitochondrial fraction was aspirated and washed via centrifugation. This was successful with the spinach mitochondria, as these were contained in a more defined band and therefore a much smaller volume was aspirated from the Percoll gradient. The spinach mitochondria formed a visible pellet and this was subsequently resuspended. The *F. japonica* samples however, often did not form a pellet after the washing stages, indicating the loss of the mitochondrial fraction entirely, or a failure to separate this fraction from the rest of the sample. The pellets formed were taken and known as purified sample. Assays were performed on these samples via oxygen electrode (methodology described in chapter 2). The *F. japonica* purified samples were found to have either very low or no mitochondrial activity.

After further investigation into bud and shoot mitochondrial isolation, a protocol detailing the isolation from immature bamboo buds and shoots was

discovered [122]. This protocol did not attempt to purify the crude mitochondrial samples from the bamboo material, therefore several changes were made to the centrifugal speeds when using the *F. japonica* material in response. This was in an attempt to increase the amount of mitochondrial sample gained from each isolation. These changes are detailed below.

- An extra debris centrifugal stage was added due to the large amount of viscous extract at the initial isolation stage and the speed was increased to 1500 x*g*.
- As illustrated in Figure 3-2, gradient purification was unsuccessful when using extract from *F. japonica* buds – the purification stages were therefore excluded when using *F. japonica* plant material.
- An extra wash centrifugal stage was added, as a replacement of the Percoll purification stage, of 100000 x*g* to remove as much debris from the 'crude' fraction as possible.

These changes to the protocol resulted in a large increase in the volume of sample gained from *F. japonica* material. Due to these results and the difficulties in obtaining a purified pellet using the Percoll purification procedure with *F. japonica*, the purification stage was removed and samples were taken and used as crude before entering the purification stage, and are referred to as "crude" in subsequent sections.

3.3.1 Development of mitochondrial isolation protocol for *F. japonica* suspension cultures

F. japonica suspension cultures were initiated as described in chapter 2. The isolation of mitochondria from these suspension grown cells was achieved using the same buffers and procedures as outlined in this chapter, however with the following adaptations compensating for the differing state of the initial material.

- Cells in suspension were filtered from the growth media using several layers of muslin. The suspension cells were scraped from the muslin and weighed for fresh weight determination.

- Approximately 2 g of cells were then placed into a pre-chilled pestle and mortar and any aggregates were ground in chilled grinding media containing 4% (v/v) protease inhibitor until in solution and nearing homogeneity. This also served to mechanically break open the cells, in the presence of protease inhibitor throughout to prevent any potential enzymatic degradation of the proteins in the homogenate.
- Once all of the cells had been ground, a Potter-Elvehjem glass homogeniser was used to ensure complete homogeneity, breaking open any cells via shearing which may have remained intact after grinding.
- The homogenate was then subjected to the centrifugal steps outlined earlier in this chapter section 0.

A comparison of suspension cell prepared samples and fresh plant material samples from *F. japonica* when run through oxygen electrode analysis and polyacrylamide gels can be seen later in this chapter, 3.4 & 3.5.

3.3.2 Mitochondrial isolation from *F. japonica* leaves

Mitochondrial isolation from *F. japonica* leaves was achieved using wild type plants that had been grown in the University of Sussex greenhouses with a 16 hour photoperiod. The details of the isolation were identical to those of the isolation of mitochondria from spinach leaves, described in chapter 2. The addition of 1% (w/v) PVP-40 was made to the isolation media to remove phenolic compounds from the leaf homogenate via adsorption. The leaf mitochondrial isolation protocols were based upon references [126] and [97]. Comparison of the isolated leaf mitochondria samples to those from differing materials of *F. japonica* can be seen later in this chapter, section 3.5.

3.4 Oxygen electrode

In order to determine if the prepared samples isolated contained mitochondria able to perform oxidative phosphorylation, they were assayed using a Clark-Rank type oxygen electrode with the use of a 400 µl cuvette. The protein

content of the samples was first estimated using a bicinchoninic acid assay (described in chapter 2) and a suitable amount of sample was used for each assay, depending on the polargraphic activity demonstrated via the oxygen uptake of the sample and the calculated protein estimation [127]. Each of the samples were added to a 400 µl chamber, containing reaction buffer, plant media A. Additions were made through a small aperture to minimise gas exchange with the surrounding environment. The functionality of the oxygen electrode apparatus is described in detail in chapter 2.

3.4.1 Buffers, Substrates & Inhibitors

Several different substrates and inhibitors were added to the chamber to test the sensitivity of the mitochondria to mitochondrial complex specific inhibitors and to give a general idea of the abundance and sensitivity of each respiratory complex to substrates, details of which are listed below.

- Plant medium A – 300 mM mannitol, 1 mM $MgCl_2$, 10 mM KCl, 5 mM K_2HPO_4, 20 mM MOPS, pH 7.2.
- NADH 1.25 mM final concentration – electron donor to NADH dehydrogenase (complex I) & provides reducing power to the oxidative phosphorylation pathway.
- Glucose/Succinate 5 mM final concentration – Glucose is provided as a substrate, which when oxidised will provide reducing coenzymes to feed into the oxidative phosphorylation pathway at complex I. Succinate also provided as a substrate, which enters the oxidative phosphorylation chain at succinate dehydrogenase (complex II).
- Ascorbate 10 mM/TMPD (N,N,N',N'-Tetramethyl-p-phenylenediamine dihydrochloride) 100 µM - when added together, asc & TMPD act as cytochrome c oxidase (complex IV) substrates by reducing cytochrome c.
- Adenosine diphosphate (ADP) 5 mM final concentration – added to mitochondrial preparations to act as a substrate, involved with ATP formation via phosphorylation.

- Carbonyl cyanide m-chlorophenyl hydrazine (CCCP) 1µM final concentration.

  CCCP is an uncoupler acting as an ionophore which causes transport of ions across the mitochondrial membrane and thereby disrupting the proton motive force.

- Antimycin a 1µM – Inhibitor of cytochrome c reductase (complex III) by preventing the reduction of ubiquinone.

- Cyanide (KCN) 0.3 mM – Inhibitor acting on cytochrome c oxidase (complex IV) and preventing oxidative phosphorylation.

3.4.2 Oxygen electrode analysis

The following figures represent the data gathered from the oxygen electrode analysis of mitochondrial samples from both *F. japonica* and *A. maculatum*.

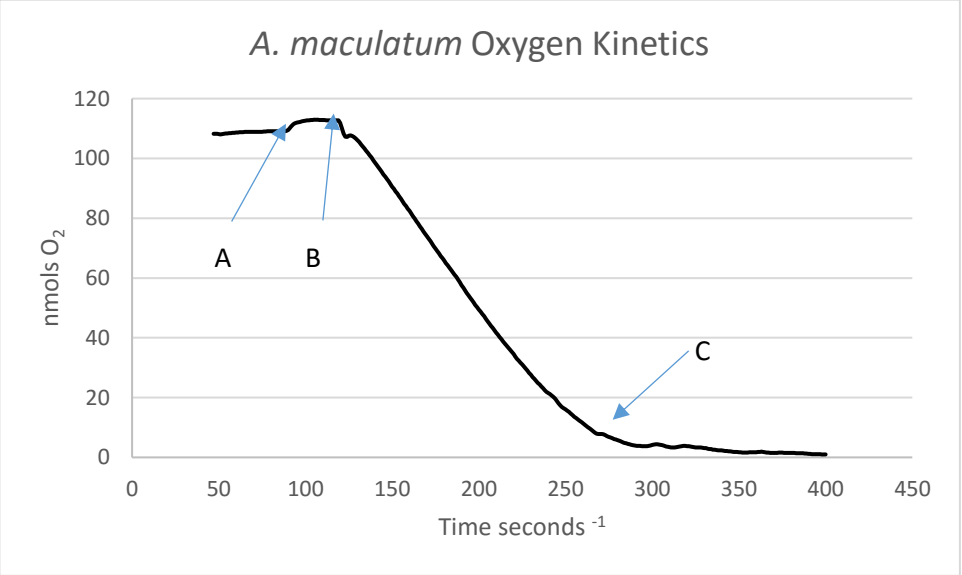

Figure 3-3 Graph showing *A. maculatum* oxygen kinetics. A - addition of antimycin a, B – indicates addition of NADH. C - point at which oxygen is depleted in the oxygen electrode chamber (anaerobiosis).

The collection of *A. maculatum* spadices took place in the spring of the years 2011 – 2015. They were harvested at a specific stage in the growth of the plant in order to maximize the amount of alternative oxidase (AOX) in the mitochondria of the spadix, which is indicated by an increase of temperature of the spadix and a fully open spathe.

The AOX reduces oxygen to water, branching from the respiratory chain at the level of complex III and the ubiquinone pool [128]. Figure 3-3 is an indication of the oxygen consumption of the mitochondria in the chamber after the addition of an inhibitor and a substrate. The first addition was antimycin a, which is a complex III inhibitor, added at the point marked A on the graph. This addition, made before any substrate is added to the chamber, ensures that any oxygen consumption rate displayed is not as a result of the conventional cytochrome pathway, inferring that the oxygen consumption is due to the AOX activity within the respiration chain. NADH is added in excess at 1.25 mM as a substrate for NADH dehydrogenase (complex I) at the point marked B on Figure 3-3. The oxygen concentration in the chamber immediately starts to decrease. This rate of oxygen reduction is 0.781 nmolO_2/sec, which, when taken in context with the amount of mitochondrial protein present in the chamber, gives an oxygen consumption rate (or specific activity) of 220 nmolO_2/min/mg protein.

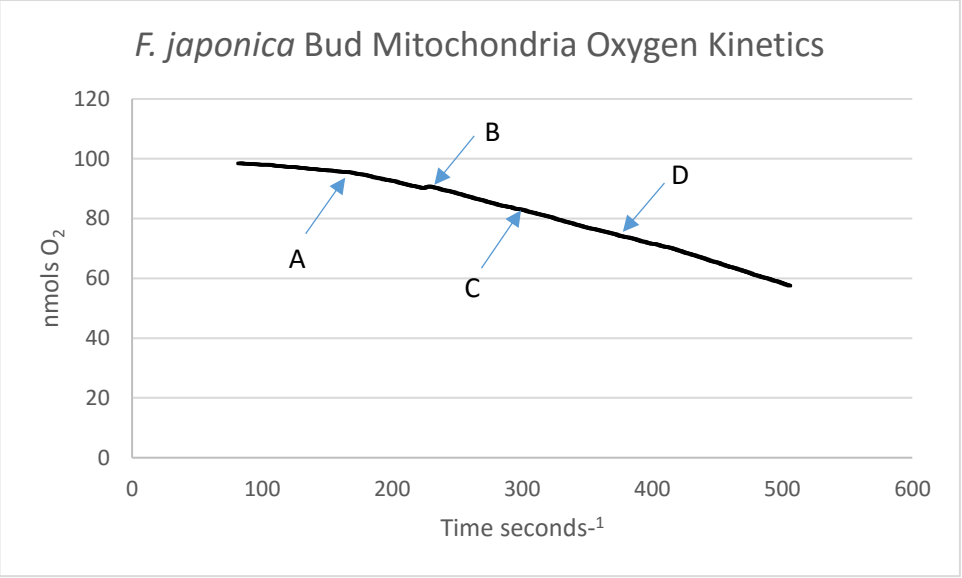

Figure 3-4 Graph showing *F. japonica* bud mitochondria oxygen kinetics. A – NADH, B – CCCP, C – Succinate rate of 0.113 nmolO2/min, D – Ascorbate, TMPD, rate of 0.138 nmolO2/min.

F. japonica samples which were used for oxygen electrode analysis in Figure 3-4 were crude mitochondrial preparations from *F. japonica* shoot and bud samples collected from the area surrounding the University of Sussex (or 'wild' sample), as previously described. The hypothesis was that the *F. japonica* mitochondria would contain a large amount of highly active mitochondria due to

the fact that the plants grow at such a rapid rate in the early growth stages (discussed in section 1.2). The point marked A in Figure 3-4 indicates the addition of NADH, followed by the uncoupler CCCP at mark B. At this point on the graph there is a small stimulation in rate compared to that of the very low rate seen with the addition of NADH. A much larger stimulation of rate would be expected if the mitochondria were intact, as CCCP should allow the rate to increase via uncoupling of the chain and allowing ions to pass freely through the mitochondrial membrane.

At mark C, the addition of succinate is made. No stimulation of rate is detected, with the initial rate of 0.113 nmolO_2/sec or a specific activity of 19.71 nmolO_2/mg/min being relative to the rate from the B mark on the graph. At mark D ascorbate is added, followed swiftly by TMPD, eliciting a small increase in oxygen reduction rate to 0.138 nmolO_2/sec, or a specific activity of 24.07 nmolO_2/mg/min. This maximum rate achieved is at a level almost 10 fold lower than the rate achieved by the *A. maculatum* mitochondria and was typical of the data gained in this set of experiments with the *F. japonica* mitochondrial samples.

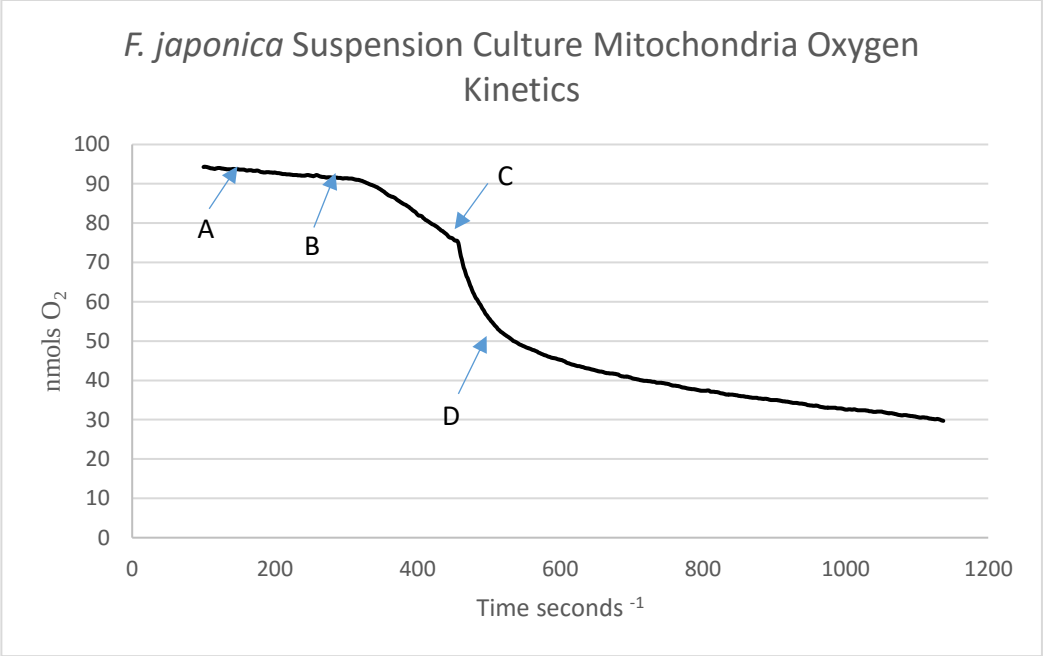

Figure 3-5 Graph showing *F. japonica* suspension culture mitochondria oxygen kinetics. Additions marked: A – glucose B –ascorbate, rate of 0.115 nmolO2/sec, C – TMPD, rate of 0.398 nmolO2/sec, D – KCN.

Figure 3-5 shows an oxygen electrode trace with a crude mitochondrial sample isolated from suspension grown *F. japonica* cells. Mark A shows the addition of glucose, which shows no significant increase in oxygen reduction rate from the auto-oxidative rate. Mark B indicates the addition of ascorbate, which initiated a rate of 0.115 nmolO_2/sec or 56.46 nmolO_2/mg/min. When TMPD was added to the chamber at mark C, the oxygen reduction rate increased to 0.398 nmolO_2/sec, or 195.56 nmolO_2/mg/min. TMPD is an artificial electron donor able to feed electrons into cytochrome c oxidase, or complex IV of the electron transport chain. In this case, ascorbate reacted strongly with the cell suspension, resulting in a considerable stimulation of rate, which was enhanced by the addition of TMPD to the chamber. At mark D, KCN was added to the chamber, which eventually slows the rate of oxygen reduction in the chamber. This led to the investigation of the relationship between the MS media and ascorbate, as the results were very different to those seen with other *F. japonica* mitochondrial samples.

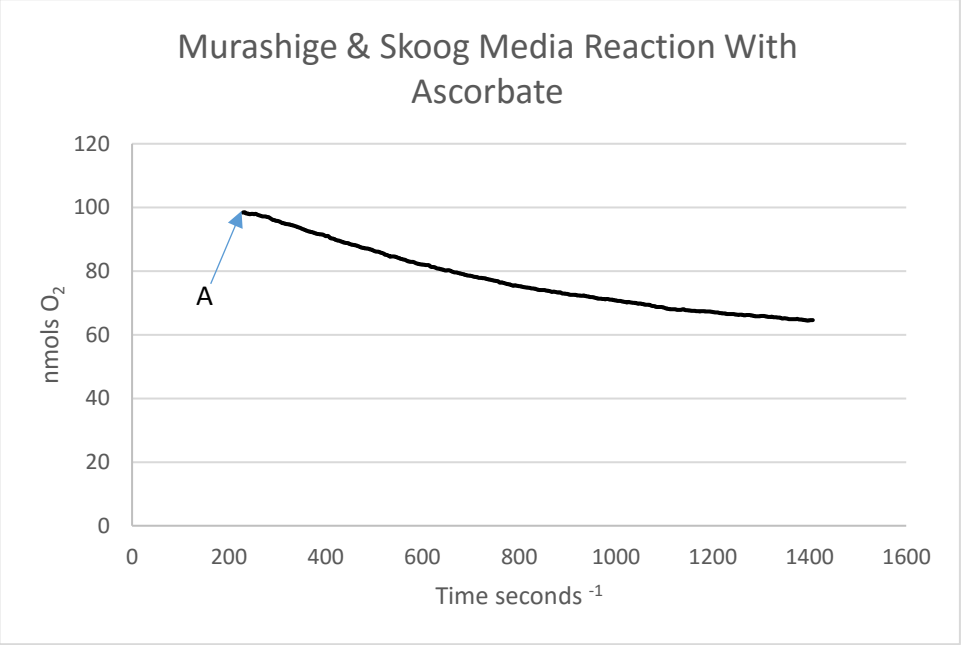

Figure 3-6 Graph showing reaction of MS media with ascorbate. A – addition of ascorbate. Rate of 0.029 nmolO2/sec

To investigate the large rate increase when ascorbate was added to the reaction mixture, the experiment was repeated with the chamber containing only the MS media with the addition of ascorbate, with the hypothesis that the ascorbate was

reacting with the growth media for the suspension cells. This proved to be the case, as the addition of ascorbate to just the MS media did indeed generate a rate, proving that the data generated with the isolated mitochondria generated from the suspension cultures were unreliable. The suspension culture mitochondria were subsequently isolated, washed, and resuspended in plant media A, which was the buffer in which the bud isolated mitochondria were assayed. The suspension generated mitochondria proved to be largely unstable after washing and resuspension in plant media A, therefore the data gathered with the oxygen electrode proved to be inconsistent.

3.5 Polyacrylamide Gel Electrophoresis

3.5.1 Sodium Dodecyl Sulphate - Polyacrylamide Gel Electrophoresis (SDS-PAGE)

In an attempt to ascertain the composition of the mitochondrial respiratory chain from *F. japonica*, given the low respiratory rates obtained in the above data (as observed in Figure 3-3 through Figure 3-6) SDS-PAGE was undertaken. Crude samples from *F. japonica* mitochondrial isolations were prepared for Sodium Dodecyl Sulphate - Polyacrylamide Gel Electrophoresis (SDS-PAGE). These were electrophoresed under the same conditions as mitochondrial samples prepared from *A. maculatum* spadices and comparisons drawn between the two. An example of an SDS-PAGE gel containing both *F. japonica* and *A. maculatum* samples is presented in Figure 3-7.

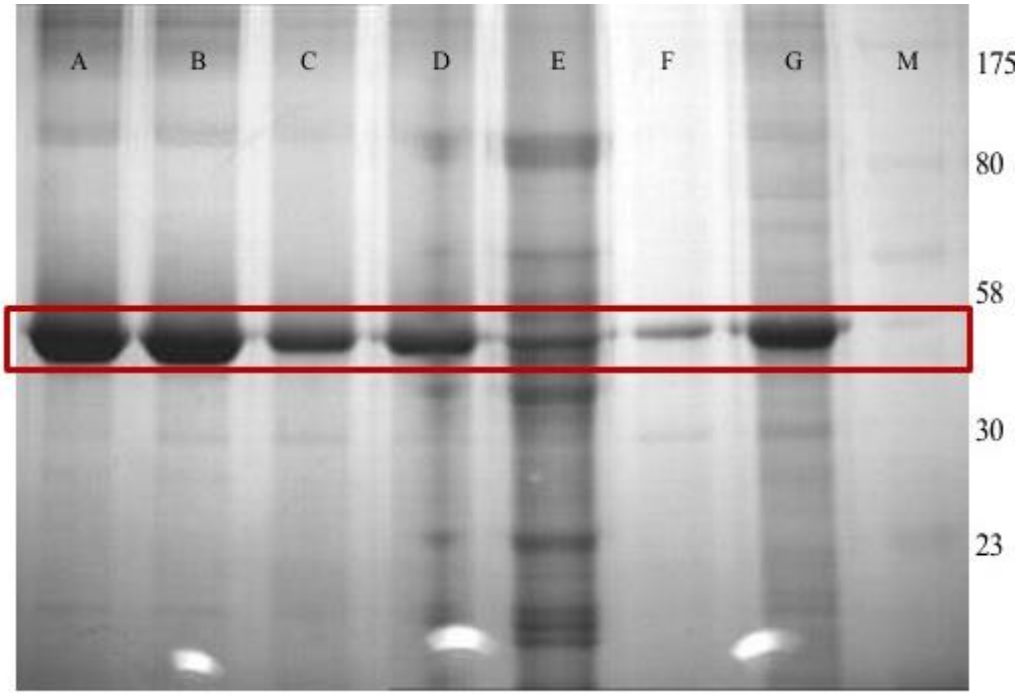

Figure 3-7 10% SDS-PAGE. A & B – Supernatant taken from final centrifugation during *F. japonica* wash stage during bud mitochondrial preparation. C & D – crude mitochondrial fraction from *F. japonica* bud mitochondrial preparation. E – *A. maculatum* purified mitochondrial sample. F & G – *F. japonica* crude mitochondria prepared from suspension cultures, 150μg and 1mg protein respectively. M – Marker proteins, numbers reprehensive of weights in kilodaltons. Red box highlights strong bands at approximately 46 kDa.

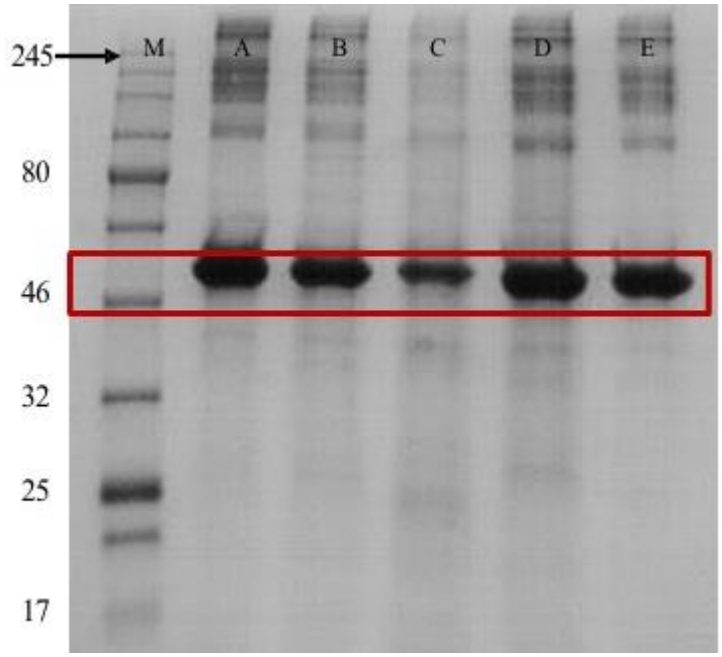

Figure 3-8 10% SDS-PAGE. A & B – crude fraction taken from *F. japonica* stem mitochondrial preparation. C– crude fraction from *F. japonica* leaf mitochondrial preparation. D & E – crude mitochondrial fractions from *F. japonica* cells grown in suspension. M – marker proteins, numbers reprehensive of weight of proteins in kDa.

As highlighted in Figure 3-7, a large band is present in all samples at approximately 46 kDa, however it is not as prominent in relation to the total protein in lane F, which represents the *A. maculatum* purified protein sample. In all lanes representing *F. japonica*, including the supernatant samples (A & B), this band is extremely prominent and represents by far the highest proportion of the protein which is visible from the sample. In comparison to the *A. maculatum* sample, it was therefore clear that there was a different pattern of distribution and/or composition of protein in the *F. japonica* samples.

Figure 3-8 illustrates that all samples from *F. japonica*, whether prepared from fresh plant material (lanes A-C) or from cell suspension (lanes D & E), contain this enriched band at approximately 46 kDa. In light of this, different forms of electrophoresis were attempted in order to investigate the protein complement in the *F. japonica* mitochondrial samples and to probe the variation between the *F. japonica* and *A. maculatum* species mitochondrial samples.

3.5.1 Blue Native PAGE

In an attempt to quantify the activities of each of the mitochondrial complexes within each of the mitochondrial samples, Blue Native PAGE (BN-PAGE) was performed with mitochondrial samples from *F. japonica* and *A. maculatum*. This method is used to separate whole respiratory chain complexes from mitochondrial samples with the use of a mild detergent which can give an indication of the size of each complex. Gradient gels were produced initially using the protocol detailed in section 2.6.3. Reproducibility was a major issue, as the gels tended not to be uniform in the gradient, polymerise within the gel casting equipment or not polymerising at all. A large amount of time was spent attempting to optimise the gradient gel production, including adjusting polymerisation temperature, altering acrylamide percentages and APS/TEMED volumes and polymerisation speed. Sample preparation for the homemade gradient gels also proved to be difficult, as the correct detergent to protein ratio had to be optimised, along with experimenting with sample storage conditions, to reduce streaking and ensure definition within the gel. In light of these factors, pre-made gradient gels

were bought in from Expedeon to ease some of the difficulties involved, increase reproducibility and to save a large amount of time.

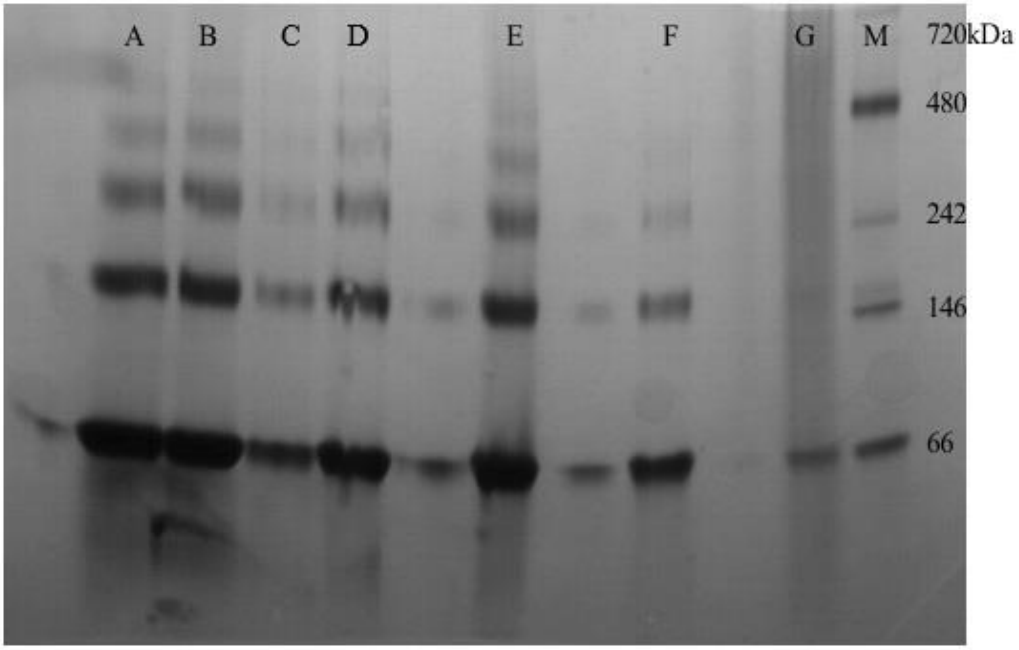

Figure 3-9 BN-PAGE gradient gels purchased from Expedeon. A-F – samples derived from *F. japonica* bud mitochondrial preparations. A – Filtrate, B – Pellet, C – 1st Supernatant, D – 2nd pellet, E – 2nd supernatant, F – crude pellet, G – rat liver mitochondrial sample, M – protein weight markers, sizes are represented in kDa.

Figure 3-9 represents a BN-PAGE 3-16% gradient gel which was purchased from Expedeon. This gel shows much increased separation of mitochondrial samples, reducing the streaking and eliminating the reproducibility issues associated with the homemade gradient gels. The samples on this gel were taken from various stages of the purification protocol, including supernatants and resuspended pellet fractions. Lane F contains the crude mitochondrial sample from the *F. japonica* bud preparation which was the most relevant to the fully purified *A. maculatum* mitochondrial samples with which comparisons were drawn throughout. The total protein decreases as the purification proceeds through the lanes A – F, indicated by the decrease in staining intensity, which would be expected as unwanted cellular fractions and debris are removed from the sample. Lane G contains a sample of solubilised rat liver mitochondria which could have been solubilised using a suboptimum ratio of detergent to protein, or

the lane of the gel overloaded with sample, causing the steaking of peptides throughout the gel.

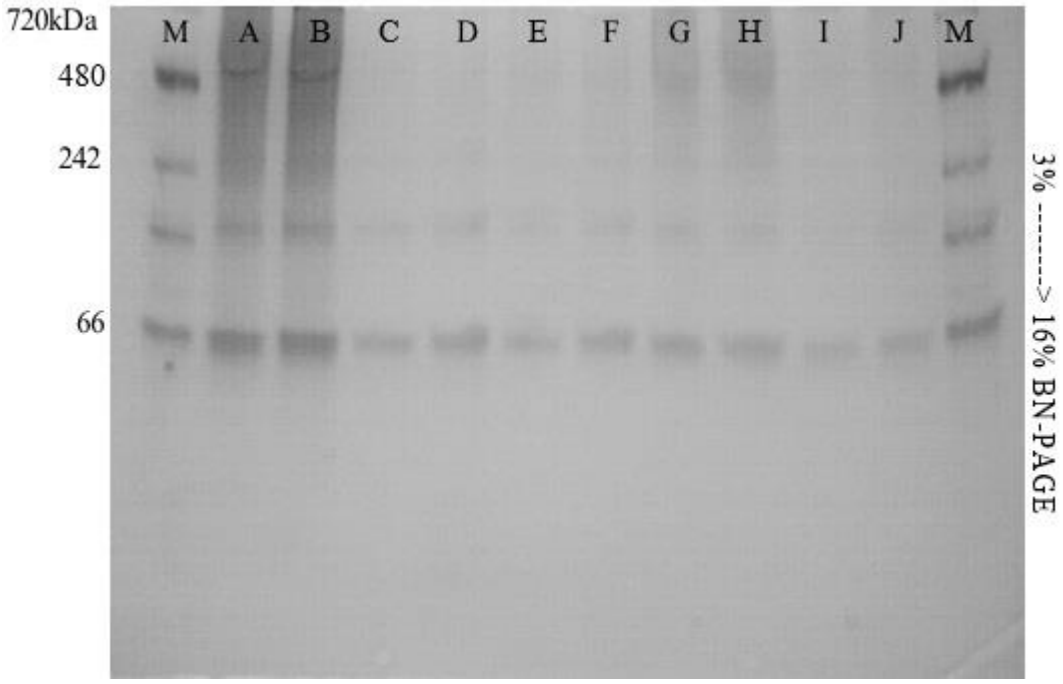

Figure 3-10 Increasing reproducibility with bought in gels. M – protein weight marker, A & B – crude mitochondria from *F. japonica* leaf preparation 10 & 20µl respectively, C -F – crude mitochondria from two *F. japonica* late bud preparations 10 & 20µl respectively,

Figure 3-10 represents an Expedeon BN-PAGE 3-16% gradient gel with samples from various preparations of *F. japonica* mitochondria. This coomassie stained gel shows much greater reproducibility than the initial tests using both homemade and prefabricated gels. The samples also show that the mitochondria from all of the *F. japonica* sources, bud, leaf and suspension, have the same features and band pattern – indicating that the cells grown in suspension have similar mitochondrial characteristics to those isolated from the plants themselves.

3.5.2 Histochemical staining

Histochemical staining was achieved with further processing of the BN-PAGE gels. Histochemical staining involved formation of insoluble precipitates within the polyacrylamide matrix of the gel, which would indicate areas of activity and give an idea as to the levels of activity of each complex. This technique

therefore gives a functional analysis of the activity of each of the isolated complexes [113] and is described in detail in 2.6.3.5.

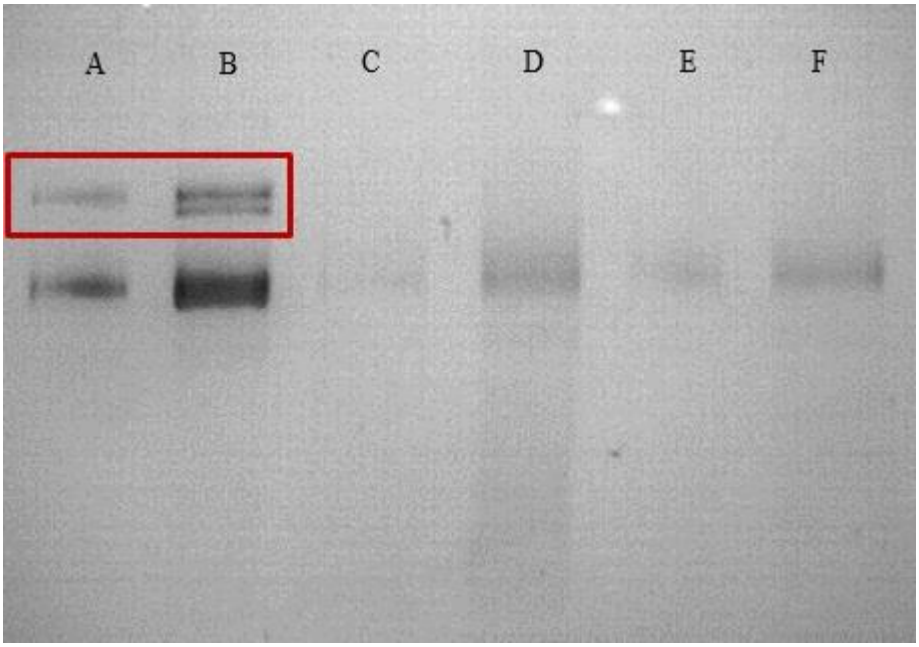

Figure 3-11 BN-PAGE gel; post histochemical staining for NADH ubiquine oxidoreductase(Complex I) A/B– 5µl/10µl fresh A. maculatum mitochondrial isolation, C/D - 80℃ stored A. maculatum sample 5µl/10µl, E/F - 20℃ stored A. maculatum sample 5µl/10µl. Highlighted area indicates higher molecular weight peptides in the freshly harvested mitochondrial samples.

The gel image shown in Figure 3-11 compares differing amounts of *A. maculatum* crude mitochondrial sample having been prepared for BN-PAGE after varying storage conditions. Lanes A & B show the greatest staining, due to the NADH ubiquinone oxidoreductase (complex I) reaction forming a build-up of insoluble formazan at the region corresponding to the enzyme. This indicated that the freshly isolated *A. maculatum* mitochondria had the most active complex I in comparison to the cold stored or frozen samples, which would be expected as studies have shown changes in oxidation rate of mitochondria after cold storage [129]. Changes in molecular ordering of lipids within mitochondrial membranes of plants have also been observed under chilling conditions [130]. Lanes A & B also both contain a small amount of protein, indicated by the staining above the main band highlighted in the above figure. This could indicate that the freshly isolated mitochondria are able to retain some of the associations with surrounding proteins, resulting in a separate, slightly higher weight when the sample is run on a BN-

PAGE gel due to the non-denaturing conditions. This is in contrast to the deep frozen (- 80℃) or frozen samples (-20℃) which may have lost these associations whilst in storage and therefore display only one band when the sample is electrophoresed on the gel.

All lanes in Figure 3-11 show a common band, indicating that all samples have some functional complex I. The size of the entire complex has been established at approximately 1 MDa in higher plants [131]. Analysis of NADH dehydrogenases from model organisms such as *Arabidopsis thaliana* and *Oryza sativa* (rice) via BN-PAGE coupled with mass spectroscopy have indicated that there are approximately 25-30 different subunits which comprise complex I in higher plants[132]. The association of these subunits within the complex when separated within a BN-PAGE gel can be changed with variation of the type and amount of detergent present whilst solublising the complex from the mitochondrial membrane [133]. As described in 2.6.3, the detergent n-Dodecyl-β-D-maltopyranoside (DDM) was chosen and several different concentrations trialled to ensure the most defined bands within each sample.

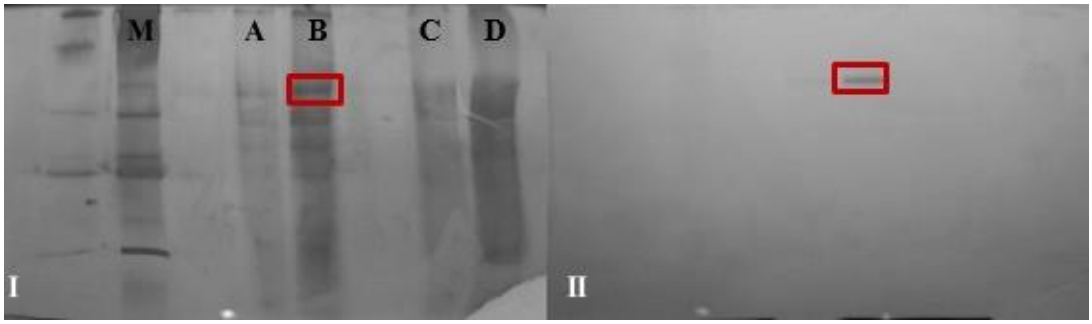

Figure 3-12 *F. japonica* crude mitochondrial isolate samples BN-PAGE gel, left (I), post histochemical staining for NADH dehydrogenase (Complex I, right, II). Lane A & B, gel A, representing crude mitochondrial sample from *F. japonica* buds stored at -80℃, 10 & 20µl respectively. Lanes C & D representing crude *F. japonica* bud mitochondrial samples stored at +4℃, 10 & 20µl respectively. Boxes highlight area on gel I which corresponds to the histochemical complex I activity on gel II.

Figure 3-12 gives an example of the initial BN-PAGE gel (I) and the histochemical staining for activity of complex I on a corresponding gel (II), using *F. japonica* crude mitochondrial samples. The marker proteins of the BN-PAGE gel on the left of Figure 3-12 appear to give an assumed weight of the reaction

centre to be between 1048 kDa and 720kDa, which corresponds to the 1 MDa estimated size of complex I [132]. The samples which had been flash frozen in liquid nitrogen and stored at -80℃ retained activity in comparison to the samples which had been held at +4℃ for the same period of time, with the higher concentration of sample giving a stronger visible reaction in gel B, corresponding to lane B on gel I, however in comparison to the *A. maculatum* sample the reaction is visibly weaker. This may be due to the lower amount of complex I in an equivalent protein concentration, as the *A. maculatum* mitochondria were fully purified in comparison to the *F. japonica* mitochondrial samples which were taken from the crude stage of the purification protocol.

Histochemical analysis of succinate dehydrogenase (complex II) and cytochrome oxidase (complex IV) were attempted but without any success. This could be due to low levels of these complexes in the mitochondrial samples from the *F. japonica,* although the technique was also tested using *A. maculatum* purified mitochondria, also without success. The original study detailing the techniques based the optimisation upon isolated mitochondria from sunflowers [113] and it may be the case that these techniques would need to be amended and optimised for different individual species of plant mitochondria for best results.

3.5.3 Two dimensional BN-SDS PAGE

Two dimensional BN-SDS PAGE was also utilised to separate the mitochondrial complexes into their components, in order to determine their composition. With the use of staining techniques, this also gave a rough estimate as to the abundance of each component within the complexes. As with the other variations of PAGE presented in this chapter, *F. japonica* & *A. maculatum* samples are compared.

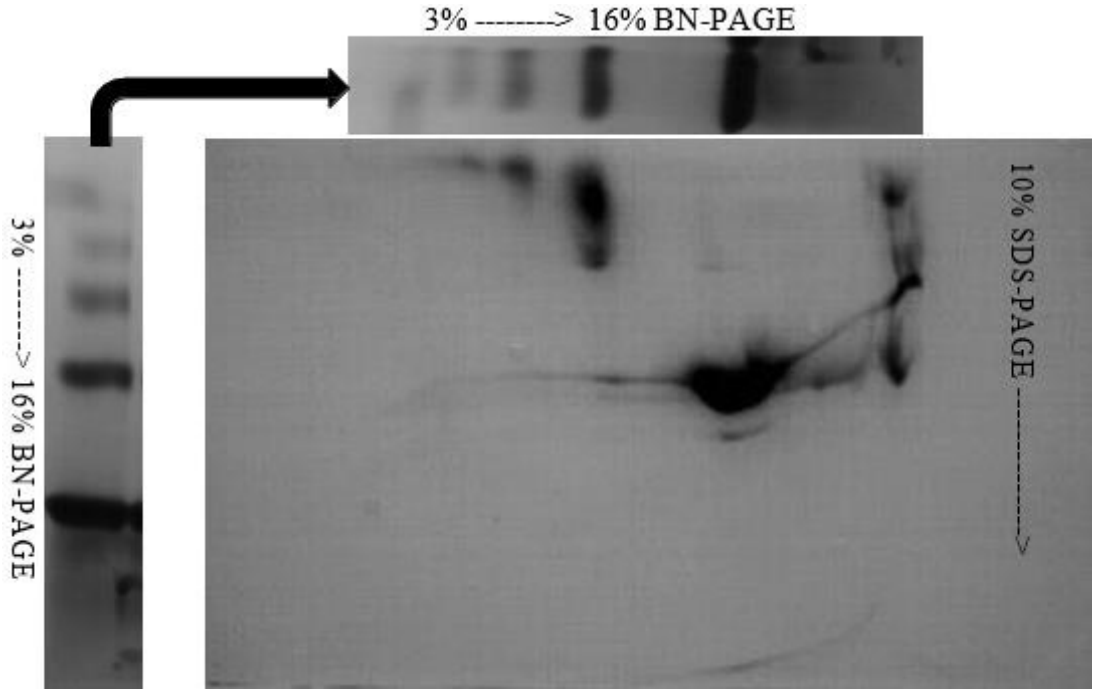

Figure 3-13 Example of second dimension BN/SDS-PAGE using *F. japonica* filtrate sample originating from bud material. The BN-PAGE gel is electrophoresed and the lane containing sample is cut from the BN-PAGE gel & prepared to be set into the SDS-PAGE gel of the second dimension as shown.

Once a BN-PAGE gel has been run in the first dimension, the lane containing the sample of interest was chosen and cut from the gel and pre-incubated in buffer before being set into an SDS-PAGE gel in the orientation illustrated in Figure 3-13. The gel is then electrophoresed in the second dimension as described in 2.6.3, which causes the complexes in the BN-PAGE gel strip to enter the second dimension gel and separate due to the presence of anionic detergent sodium dodecyl sulphate (SDS).

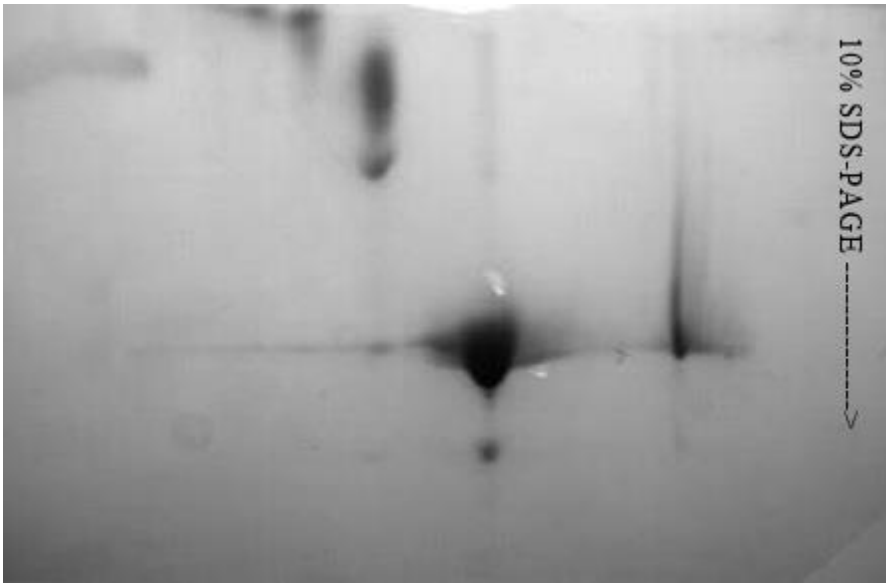

Figure 3-14 *F. japonica* filtrate sample originating from bud material improved BN-PAGE gel. Optimising run conditions gave clearer separation in comparison to Figure 3-13.

Figure 3-14 shows some progression in this technique, where the sample can be seen to have separated in a more distinct manner, with slightly more defined areas in the second dimension. Both of the gels depicted in the figures had been silver stained (methodology described in chapter 2), which is a much more sensitive method of protein staining in comparison to coomassie based staining, able to detect protein in as little as the low nanogram range [134].

In these gels, filtrate samples were used as they contained the greatest amount of protein from all of the fractions taken from the mitochondrial isolation from the *F. japonica* suspension cultures. Tricine SDS-PAGE was used as an alternative to glycine SDS-PAGE for the second dimension as it is preferable for the resolution of low molecular weight proteins and superior in the separation of proteins in 2D SDS/BN-PAGE gels [135].

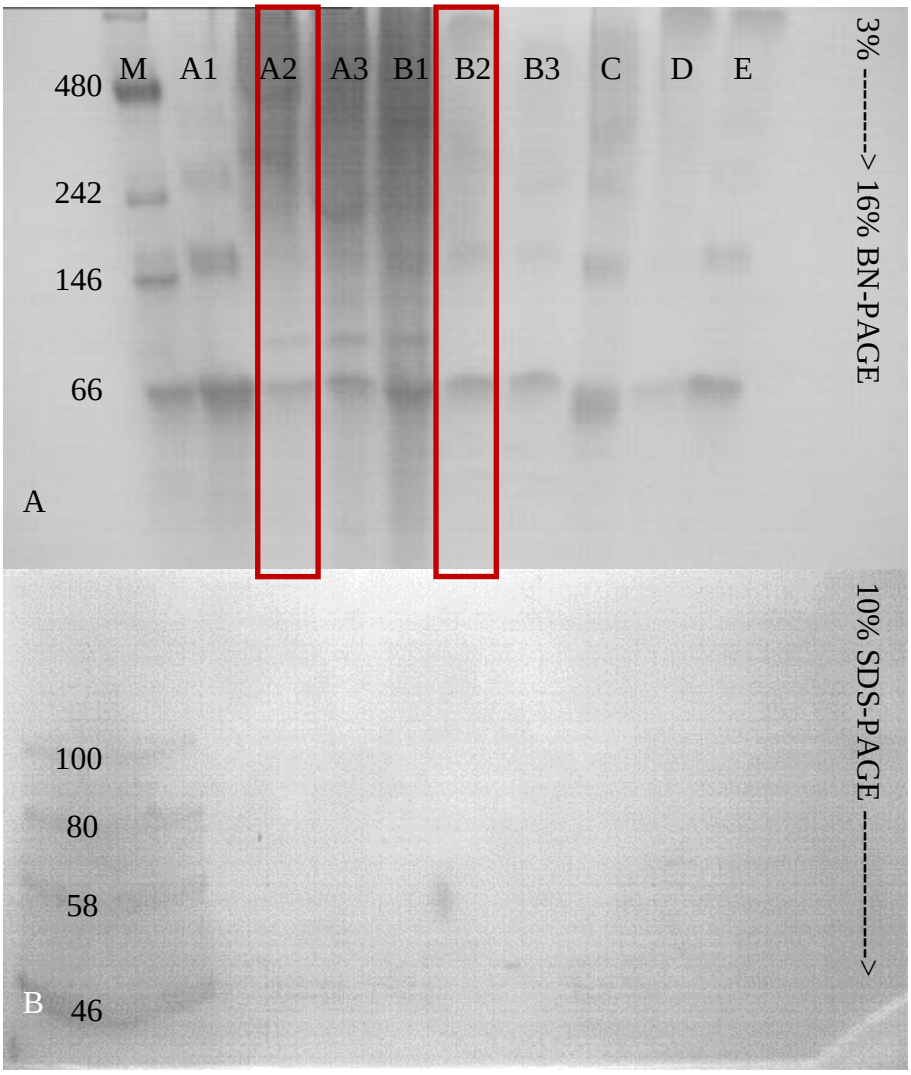

Figure 3-15 – GEL A: First dimension BN-PAGE gel – M – Marker proteins, A1 – non solubilised *A. maculatum* mitochondrial samples, A2 – digitonin solubilised *A. maculatum*, A3 – DDM solubilised *A. maculatum*. B1 – non solubilised *F. japonica* bud mitochondria sample, B2 – digitonin solubilised *F. japonica* bud mitochondrial sample, B3 – DDM solubilised *F. japonica* bud mitochondrial sample. A2 & B2 highlighted indicate lanes taken for 2D SDS-PAGE. GEL B – BN-SDS 2D-PAGE representing lane A2 in the second dimension.

Figure 3-15 gel A illustrates *A. maculatum* and *F. japonica* mitochondrial samples prepared for BN-PAGE without addition of detergent (A1, B1), or solubilised using the detergents DDM (A2, B2) or digitonin (A3, B3). It was found that for both *A. maculatum* and *F. japonica* that digitonin was the better of the two detergents for clarity of band separation within the gel and these lanes are highlighted in gel A. Both of the species mitochondrial samples were electrophoresed on the same gel so as to ensure identical conditions for comparison

of their separation profiles. The *A. maculatum* A2 lane appears to have a higher abundance of higher molecular weight proteins in comparison to that of the *F. japonica* B2 lane, although these are present in a 'streak' and not in defined bands. The streaking could be due to overloading of the protein, as the *A. maculatum* samples were often of high (<30mg/ml) protein concentration and required dilution before preparation for BN-PAGE. The digitonin solubilised *F. japonica* mitochondrial sample, B2, also contains streaking and contains visibly less protein than the *A. maculatum* sample, A2.

Both gels in Figure 3-15 are Coomassie stained, as the silver staining technique described in 2.6.2.2 is not compatible with 2D analysis or mass spectroscopy, meaning that proteins which are present in low concentrations are not viable on these gels. Gel B represents the 2D SDS/BN-PAGE of the A2 lane from gel A and the resulting protein spots in the second dimension. The equivalent 2D gel was run containing the B2 lane from gel A and the protein spots from both of these gels were compared and analysed using mass spectroscopy.

3.6 Conclusion

This chapter describes the development and optimisation of *F. japonica* mitochondrial isolation from buds, leaves and cell suspension. As discussed, many attempts were made to fully purify mitochondria from these samples, all of which were deemed unsuccessful as no clear respiratory activities were obtained, as is displayed in Figure 3-3 through Figure 3-6. The main issue affecting purification was the amount of tissue or suspension available for the isolation as a very large initial amount of sample was required. At each stage of the purification technique a large portion of the sample was lost, resulting in a very small yield of mitochondria, even at the crude stage. One improvement which could be made would be to adapt the percoll gradients protocol described in section 2.1.2 in order to increase the yield of *F. japonica* purified sample at this stage. However, put into perspective with the further results in this chapter, the yield of *F. japonica* mitochondria, albeit low, may be a true reflection of the abundance of mitochondria

in the cell. Morphometric evidence points to an overall smaller number of mitochondria in the *F. japonica* cells than anticipated, especially in comparison to other tissues, such as *A. maculatum* spadices. This data can be seen in later chapters.

The oxygen electrode was used to analyse the activity of the mitochondrial samples when obtained from these various sources and the results compared to that of *A. maculatum* mitochondria, shown in Figure 3-3. Surprisingly, the *F. japonica* bud mitochondria had very little respiratory activity, where large rates could have been expected due to the very fast growth of the plant at this stage – the buds were anticipated to be full of mitochondria which would have been generating the energy necessary for this type of growth. Mitochondria isolated from the *F. japonica* suspension cultures seemed initially to have a much greater activity in comparison to the bud mitochondria, however as seen in Figure 3-6, the MS growth media was reacting with the substrates in the oxygen electrode chamber. Therefore the results were unreliable and further testing of the mitochondria via resuspending in plant media A for analysis proved impossible due to the instability of the organelles.

SDS-PAGE was performed on the mitochondrial samples and indicated a very similar protein band pattern in *F. japonica* from all sources. This same pattern was observed when the *F. japonica* samples were run on the same gel as *A. maculatum* mitochondrial samples, ensuring that the protein pattern was not an artefact of the electrophoresis. All of the *F. japonica* samples proved to have a prominent band at approximately 46 kDa in comparison to that of the *A. maculatum* sample, which had a much less pronounced band at this region. A literature search of known mitochondrial proteins of approximately 46 kDa was performed, which indicated a potential NADH dehydrogenase [136], or potentially a part of the mitochondrial protein import apparatus [137].

To further explore the mitochondrial samples, BN-PAGE was utilised. This technique was developed with increasing reproducibility, allowing the separation of the respiratory complexes in their native form. This allowed the comparison of different solubilisation techniques, which were eventually utilised with histochemical staining. The histochemical staining for complex I in the respiratory

chain confirmed the presence of this complex and also indicated that the *A. maculatum* samples contained a larger concentration of complex I in comparison to the *F. japonica* samples. The histochemical staining of the other complexes was not successful. This may be due to the fact that full optimisation of this technique was not undertaken in this series of experiments.

2D BN-PAGE development allowed for the separation of the complexes into their constituent proteins and allowed comparisons to be drawn between *A. maculatum* and *F. japonica* mitochondrial compositions. This work suggested that mass spectroscopy would be a useful technique to use in this case in order to identify and quantitate the differing protein spots within the gels.

4 Transmission Electron Microscopy

4.1 Introduction

Transmission electron microscopy, or TEM, is a powerful technique allowing the visualisation of the ultrastructures of both biological and inorganic materials. The first prototype electron microscope was built in the 1930's and had roughly the same magnification power as an ordinary light microscope [140]. As technology continued to advance, so did both the magnification levels and the resolving ability of the electron microscopes. The main components of the TEM have not significantly changed since the 1930's – however, lens, circuitry and voltage stability have all greatly improved [141].

The use of a beam of electrons as an illumination source greatly improves the resolution attainable in comparison to that of light-based magnification resolution. The resolution of a light microscope is limited by the wavelength of visible light, which is in the range of approximately 390-700 nm [142]. The electron microscope produces a beam of electrons which acts as a wave and has a wavelength of less than 1nm. This much shorter wavelength enables the distinction of much finer detail within a sample and at much greater magnifications.

The basic components of a TEM microscope are the electron gun, electromagnetic lenses, specimen rod and the observation level. The electron source is a filament of tungsten which is heated via the application of high voltage and electrons are emitted from the end of the wire in a process referred to as thermionic emission. The filament is within a housing known as a cathode gun, from which the electrons are emitted and pass to an anode plate with a small aperture, which acts to focus the electron beam to pass down the TEM column [143]. Electromagnetic lenses focus the beam of electrons inside the column of the microscope, which is under a high vacuum to allow the electrons to be transmitted without any unwanted collisions with other molecules such as gases or water [144].

The electron beam is then focussed upon the sample, which is inserted into the microscope column via a specimen rod. Sample preparation for TEM is covered in detail in chapter 2, although a brief outline will be presented here. It is essential that the sample is very thinly sectioned, less than 100 nm thickness, in order to allow the electron beam to pass through the unstained areas and form an image on the phosphor-coated florescent screen for imaging. Adjustments are made to the currents in the electromagnets controlling the electron beam to change the focus or magnification of the image. A 'low mag' mode is used initially to centre the electron beam on the sample to find a general area of interest and also to pre-irradiate the sample on the support grid. Pre-irradiation helps to prevent any damage to the thin sample by the electron beam over-heating and potentially causing splits in the specimen. Figure 44-1 is an image of the Hitachi -7100 TEM used in this project with some of the key components labelled. Images are acquired digitally from the TEM via the use of an axially mounted Gatan Ultrascan 1000 charged coupled device (CCD) camera.

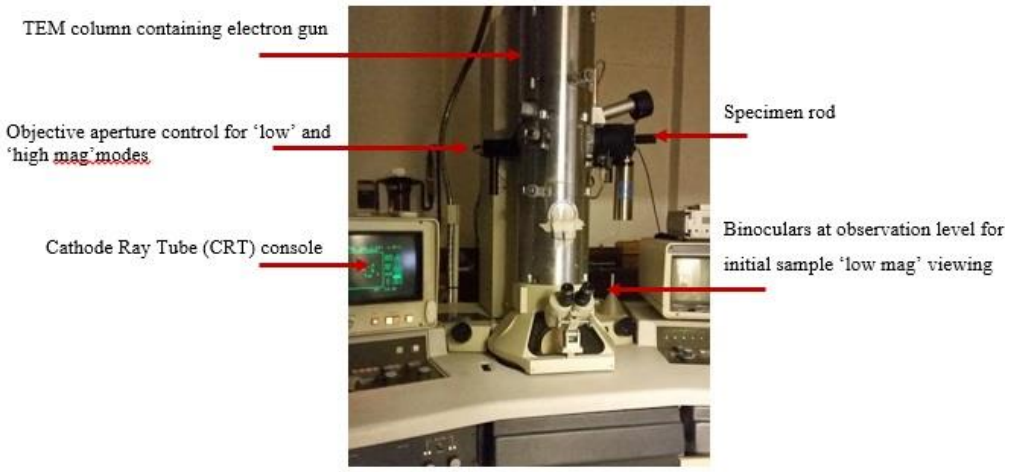

Figure 44-1 The HITACHI-7100 TEM microscope used for this project.

The impetus for the use of TEM in this project was to determine the amount, size and distribution of mitochondria throughout cells of *F. japonica* from various sources. Initially, this chapter examines samples of *F. japonica* early buds with the hypothesis that they would contain a large amount of mitochondria due to the extremely rapid growth rate exhibited at the early growth stage. Samples from *A. maculatum* spadices, which are known to contain a large amount of mitochondria in

order to produce heat during thermogenesis, were also investigated in order to provide a comparison to the *F. japonica* samples. Sections were also taken and prepared from *F. japonica* callus, as well as samples from *F. japonica* suspension cultures to determine any differences between cell or mitochondrial morphology in these differing sources of *F. japonica* cellular material.

4.2 Sample preparation

4.2.1 Preparation and fixatives

In order to prepare the plant material for TEM, the *F. japonica* bud material and the *A. maculatum* spadix material was cut into small rough cubes, approximately 2 mm^3 before being introduced to a fixative solution. The sectioning procedure can be visualised in figure 3 chapter 2, with detailed methodology described in section 2.1. The *F. japonica* callus material and *F. japonica* suspension cell material preparation for TEM are described in section 2.2.1.2.

The fixative used at the initial stages was 2.5% (v/v) glutaraldehyde, which effectively fixes proteins in place by forming cross-links or methylene bridges between nitrogen atoms of proteins very rapidly [145]. The buffer used throughout was sodium cacodylate, either at 0.05 M or 0.1 M concentration in order to maintain stable pH within the samples during fixation and preserve the ultrastructure of the cells. A secondary fixation was accomplished with the use of 1% (v/v) osmium tetroxide in sodium cacodylate buffer. This was applied to the sample after a thorough rinse in buffer to remove any excess glutaraldehyde. Osmium tetroxide is an effective fixative of lipids within a sample via oxidation of unsaturated bonds of fatty acids, producing metallic osmium. Osmium is electron dense and therefore added contrast to lipid rich areas, such as membranes within the sample.

4.2.2 Dehydration and epoxy resin infiltration

Once samples had been fixed and rinsed in distilled water thoroughly, they were dehydrated in stages through an ethanol series – 50%, 75% and 100%. This was done in order to remove any residual water in the sample, as any water molecules

introduced into the TEM microscope would interfere with the electron beam and cause blurring of the image. The samples were then rinsed twice in propylene oxide in order to remove any residual ethanol from the dehydration stages. A 50/50 solution of propylene oxide and epoxy resin was prepared and the samples were incubated in this solution overnight to aid the integration of the resin into the samples. This was followed by several changes of pure resin for each sample. The samples were considered to be ready for polymerisation after approximately 48 hours post resin infiltration. The resin containing the sample was polymerised in an oven set at 60℃ for 24 hours, after which time the samples were fully embedded in the resin and ready for sectioning.

4.2.3 Sectioning and staining of samples

Initial sectioning was achieved using a razor and glass knife to trim away excess resin from around the embedded sample. Once as much excess resin had been removed as possible, an ultra-microtome was used to prepare samples from the sample in the region of 60-100 nm thick. The sections were cut from the resin block using a diamond blade with an attached boat containing distilled water. The samples were then picked from the boat and placed onto supports and were allowed to dry. All sectioning of samples throughout this project was performed by Dr. Julian Thorpe.

Once the sections were dried onto the support grids, they were further stained using 0.5% (v/v) aqueous uranyl acetate for 1 hour. This was achieved by placing a drop of the uranyl acetate onto parafilm and placing the support grid with sample side down on top of the drop. The samples were then thoroughly rinsed and stained further with lead citrate for approximately 15 minutes. These stains offer more heavy metal into the sample and therefore provided greater contrast when viewing in the TEM.

4.3 Imaging of *F. japonica* bud sections

For initial imaging of *F. japonica* bud samples, sections were taken from the base, centre and tip of the bud, to determine whether there was a difference in cellular content in these three regions within the bud. Sectioning of the *F. japonica* buds and clarification of the regions can be seen in chapter 2.2.1.2 & visualised in figure 2-4.

Figure 4-2 Base *F. japonica* bud section fixed in 0.05M sodium cacadolyte buffer. 1000x magnification. Black arrows indicate cell membranes. White circles potential mitochondria. A – split in sample. B – aggregate of stain & possible artefact. Scale bar = 2μm.

Figure 4-2 is a representation of a typical low magnification image of a base section of a *F. japonica* bud sample. The cells generally contained large vacuoles,

with any organelles located within a small margin of cytoplasm near the cell membrane. The area depicted shows five visible potential mitochondria, highlighted by white circles, within this region. There is also an indication of the damage which can be caused during the sectioning and viewing of the samples, showed by a split in the section, marked A in this figure.

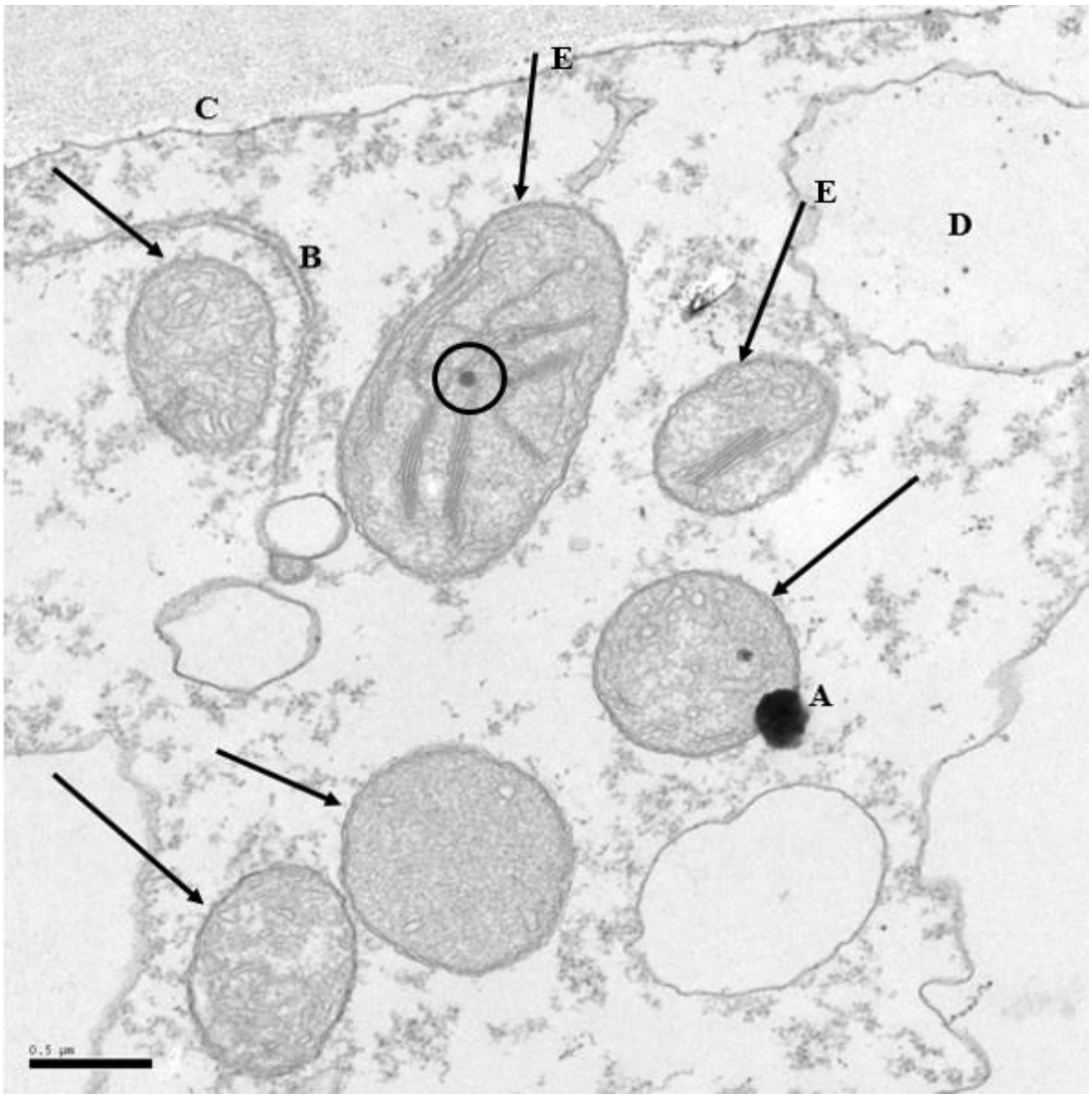

Figure 4-3 *F. japonica* bud base section - fixed in 0.05M sodium cacadolyte buffer. 5000x magnification. Black arrows indicate potential mitochondria. A – staining artefact. B – Possible rough endoplasmic reticulum. C – Cell membrane. D – Vesicle. E – Potential early plastid. Black circle indicates potential ribosome or lipid droplet. Scale bar = 0.5μm.

Figure 4-3 is a higher magnification image of a base section of an *F. japonica* bud sample. Potential mitochondria are marked with black arrows, with clear membranes and visible internal cristae. Again, these organelles are located within a

small margin of cytoplasm near the edge of the cell, with the cell membrane marked C in this image. Another organelle is marked B in this image which may be representative of rough endoplasmic reticulum, with potentially more free ribosomes present in the cytoplasm. D represents a vacuole within the cell. The organelles marked E in this figure show similar characteristics to the potential mitochondria marked with the black arrows, although the visible stacking of the membranes in these organelles could indicate the potential to mature into plastids – possibly into chloroplasts, where the stacked membranes would become thylakoid membranes involved in the light-dependent reactions of photosynthesis. If this was the case, the dense staining indicated by the black circle in the Figure 4-3 could be indicative of a ribosome or a lipid droplet within the chloroplast. At this stage of development it is difficult to distinguish with confidence between the potential mitochondria and the plastids/pro-plastids present in this sample.

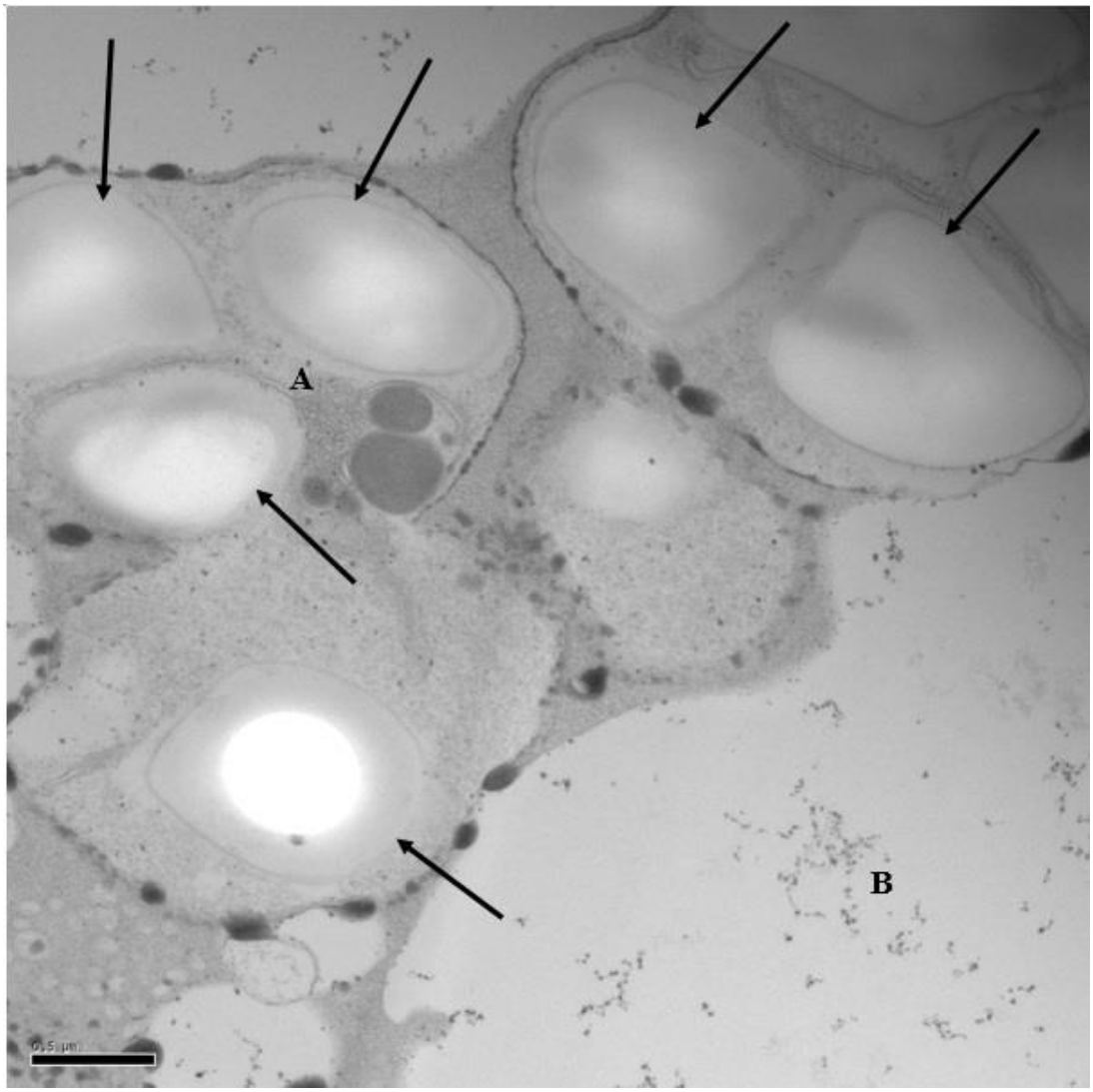

Figure 4-4 Centre *F. japonica* bud sample fixed in 0.05M sodium cacadolyte buffer. 5000x magnification. Black arrows indicate potential plastids. A – Golgi apparatus. B- Vacuole. Scale bar = 0.5 µm

Figure 4-4 is a representation of a typical image of a centre section of an *F. japonica* centre section of bud sample at 5000x magnification. The centre section sample shares the characteristic of containing organelles in the cells cytoplasm margin near the cell membrane, as seen in the base sample, Figure 4-3. Black arrows indicate potential pro-plastids which may become a number of different specialised organelles within the cell, for example leucoplasts or chloroplasts. The white areas within these plastids contain lipids or starch depending on the development or differentiation of the plastid, although the large white areas would indicate the probable development of these organelles into storage plastids. This is in comparison to the organelles marked E in Figure 4-3, which appear to have stacks of membranes indicative of chloroplast development. Marked A in this image are potential Golgi

apparatus which appear as a group of membranes located around the putative early chloroplasts. The area marked B indicates a large vacuole, which is characteristic of all of the *F. japonica* bud section samples. This image shows no clear indication of the presence of mitochondria, as was typical in the centre sections taken from the *F. japonica* buds.

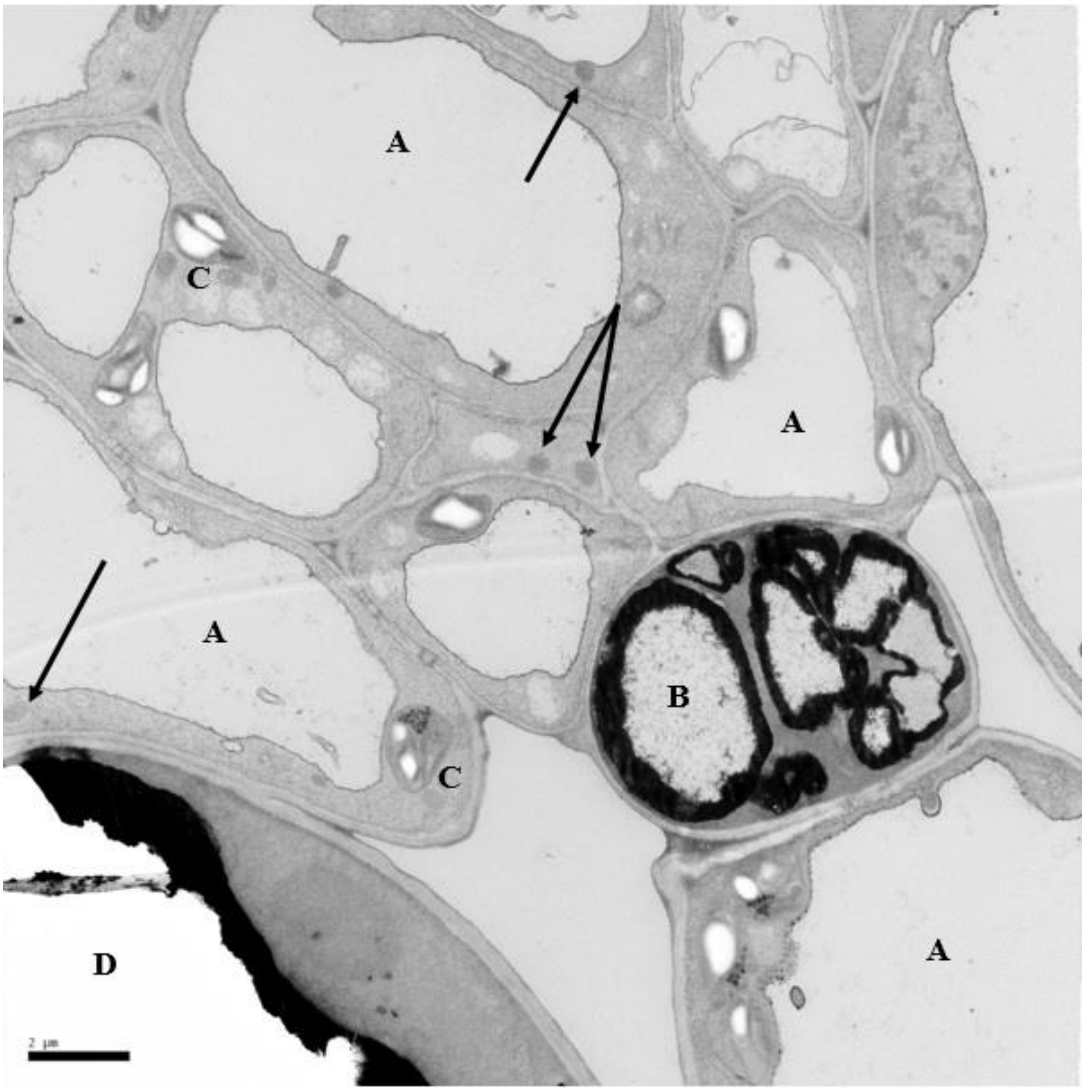

Figure 4-5 *F. japonica* tip bud sample fixed in 0.05M sodium cacadolyte buffer at 1000x magnification. A – large vacuoles (not all labelled) B – Lipid –dense storage vesicles. C – plastids/early chloroplasts. D – split in sample. Black arrows indicate potential mitochondria. Scale bar = 2 µm

Figure 4-5 is a representation of a typical low magnification (x1000) *F. japonica* bud tip sample. The image is dominated by the large vacuoles present in all visible cells, marked A and again the characteristic cytoplasm around the margins of the cells. It is common in plant cells to have a large central vacuole in order to

maximise the access of light harvesting organelles to the cell periphery, where maximum light energy could be harvested[146]. The marker B indicates an area which appears to contain darkly stained material. This could potentially indicate some storage vesicles, although taken in context with the rest of the image, it may be more likely that it is a cell which has been sectioned at a level, theoretically through the membrane, which is more heavily stained due to the high lipid content of the membrane. The marker C indicates putative pro-plastids, although not all (approximately 7) of these organelles are marked in this image. The black arrows in this image indicate potential mitochondria, which are noticeably few in number in comparison to the number of cells in this image.

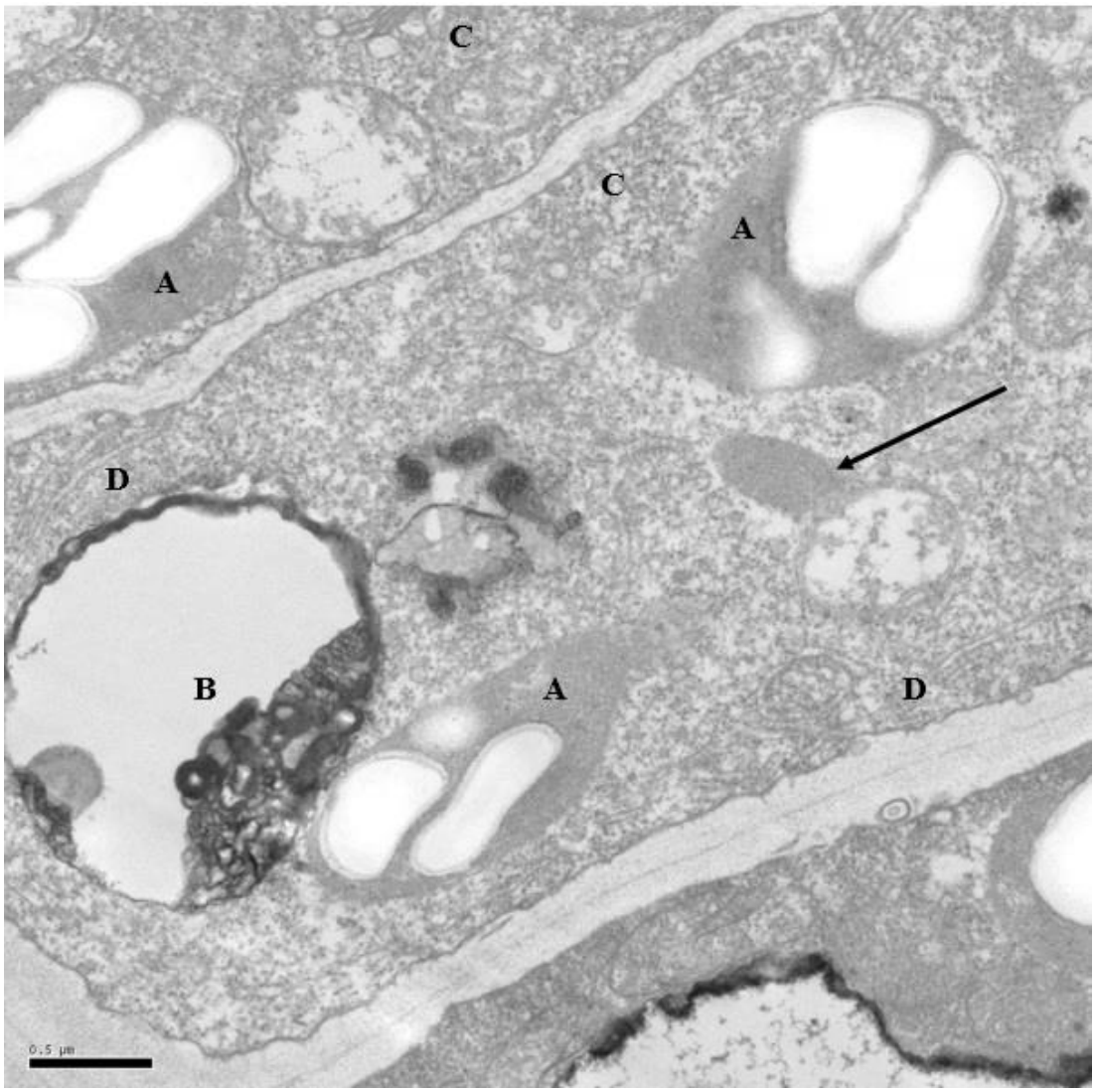

Figure 4-6 *F. japonica* tip bud sample fixed in 0.05M sodium cacadolyte buffer at 5000x magnification. A – plastids/early chloroplasts. B – lipid dense vesicle. C – Golgi apparatus D – rough endoplasmic reticulum. Black arrow indicates a potential mitochondrion. Scale bar = 0.5 µm

Figure 4-6 depicts an image taken of a tip section from a *F. japonica* bud sample at 5000x magnification. The marker A indicates plastids or early chloroplast organelles, which have a defined membrane separating them from the rest of the cytoplasm, as seen in the previous figures in this chapter. Marker B shows what could potentially be a large lipid storage vesicle within the cell, indicated by a large amount of dark stained material around the periphery of the vesicle. The areas marked with C indicate areas in two adjacent cells containing what appears to be large amounts of Golgi apparatus near the cell periphery. Marked D in the image is an area which potentially contains rough endoplasmic reticulum, which is also surrounded by what appears to be a large amount of ribosomes free in the cytoplasm.

The black arrow indicates the single potential mitochondrion visible in this section image.

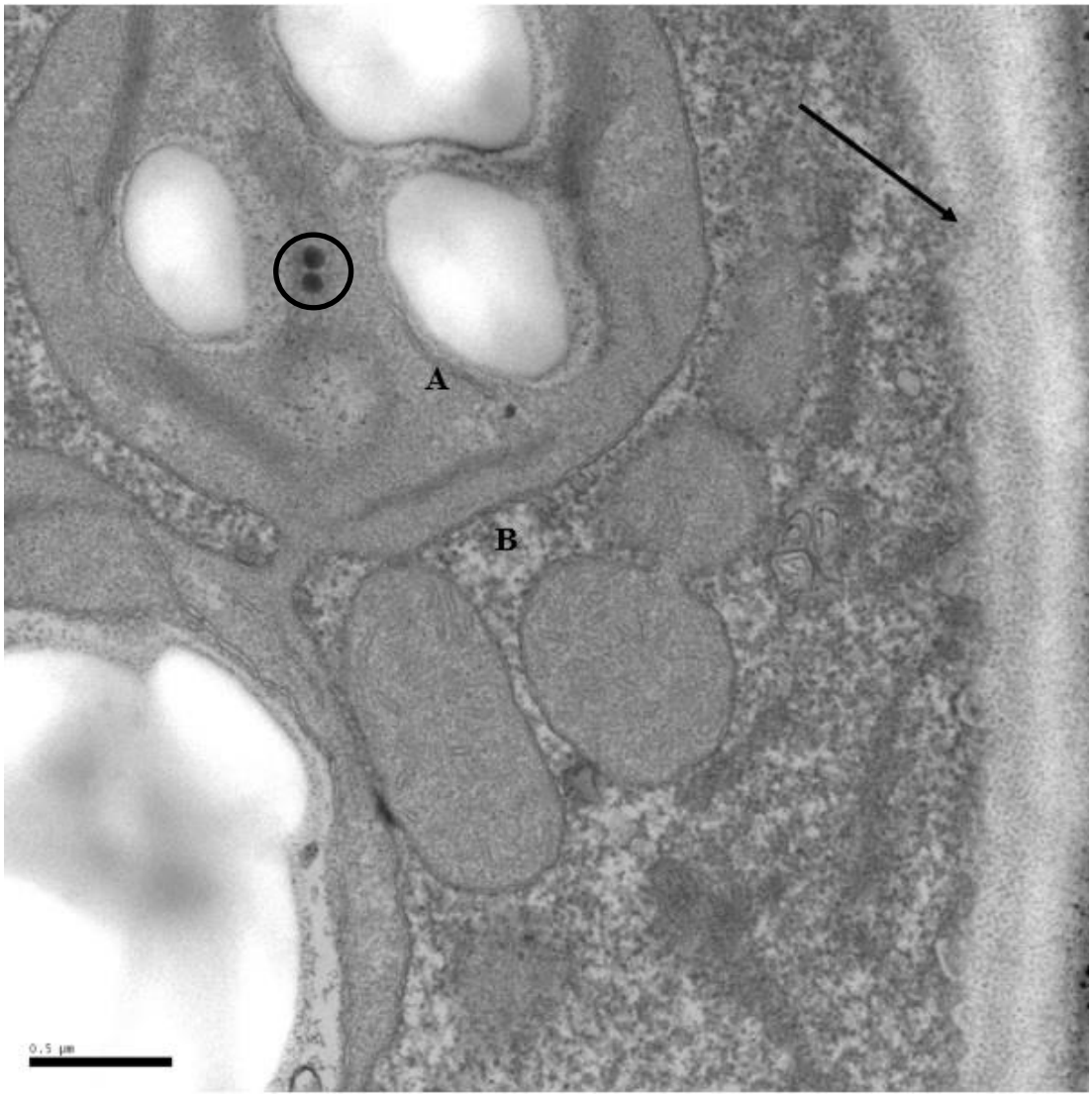

Figure 4-7 *F. japonica* tip bud sample fixed in 0.05M sodium cacadolyte buffer at 6000x magnification. A – plastid /early chloroplast. B – Potential mitochondria. Black arrow indicates cell membrane. Black circle indicates potential ribosome or lipid droplet. Scale bar = 0.5 µm

Figure 4-7 shows the highest magnification image of the tip of a *F. japonica* bud sample. Marker A indicates a potential early chloroplast, with the large white areas characteristic of starch storage within the organelles. Also visible are developing stacks of membranes, which have the potential to develop into thylakoid membranes. The dark stained areas highlighted by the black circle in the organelle are most likely plastoglobuli lipid droplets, which are known to react strongly with the osmium stain used in the sample preparation.

The marker B shows an area with three potentially distinct mitochondria, with the organelle on the left of the image displaying the most distinct membrane and cristae. The mitochondria to the right appears to be undergoing fission, which is the mechanism of replication of mitochondria within the plant cell [147]. It is not clear if the shape on the right of the 'budding' organelle is a mitochondria, although it could be a section through the centre of an organelle, therefore not demonstrating the same distinct membrane as displayed in the other mitochondria seen in this image. If the mitochondria in this image are, as is suggested here, undergoing fission – it could be argued that a higher demand for energy in the plant cell is the impetus for this replication.

As has been displayed in the low magnification images in this chapter section, the mitochondria are fairly low in number and where present, tending to be grouped together in the periphery of the growing cells. Typically, all three regions sectioned from the *F. japonica* buds were not at all rich in mitochondria, involving thorough searching through the section to find a region which contained visible and discernible mitochondria. The tip sections gave the best, most distinct images of potential mitochondria within the cell at higher magnification and these sections also appeared to have the densest cytoplasm. The vacuoles of the cells of all three regions imaged here, base, centre and tip are large, dominating the majority of the cells.

4.4 *Arum maculatum* spadix imaging

In order to provide a comparison to the *F. japonica* bud sections, *A. maculatum* spadix sections were prepared and imaged following the same protocol. Images of spadix section preparation can be seen in chapter 2, figure 2-3.

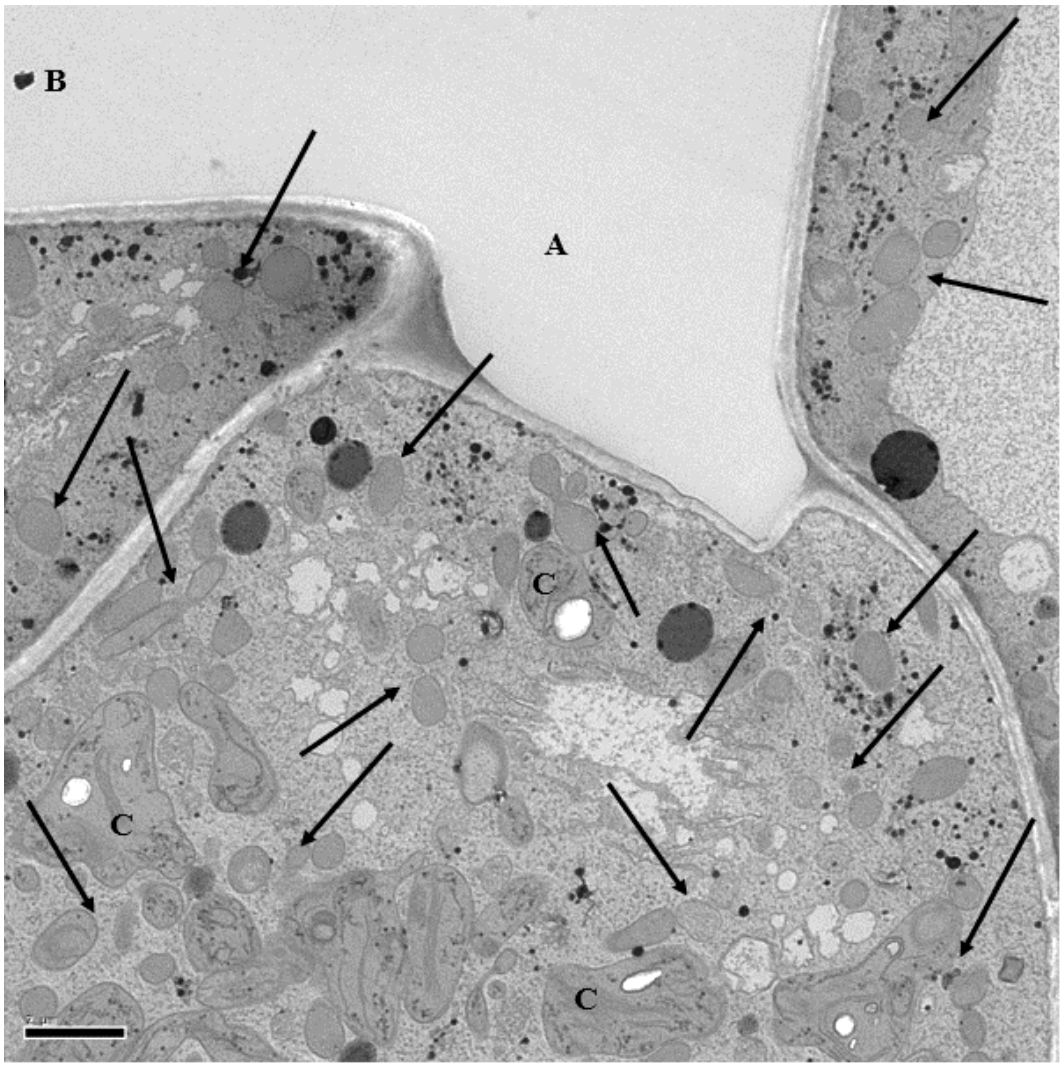

Figure 4-8 *A. maculatum* spadix section, fixed in 0.1M sodium cacodylate buffer. 1000x magnification. A – Vacuole. B – Staining artefact C – Plastids/chloroplasts. Black arrows indicate groups of mitochondria. Scale bar = 2µm

Figure 4-8 is an image taken of an *A. maculatum* spadix section at low magnification. Marker A indicates a large cellular vacuole at the junction of four cells. Mark B is likely an artefact from the staining procedure and sample preparation. Areas marked C indicate potential chloroplasts, with white areas

indicating stored starch within these organelles. Areas marked with the black arrows indicate groups of mitochondria. Mitochondria in this sample are numerous and well defined, with evidence of mitochondrial fission in some areas.

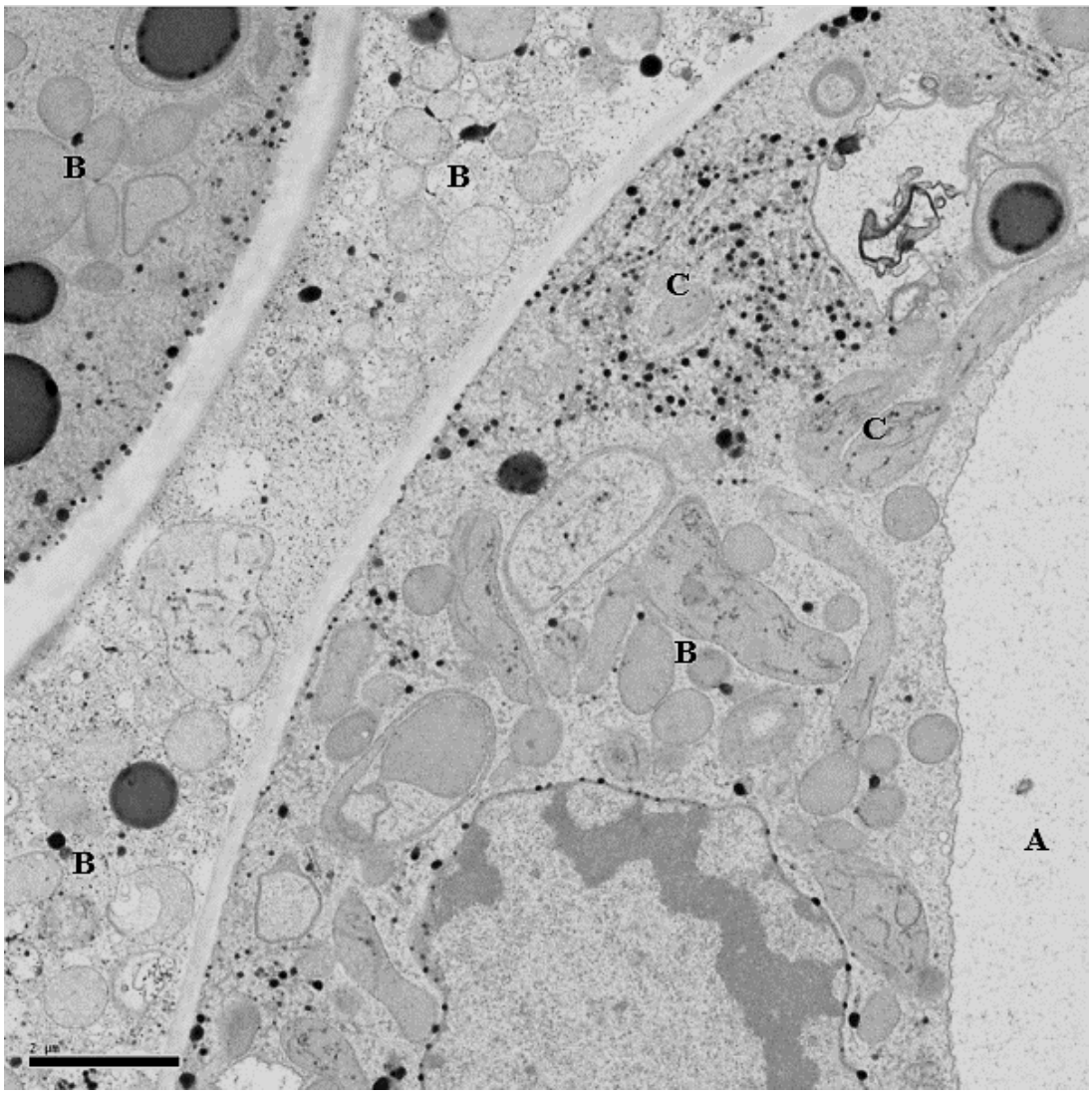

Figure 4-9 *A. maculatum* spadix section, fixed in 0.1M sodium cacodylate buffer. 1500x magnification. A – Vacuole. B – group of mitochondria. C – Plastids/Chloroplasts. Scale bar = 2 µm

Figure 4-9 shows another low magnification image of the *A. maculatum* spadix section, this image comprising of three cells closely packed together. Marker A indicates the large vacuole visible in the right cell. The B marker indicates groups of mitochondria, which are the most numerous organelle in all three cells. The C markers indicate small potential pro-plastids present in the right cell.

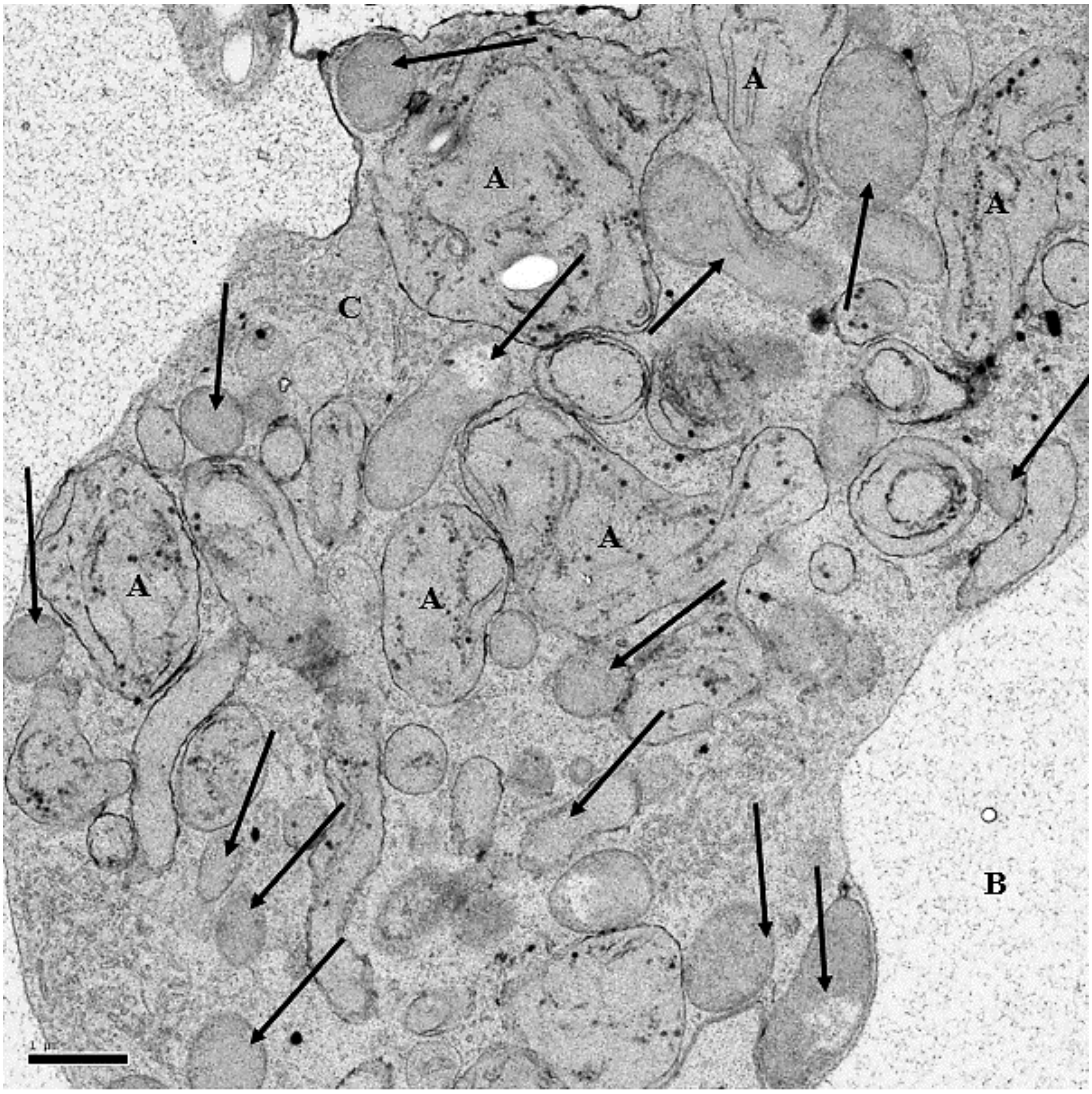

Figure 4-10 *A. maculatum* spadix section, fixed in 0.1M sodium cacodylate buffer. 2000x magnification. A – plastids/potential chloroplasts B – Vacuole C – Golgi apparatus. Black arrows indicate mitochondria or areas of multiple mitochondria. Scale bar = 1 µm

Figure 4-10 represents another region of *A. maculatum* spadix section, at 2000x magnification. Areas marked with A indicate potential chloroplasts, containing what appear to be stacks of thylakoid membrane. Marker B indicates a large cellular vacuole. Marker C specifies a region potentially containing Golgi apparatus. Arrows indicate areas which contain mitochondria which are grouped very closely together in this cell. Unfortunately, in this image, very little detail can be distinguished within the mitochondria themselves, although the numbers of them in the cell are great.

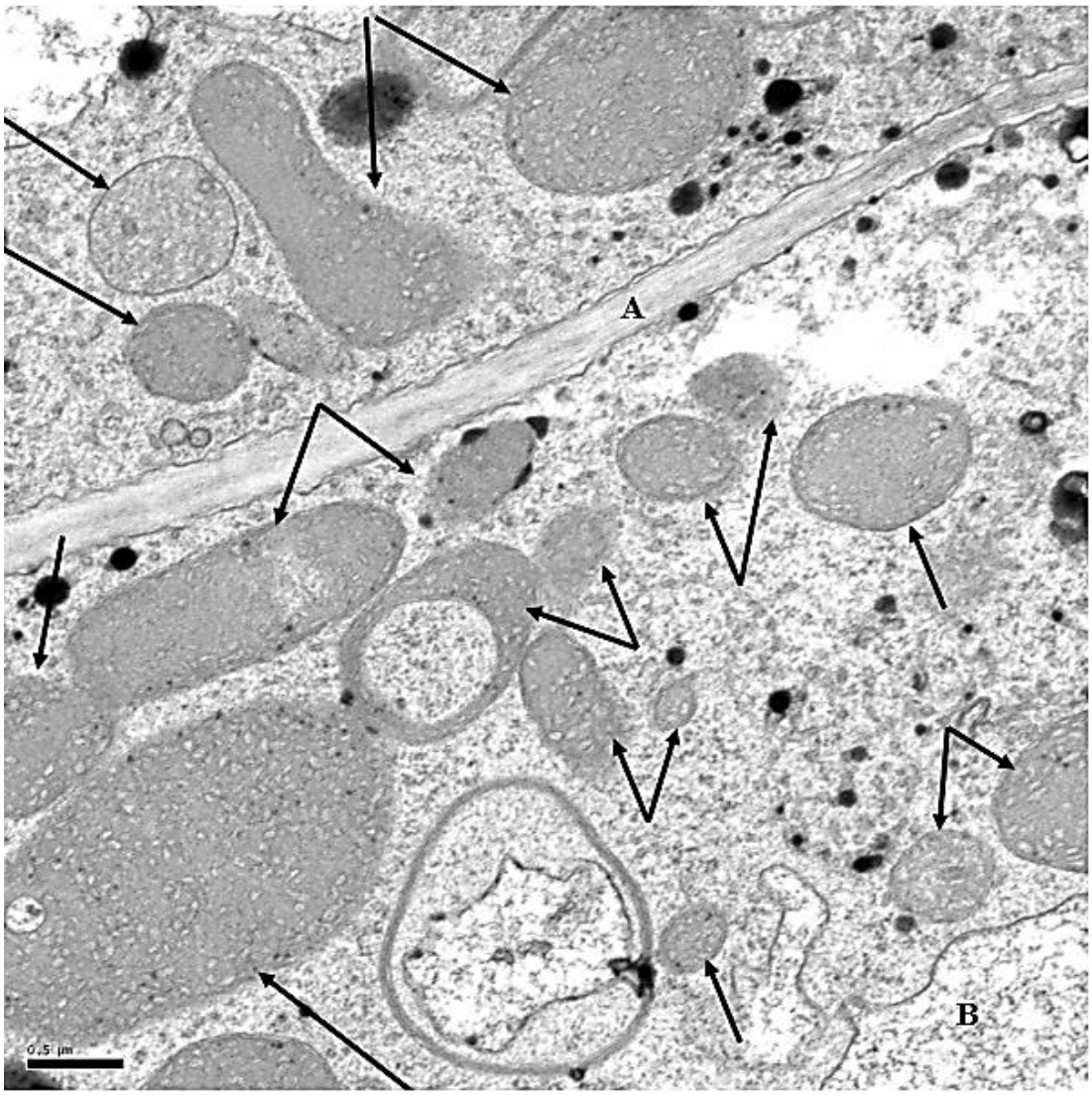

Figure 4-11 *A. maculatum* spadix section, fixed in 0.1M sodium cacodylate buffer. 4000x magnification. A – Cell membrane. B – Vacuole. Black arrows indicate mitochondria. Scale bar = 0.5 µm

Figure 4-11 is a section of the *A. maculatum* spadix under a higher magnification. Marker A indicates the cell membrane between the two cells shown in this image. B shows a cellular vacuole visible in the bottom cell. Black arrows indicate the many mitochondria in this image. This area of the section is very well preserved, with the mitochondrial membranes and internal cristae clearly distinguishable.

After comparison of the images obtained from the *F. japonica* bud sections and those from the *A. maculatum* spadix, it was clear that the *Fallopia* samples had much fewer mitochondria, less cytoplasm and had much larger vacuoles. To

determine if these characteristics were present throughout all of the sources of *Fallopia* cellular material used during this project, TEM was also performed on callus and suspension material from *F. japonica*.

4.5 ***F. japonica*** **callus imaging**

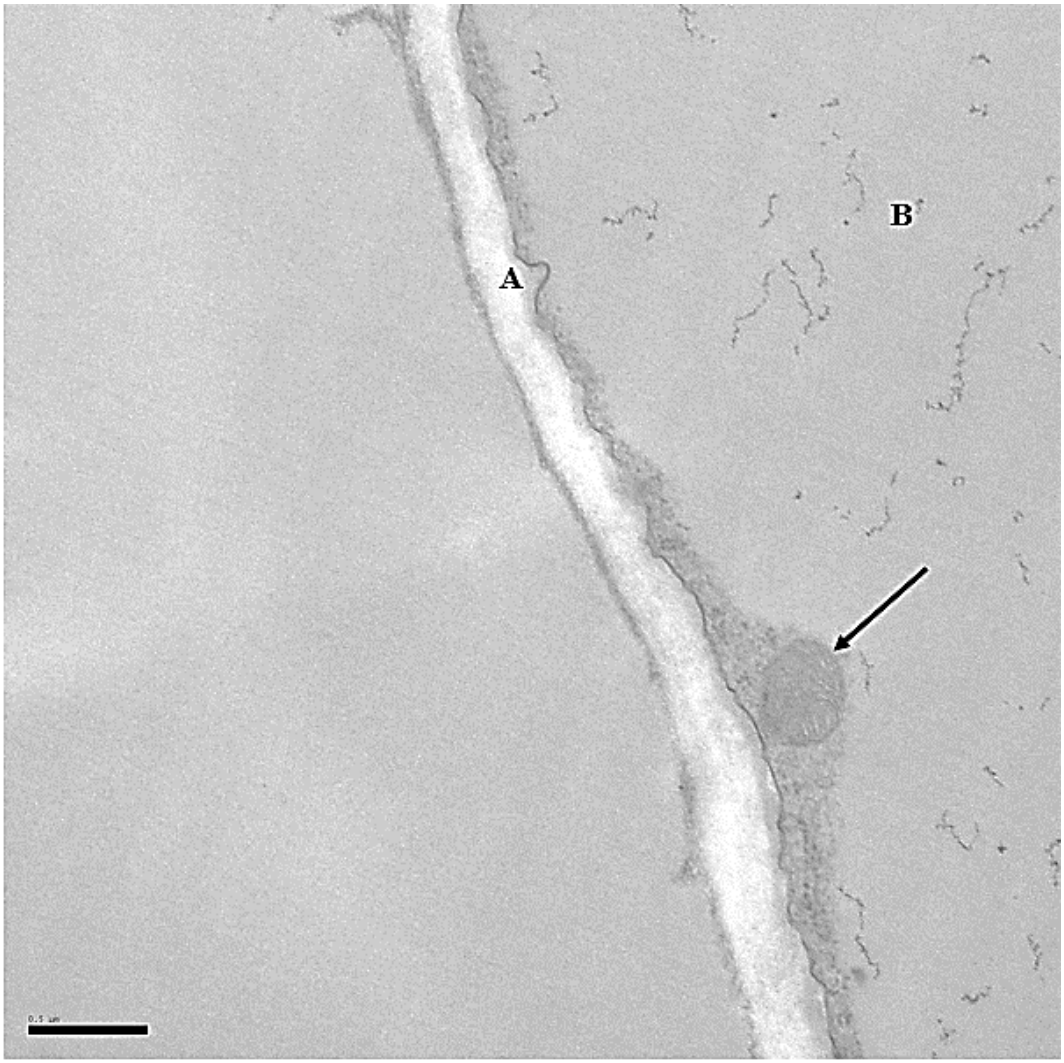

Figure 4-12 *F. japonica* callus section, fixed in 0.1M sodium cacodylate buffer. 5000x magnification. A – cell membrane. B – Vacuole. Back arrow indicates a mitochondrion. Scale bar = 0.5 μm.

Figure 4-12 represents a section of *F. japonica* callus material at a high magnification. This image is typical of the regions seen throughout the sample - very little cytoplasm was present in the cells, with the majority of the organelles within a small margin at the cell periphery. Marker A indicates the cell membrane, B a

cellular vacuole. The black arrow indicates a small potential mitochondrion with detailed matrix cristae visible.

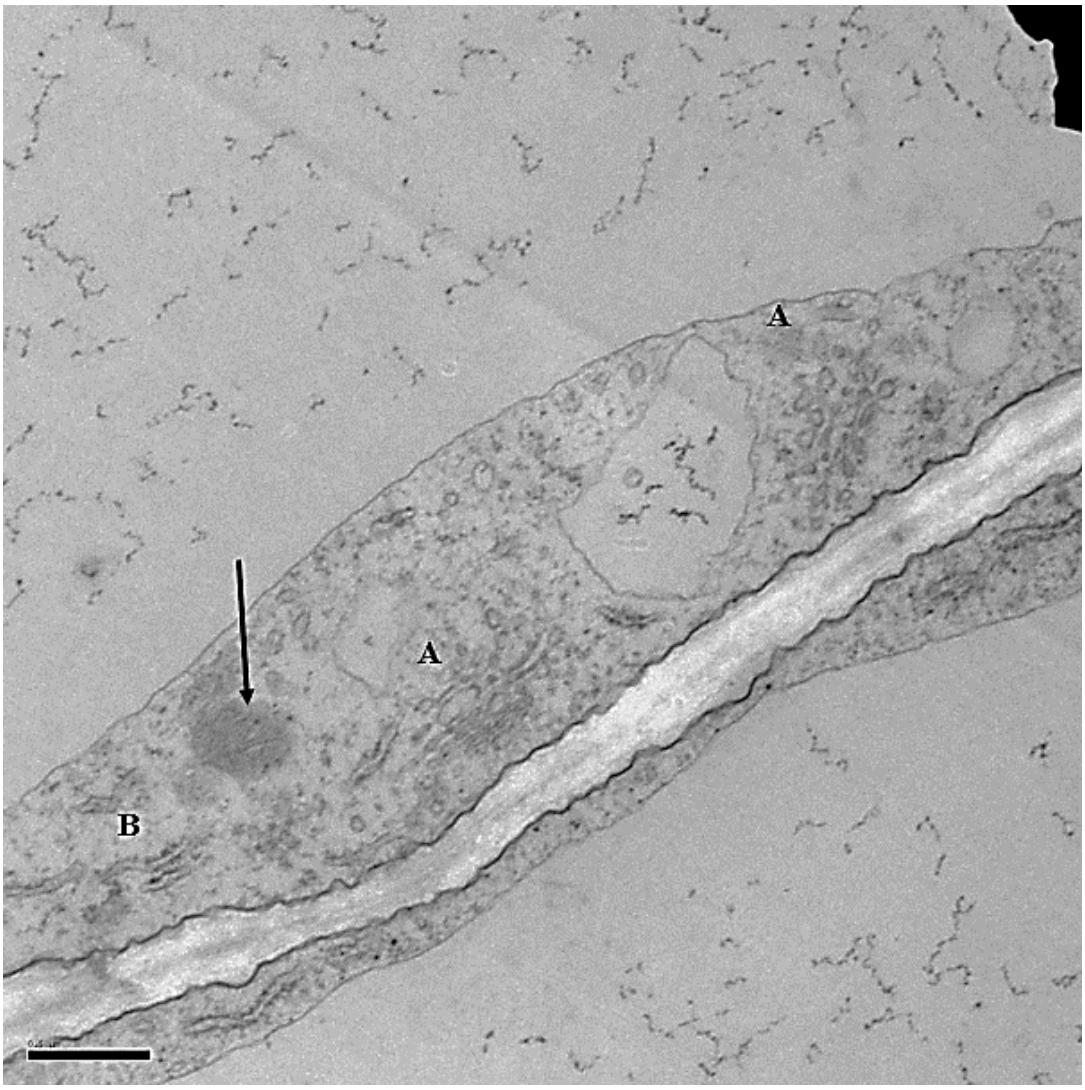

Figure 4-13 *F. japonica* callus section, fixed in 0.1M sodium cacodylate buffer. 5000x magnification. A – Golgi apparatus B – rough endoplasmic reticulum. Black arrow indicates potential mitochondria. Scale bar = 0.5 μm

Figure 4-13 represents a second section of *F. japonica* callus material at a high magnification. The A markers represent areas of the cell containing Golgi apparatus, B indicates potential rough endoplasmic reticulum. The black arrow again represents what is a small potential mitochondrion within the cytoplasmic region around the cell periphery.

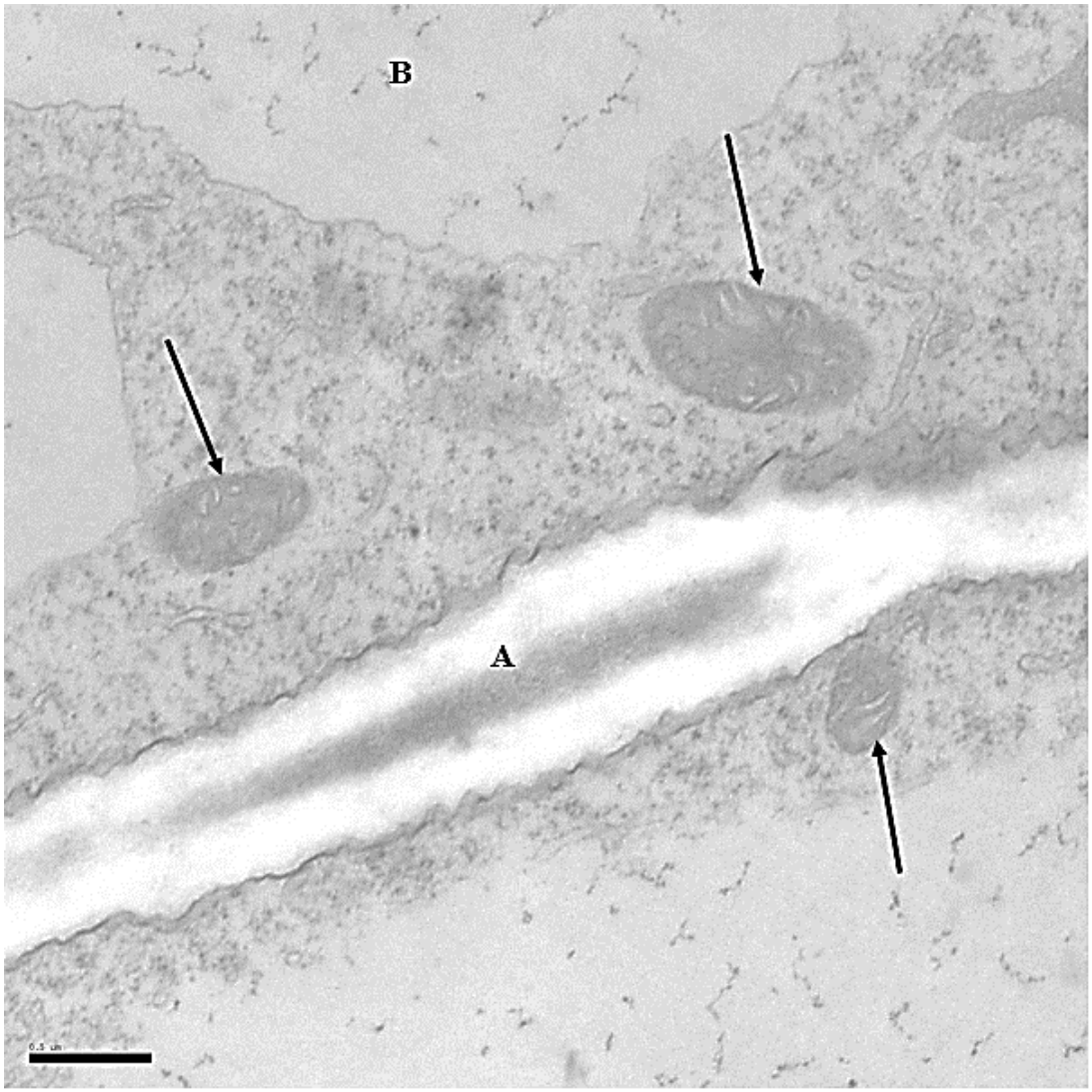

Figure 4-14 *F. japonica* callus section, fixed in 0.1M sodium cacodylate buffer. 5000x magnification. A – Cell membrane B – Vacuole. Black arrows indicate mitochondria. Scale bar = 0.5 µm

Figure 4-14 represents *F. japonica* callus material at high magnification. This section contains several small potential mitochondria, present in the cytoplasm around the periphery of the cell, as indicated by the black arrows in this image. Marker A represents the cell membrane, marker B indicates the large cell vacuole.

As has been shown clearly in

Figure *4-12* through Figure 4-14, the *F. japonica* callus cellular material contains very few organelles. The mitochondria which are present in the sections are small and seemingly dense, without visible complex internal cristae. The cells in these sections were very large, which resembled the cells from the sections taken

from the *F. japonica* bud base sections and shown in Figure 4-2. As the callus cells were intentionally dedifferentiated with the aid of plant hormones in culture, the lack of specialised organelles such as chloroplasts within these cells was not surprising.

4.6 *F. japonica* suspension culture imaging

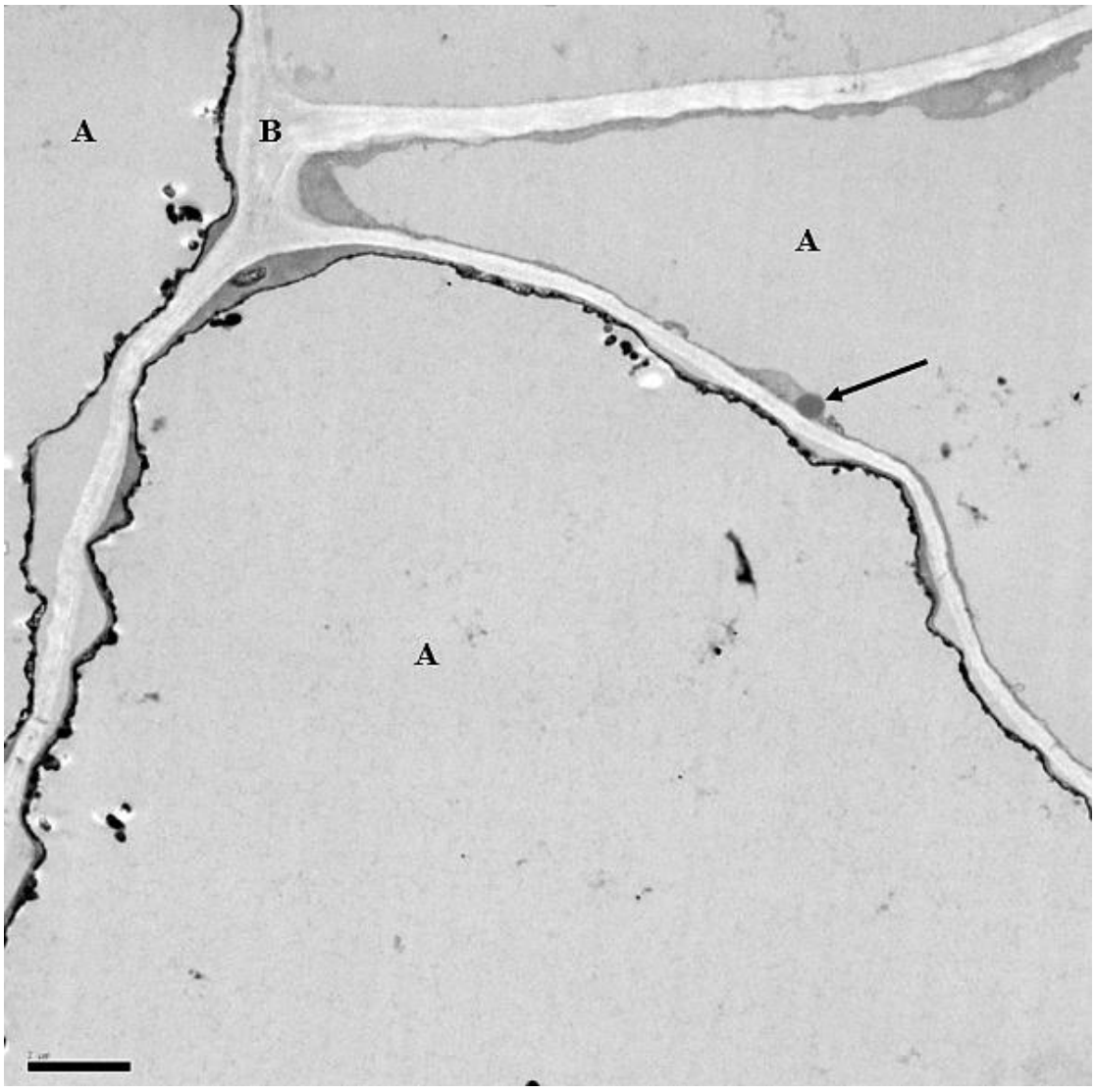

Figure 0-1 *F. japonica* suspension culture section, fixed in 0.05M sodium cacodylate buffer. 1000x magnification. A – Vacuole. B – Cell membrane. Black arrow indicates mitochondria. Scale bar = 2 µm.

Figure 0-1 shows a low magnification image of a *F. japonica* suspension culture section. Markers A show the multiple large vacuoles present in all four cells visible in this section, with marker B showing the convergence of the cells at a cell

membrane junction. The black arrow indicates a potential mitochondrion present in a small amount of cytoplasm detectable in this image. Darker staining around the vacuoles in this image could be due to the presence of concentrated lipids within the internal vacuolar membrane.

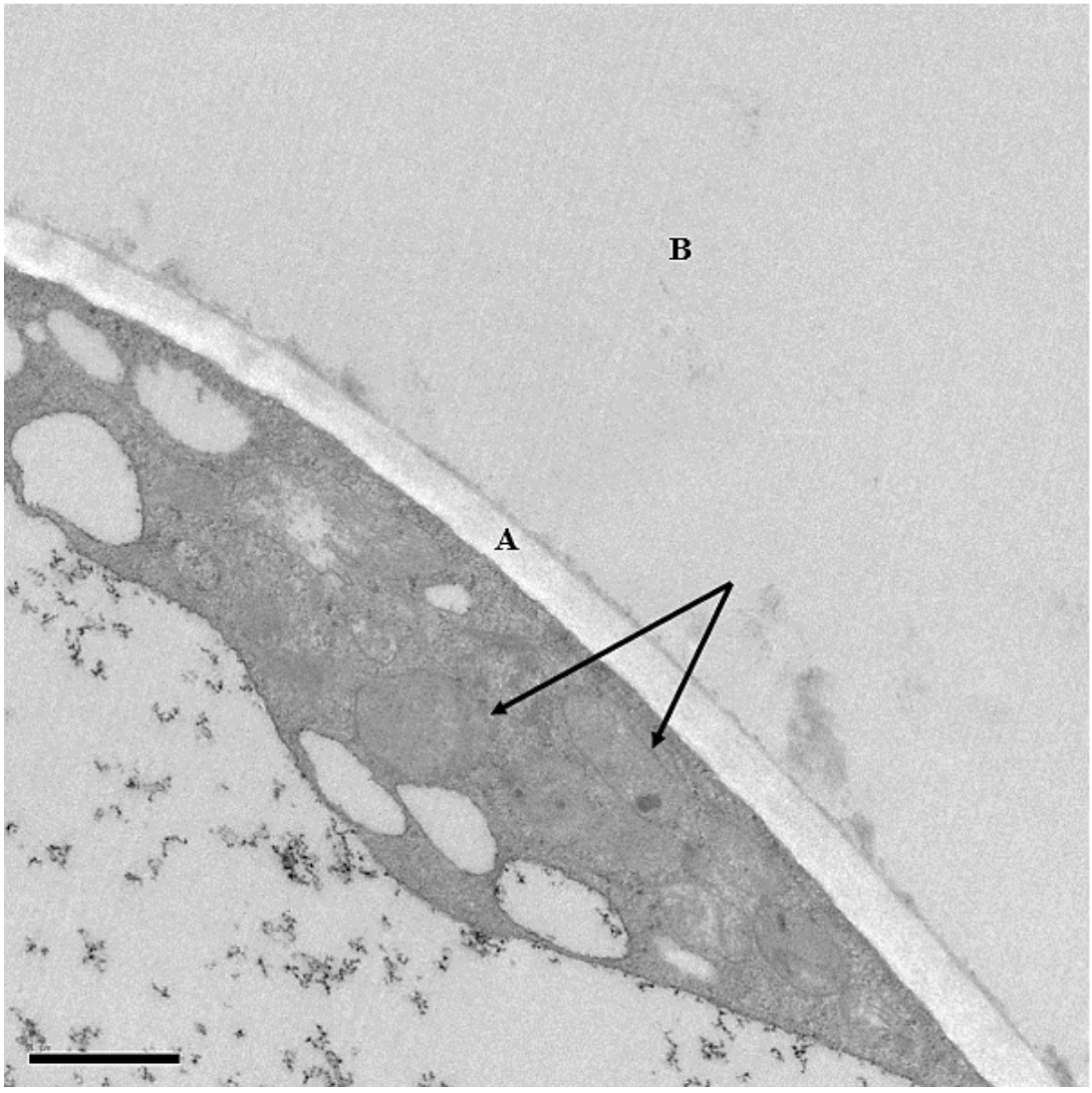

Figure 4-2 *F. japonica* suspension culture section, fixed in 0.05M sodium cacodylate buffer. 3000x magnification. A – Cell membrane. B – Vacuole. Black arrows indicate mitochondria. Scale bar = 1 μm.

Figure 4-2 represents a higher magnification image of a *F. japonica* suspension section. Marker A represents the cell membrane, marker B the vacuole of an adjacent cell. The black arrows indicate the potential mitochondria present in this sample, which are not immediately obvious due to the lack of detail in the image. The cytosol in this sample is highly dense and appears to have several plastid-like organelles present.

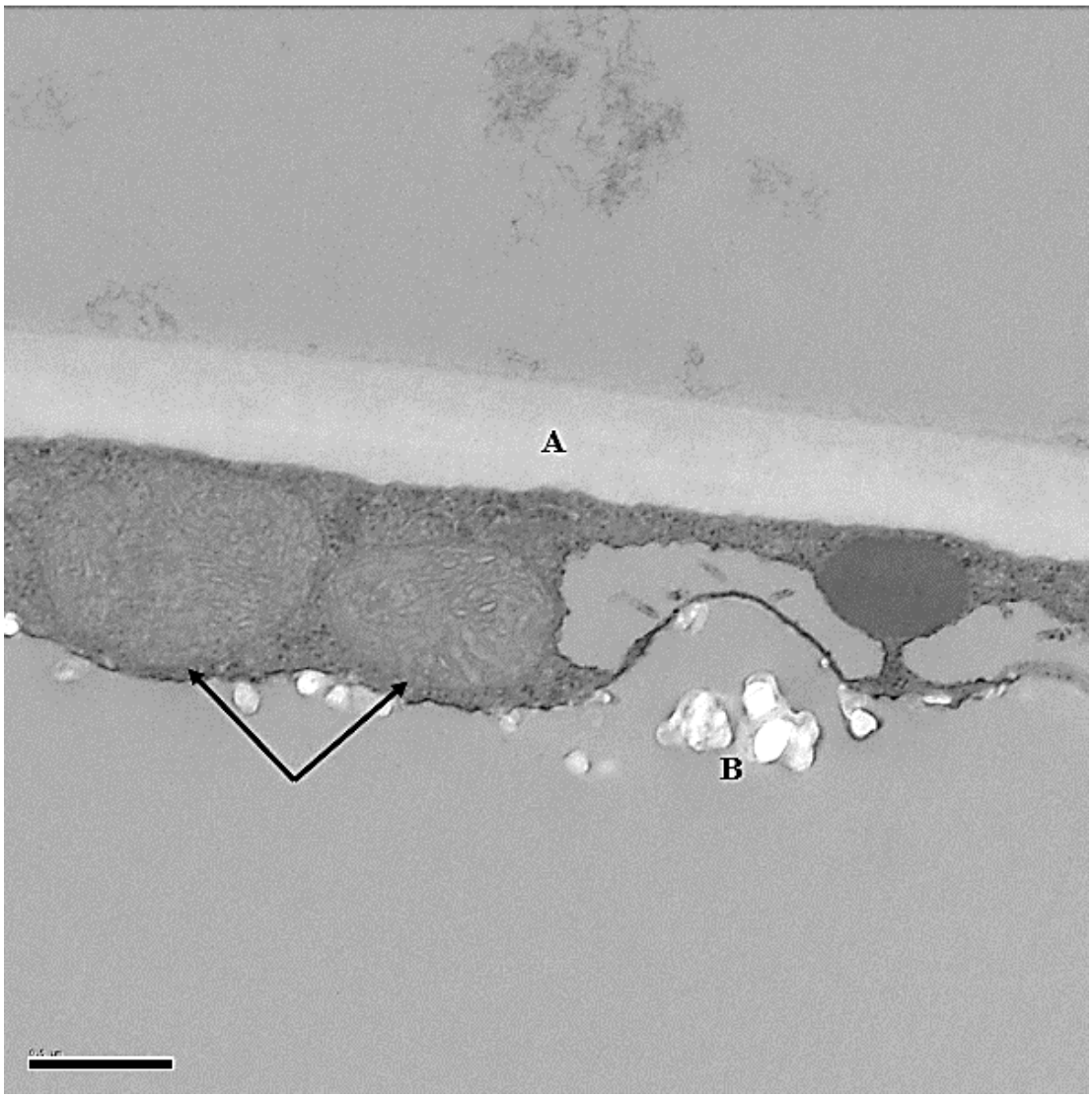

Figure 0-3 *F. japonica* suspension culture section, fixed in 0.05M sodium cacodylate buffer. 6000x magnification. A – Cell membrane. B – Splitting of sample artefacts. Black arrows indicate potential mitochondria. Scale bar = 0.5 μm.

Figure 0-3 represents the highest magnification of a *F. japonica* suspension section. The cell membrane is indicated by the A marker in this image, whereas marker B indicates some damage to the sample through splitting of the thin section. The potential mitochondria are marked with black arrows in this figure. The cristae of the mitochondria and the dense cytoplasm around the periphery of the cell are clearly visible in this image.

4.7 Conclusion

The objective of using TEM to investigate the *F. japonica* samples was to gain an insight into the composition of the cells and determine if any structural or organisational factors contribute to the exceptional growth rates seen in the *F. japonica* plants. Sections were first taken from buds of wild growing plants and fixed successfully using 2.5% glutaraldehyde, which is within the general range of concentration used for the fixation of plant cells [148]. Buffer concentration was found to be most effective for the bud sections at 0.05M sodium cacodylate as solutions of higher molarity resulted in loss of some ultrastructure within the cells.

Initial viewing of the base sections from the *F. japonica* bud samples showed large vacuoles within cells, with a small amount of overall cytoplasm which was located around the periphery of the cells, as can be seen in Figure 4-2. The cytoplasm in these cells contained very little in the way of organelles, although some few putative mitochondria are marked, along with some rough endoplasmic reticulum (RER). The presence of RER in this sample indicates that protein synthesis is active within the region, as the ribosomes on the surface of the ER provide the sites for manufacture of essential membrane proteins and proteins destined for secretion from the plant cell [149].

Within the centre section taken from the *F. japonica* bud sample shown in Figure 4-4, large vacuoles are again present in the cells. As mentioned previously, plant cells often have a dominant central vacuole, often occupying from 30% of the cell volume in meristematic cells [146], as is true in all of the *F. japonica* images seen in this chapter. The centre section contains dominant structures which are putatively identified as plastids or pro-plastids, containing what appear to be starch grains [150]. Again, very few mitochondria are present, which was a representational result based on multiple centre bud sections viewed in the TEM.

The tip sections taken from the *F. japonica* buds in Figure 4-5 to Figure 4-7 showed smaller cells with developing vacuoles which is typical of apical meristematic tissues [151]. In the higher magnification images some RER and Golgi

apparatus are visible. The Golgi apparatus have an important roles in growing plant tissues, by way of synthesis of cell wall polysaccharides and sorting and glycosylation of proteins [152]. As seen in all of the *F. japonica* bud sections examined, the mitochondria are small and few in number – often grouped together in the cytoplasm.

For a comparison, *A. maculatum* tissue sections were examined following the same preparative protocol for TEM. It is immediately obvious upon viewing of Figure 4-8 through Figure 4-11 that the cellular composition is inherently different to that of the *F. japonica* sections observed, in that the dominant organelles are mitochondria. This spadix of *A. maculatum* are known to be highly thermogenic and contain a large amount of AOX containing mitochondria during this period, so the results are not surprising in this regard. The main conclusion gained from the comparison of these plant sections is the scale of the difference between the number of mitochondria present in these two species, where one would expect an energy demanding, rapidly growing *F. japonica* bud to contain many more mitochondria to provide the energy needed during this stage.

To gain an understanding of the cellular composition of *F. japonica* cells in culture and how the structure relates to that of *F. japonica* bud cells, TEM was also performed on sections taken from both callus and suspension culture. As can be seen in

Figure *4-12* through Figure 0-3, the cellular structure is comparable to that of the base sections taken from the buds of *F. japonica*, in that the cells are large and contain large vacuoles. The main difference between the cultured cells and those sections taken from the plants are the lack of any specialised organelles within the cultured cells. This is again not surprising, as the cultured cells had been grown in an environment which encouraged dedifferentiation, therefore any location specific organelles, such as chloroplasts, are understandably absent from these cells. The cultured cells did have evidence of the presence of Golgi apparatus, which due to their role in generation of cell wall polysaccharides, would be logical in these growing tissues.

	Total mitochondrial area (um)	**Average % cell volume**
Fig 2-3 *F. japonica* BASE	4.489	1.354
Fig 4 *F. japonica* CENTRE	0.138	0.146
Fig 5-7 *F. japonica* TIP	2.216	0.552
Fig 8-11 *A. maculatum* SPADIX	65.677	16.427
Fig 12-14 *F. japonica* CALLUS	0.942	0.322
Fig 15-17 *F. japonica* SUSPENSION	2.533	0.631

Table 4-1 Comparison of mitochondrial area and percentage cell volume in *F. japonica* material

Table 4-1 shows a summary of data gathered from the TEM images presented in this chapter gathered and analysed using ImageJ. Total mitochondrial area represents the area in micrometres occupied by potential mitochondria in the figures presented in this chapter. Similarly, the average mitochondrial cell volume is an average of the percentage of the cell volume occupied by mitochondria within the given figures in this chapter. The quantification of the numbers and volume of mitochondria show clearly the difference between the *A. maculatum* and *F. japonica,* with the *A. maculatum* spadix sections having a much greater area and volume of mitochondria within the cells. Base regions of the *F. japonica* buds are shown to have the greatest area and volume of mitochondria when compared to the other *F. japonica* samples analysed, which could be due to this area consisting of more mature cells. Further analysis of this data will be presented in chapter 6.

Overall, the results presented in this chapter go some way to explaining the lack of high levels of respiratory activity during assays and the difficulty of isolation of mitochondria from *F. japonica* plant tissue and cultured cells. The numbers of mitochondria are seen to be very low within all of the areas examined using TEM, especially when compared to the numbers in the *A. maculatum* sections. These results are at odds with the rapid growth rate seen in the plants. This could be an indication that mitochondria play a smaller role in the generation of energy within the *F. japonica* cells in comparison to other plant species. The ramifications of these results are discussed further in chapter 6.

5 Generation and Development of *Fallopia japonica* cell culture

5.1 Introduction

Plant cell culture - the sterile culture of plant cells and organs under defined *in vitro* conditions - is a technique used throughout most plant research laboratories [153]. In 1902, Austrian botanist Gottlieb Haberlandt is considered to be the first person to discover the potential of a single plant cell to regenerate into a whole plant – which is recognised as totipotency in modern botany [154].

Plant cell culture has many important applications in modern science. In this chapter it is introduced as a platform through which to provide an *in vitro* culture of dedifferentiated *F. japonica* cells. The dedifferentiated cells provide an ideal model on which to perform characterisation experiments detailed later in this chapter.

Established protocols for the generation of cell culture from different organs of plants, such as leaves, root or seed are available for several plant species. *Arabidopsis thaliana* is a prime example. *A. thalaina* was the first plant species to have its genome completely sequenced [105] and its status as a model organism make it a very attractive species to study via cell culture. Many published protocols detailing collection & preparation [155], media selection [156], plant growth regulator selection and concentration [157], callus growth and liquid media stages [158] are available for *A. thaliana*. To the best of our knowledge, no protocols are available in the literature at the time of writing for the generation of cell culture for *F. japonica*.

As each species of plant have different requirements for optimal growth in cell culture, the protocol presented for growth of *F. japonica* cell culture has been adapted and optimised from established protocols of several different plant species. These include *Nicotiana* species (tobacco) [159], *Petunia* species [160], *Stevia*

rebaudiana [161], *Coffea arabica* (coffee) [162] and as previously mentioned, *A. thaliana* [163].

This chapter contains a detailed walkthrough of all stages of cell culture, from selection and preparation of explants, to analysis and characterisation of suspension cultures.

5.2 Collection and preparation of *F. japonica* plant material

F. japonica plants were grown in the greenhouses at the University of Sussex from February 2012 – August 2015. These plants were a selection of 'wild type' - which were exhumed from a large naturalised patch growing near the University of Sussex grounds - and additionally hybrids generously donated from Dr. John Bailey of the University of Leicester. For generation of cell culture, the wild type plants were selected for use – as these would represent the dominant sub-species of *F. japonica* present in the UK and Europe in its naturalised invasive state.

Plants were chosen which were actively growing, indications of which were increased biomass, new leaf production and increase in height. Leaves were selected as explant material as they represent the most simple plant organ to sterilise, they are numerous and several papers are available detailing the treatment of various species of plant leaves in generation of cell culture, which allowed the adaptation of protocols from existing and successful experiments [155, 164, 165]. Leaves which were fully unfurled yet not fully mature were selected, as immature tissues are likely to contain more dedifferentiated cells which increase the likelihood of callus formation in comparison to fully mature regions [166, 167]. The leaves were then washed thoroughly in distilled water for 20 minutes, with the aim of removing any soil, insects or other dirt which may be present and cause contamination. The washed leaves were subsequently wholly immersed in pure ethanol for approximately 30 seconds. At this stage, the leaves were transferred to sterile conditions and treated as sterile from this point onwards throughout the protocol.

The leaves were washed with a mixture of household bleach and a detergent (tween) and were then considered to be sterile. After removal of any residual surfactants via repeated washing in distilled water (as described in chapter 2) the explants were prepared from the leaves. Any browning around the edges of the leaves was removed using a sterile scalpel as browning was an indication of cell death and would therefore potentially not yield viable growth in subsequent stages.

The internal areas of the leaf were then cut into squares, approximately $1cm^3$. These were scored lightly using a scalpel to induce the formation of dedifferentiated cells and callus as a reaction to wounding [168]. The wound response is a complex process which, in *A. thaliana*, involves the upregulation of specific transcription factor WOUND INDUCED DEDIFFERENTIATION 1 (WIND1). Wounding enhances the cells response to cytokinin which in turn promotes the formation of callus tissue [169]. Wound response calli are highly pluripotent as they are most frequently able to regenerate new organs and tissues in comparison to either callus-inducing-media (CIM) type callus or callus derived from pathogen infection [168].

5.3 Media considerations

5.3.1 Media selection

In order for the explants to continue to grow in an *in vitro* environment, certain nutritional requirements were necessary. While there are several different available media specifically for the growth of explants and the initiation of cell culture, two media types were chosen and trialled for the growth of *F. japonica* explants. These were Murashige and Skoog (MS) [170] and Gamborg B-5 (GB5) [171] media as detailed in chapter 2, table 2-6 and 2-7. MS media was chosen for the trial as it was the most commonly used basal medium for callus growth from plant explants, GB5 media chosen as it was originally developed for generation of callus for use in suspension culture [172].

5.3.1.1 Agar percentage selection

For all of the callus growth stages, a gelling agent was required to solidify the media for use as a support for the explants. Plant cell culture grade agar was used for this purpose, purchased from Sigma, with a quoted working concentration of 6-12 g/L, or between 0.6 – 1.2 % concentrations.

Lower concentrations of agar were added to both types of media, 0.6% was trialled initially and found to be too low – it would often not support, or would entirely engulf the explant. 1% was also found to not have enough rigidity, therefore 1.2% agar final was used throughout the explant and callus stages.

5.3.1.2 Explant pH range determination

The explant media was also a factor of consideration when the initial cultures were set up. Many cultures are known to tolerate a range of pH, from 5.2 to 5.8 [173]. Many cultures are known to be stable for at least 21 days at pH 5.5 [174, 175]. In light of this, both MS and GB5 media types were adjusted to pH 5.5 with 0.1M potassium hydroxide before autoclaving and use. Some variation in pH was trialled, with no visible effects on the cultures, therefore pH was kept within pH 5.5 ± 0.1 during the growth of the cultures.

5.3.1.3 Growth regulator selection

Cytokinins and auxins are natural plant growth regulators (also known as plant hormones, although this term is archaic), produced by all plants to self-regulate their development and even react to changing environmental conditions.

Auxins can be natural or synthetic, examples of which are Indole-3-butyric acid (IBA) and 2,4-Dichlorophenoxyacetic acid (2,4-D) respectively [101]. The primary action of all auxins is the promotion of cell elongation; which, when acting in combination with cytokinins, cause normal growth, development and differentiation of plant organs [176]. When used in plant cell culture, auxins are thought to enhance callus growth. Synthetic auxin 2,4-D has a history of use as a

selective herbicide, as follicular application of high doses causes abnormal overgrowth of plant tissues [177].

Cytokinins, such as Kinetin (Kin) and 6-Benzylaminopurine (BAP) work in concert with auxins and have primary roles in cell growth and division within plant cells [178]. Examinations of effects of many trials have elucidated that both auxin and cytokinin are required for successful proliferation of cells [178]. The balance of these two phytohormones is crucial to the growth of plant cells in culture [179].

Primarily, a matrix was prepared which detailed the components of each of variations of growth regulators, which can be seen in Table 5-1. IBA and BAP were chosen as the first auxin/cytokinin pairing to trial in the media. The IBA (Sigma: I5386) working concentration was provided by Sigma as between 0.1 – 10 mg/L; the BAP (Sigma: B3408) concentration as 0.1 – 5.0 mg/L [180]. Each culture trial was assigned a number from 1-36 and a plate of either MS or GB5 media containing the corresponding concentration of IBA and BAP was prepared. Explants were plated onto each culture and observed at regular intervals to assess the quality and speed of callus formation.

Figure 5-1 shows an image of the explants on a variety of media concentrations, as indicated by the culture numbers indicated highlighted in red from Table 5-1.

BAP Concentration mg/ml	IBA Concentration mg/ml						
		0.1	**0.5**	**2.0**	**5.0**	**7.5**	**10.0**
	0.1	1	2	3	4	5	6
	0.2	7	8	9	10	11	12
	0.5	13	14	15	16	17	18
	1.0	19	20	21	22	23	24
	2.5	25	26	27	28	29	30
	5.0	31	32	33	34	35	36

Table 5-1 Matrix showing initial trial matrix for growth regulator concentrations - numbers in red indicate culture numbers which were attempted. For example; 0.5mg/ml IBA + 0.5 BAP concentration = culture number 14.

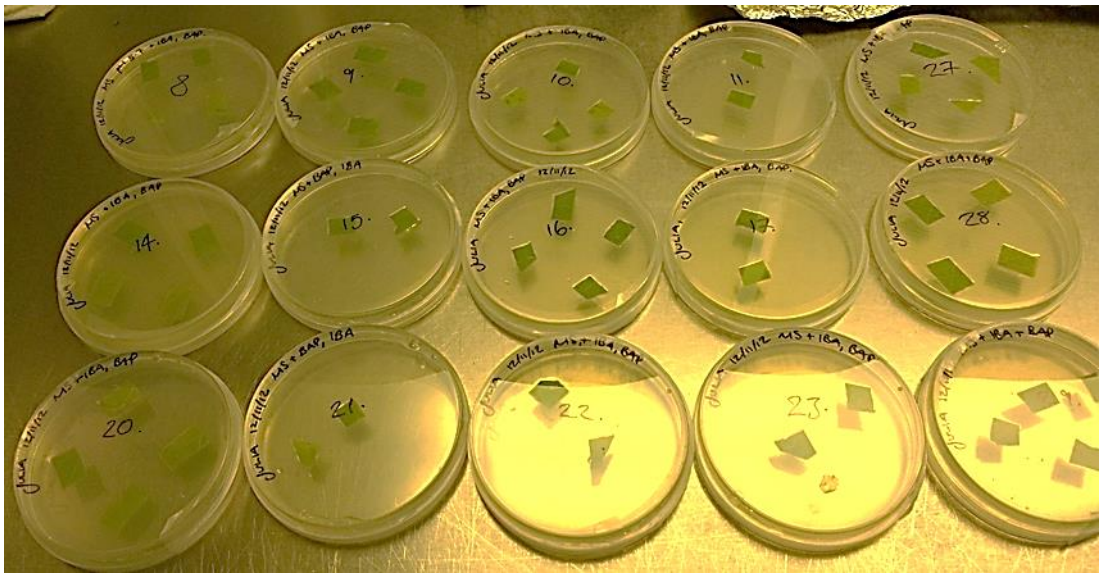

Figure 5-1 *F. japonica* leaf explants on a range of growth regulator concentrations for callus growth trial.

5.4 Callus Growth

Following the preparation of the solid media into plates and the sterilisation of the *F. japonica* leaves, the wounded explants were pushed gently into the surface of the solidified media under sterile conditions in a flow cabinet. The plates were then sealed with parafilm and transferred to be incubated in a Weiss cabinet at 22℃ with constant lighting. The incubation period varied initially as the time required for callus tissue to generate from the explants was unknown. Estimations were made from the literature [163, 181-183] as to the amount of time in which the growth of callus would occur and observations were taken periodically based on these estimations.

Explants were checked three times a week for outgrowths, which were initially observed from the cut edges of the leaves and also from the 'wounding' scores on the leaf surface. The explants initially became swollen and were seen to curl in on themselves slightly. There was also a tendency for browning of some parts of the leaves, most commonly around the edges and the scoring wounds on the surface. Outgrowths first appeared as small whitish/brownish clumps of cells growing from the explants. Figure 5-2 shows a typical example of a leaf explant under medium regulator conditions, after two weeks of incubation – swelling and curling of the leaf, with the very beginnings of callus outgrowth from the edges of the explant.

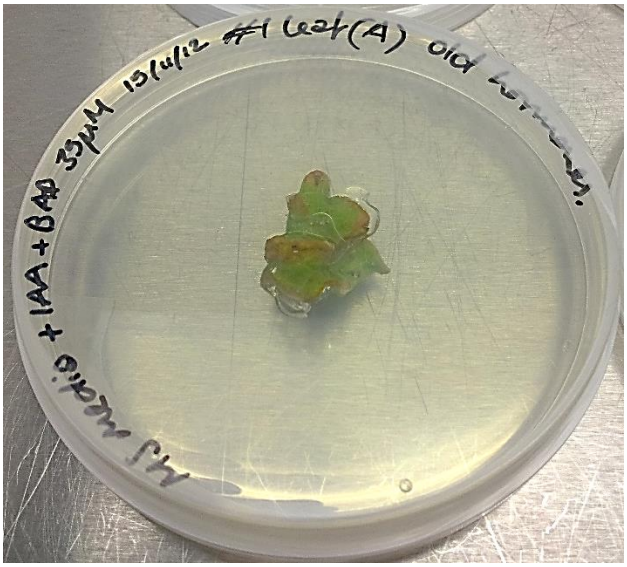

Figure 5-2 *F. japonica* leaf explant after two weeks of incubation.

5.4.1.1 Callus plate contamination

Contamination was at first a major hindrance to setting up cell culture, as it was frequently found that bacterial and fungal growths were present on early attempts to form callus tissue. Any plates which were found to have bacterial or fungal growth were immediately discarded. Examples of typical contamination on the explant plates can be seen in Figure 5-3. The left plate has fungal contamination highlighted, in the right plate, yellow bacterial growth can be seen around the explant material.

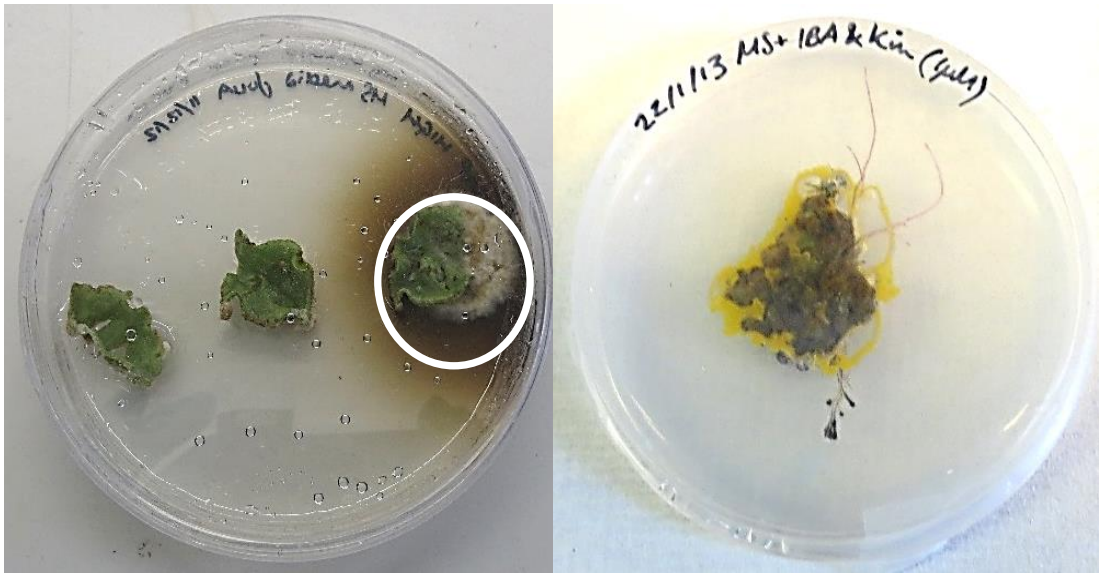

Figure 5-3 Examples of contaminated explants on solid media.

As a result of the initial high contamination rate observed, sterilisation techniques and procedures were reviewed and updated significantly. Firstly, all apparatus which was used to prepare the explants, including scalpel handles and blades, tweezers and spatulas were autoclaved before use. Secondly, all equipment which was used in the flow hood whilst the preparation of the explants and transfer of transplants occurred, including bottles of media, plates and pipettes were thoroughly surface sterilised with 70% IMS before being placed into the flow hood. Thirdly, any stages involving sterile conditions were performed in a larger flow hood which had UV light capability. The flow hood (microflow laminar flow workstation) was run on full with UV lighting for at least 5 minutes with 70% IMS surface sterilisation before use.

Finally, during any procedure involving the explants, breaks were taken on a regular basis between sessions; during which the flow hood was re-sterilised and the UV lamp was switched on for a minimum of five minutes. This was done in order to prevent any microorganisms which may have been introduced in the previous session to be eliminated and prevented from infecting further plates and explants. These changes dramatically reduced the frequency of contamination on the explant plates and allowed generation of callus material from a greater number of explants.

5.4.1.2 Callus grading

Once a substantial amount of callus had been produced, variations were obvious between the different types. Callus can be 'graded' as either friable or solid and also the colouration of the callus differs markedly – red, brown, white or a mixture of the three [168]. Callus tissue was judged by sight as to its colour and texture; these observations were collected and any associations with the media type and regulators used were noted.

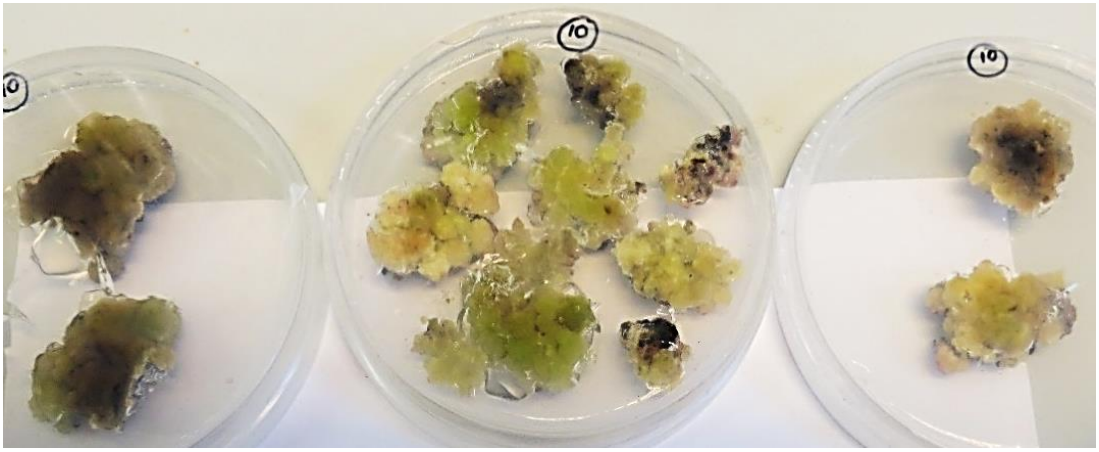

Figure 5-4 Callus development – medium balanced auxin/cytokinin ratio.

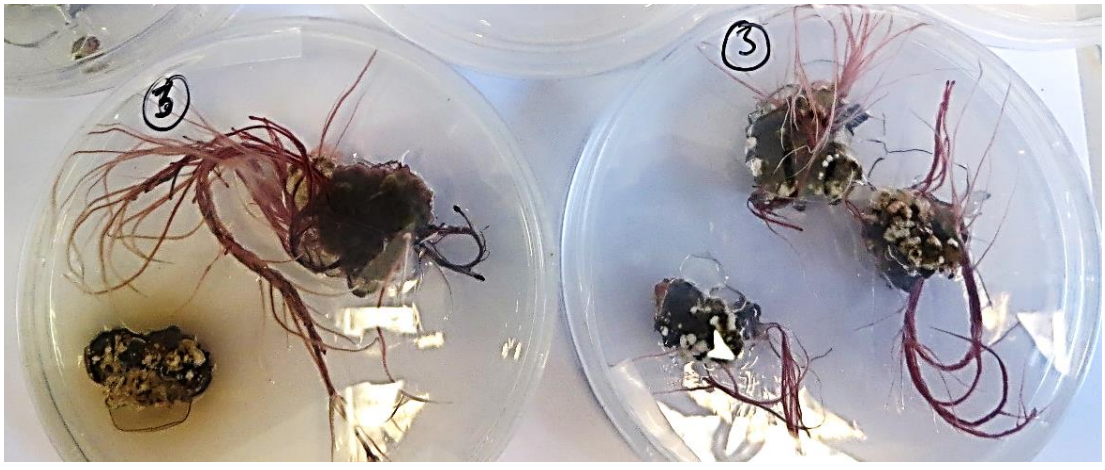

Figure 5-5 Medium auxin low cytokinin root development.

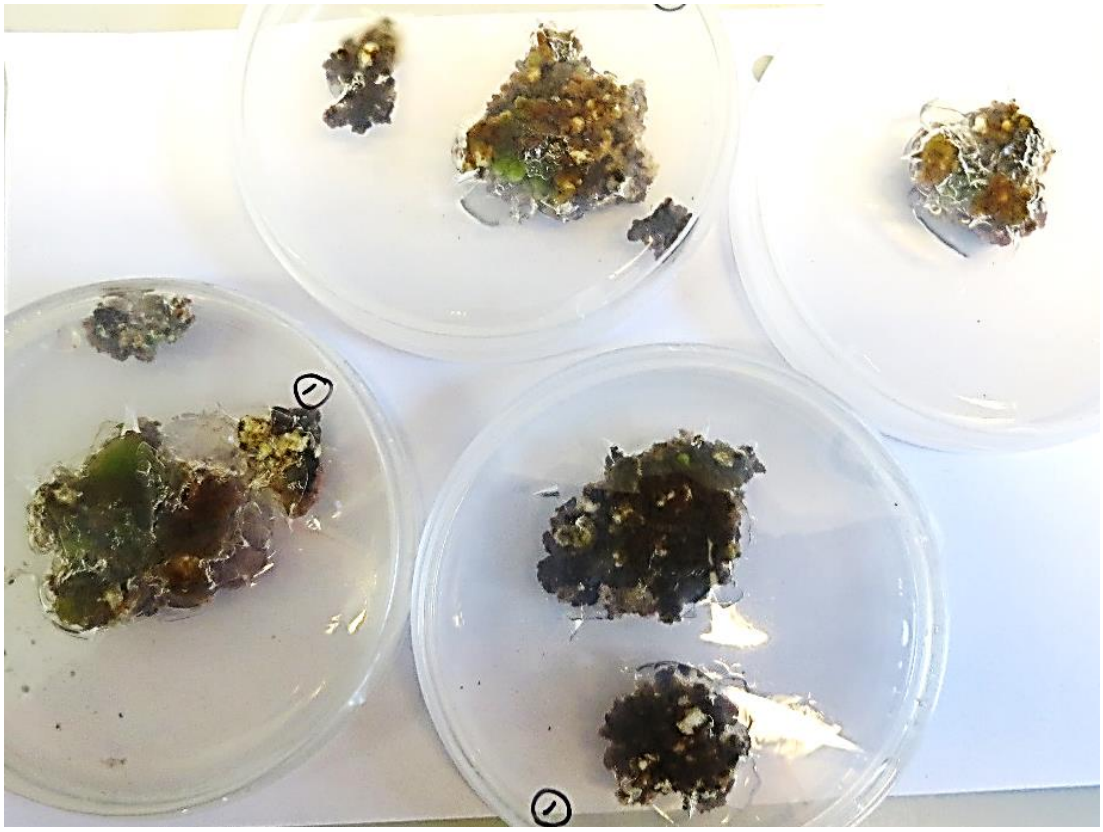

Figure 5-6 Dense callus development.

After analysing the types of callus generated by varying media types and growth regulators, it was found that MS media with a 0.5 – 5.0mg/L IBA and 0.2mg/L BAP balance generated the most friable and fast-growing callus – this corresponds to culture numbers 8 through 10 as seen in Table 5-1. This type of friable callus can be seen in Figure 5-4 and was the most suitable for the initiation of suspension cultures. Characteristics of this type of friable callus were fast growth, a 'fluffy' appearance and soft texture, making pieces easy to separate from the main callus growth to be used for suspension initiation. Figure 5-5 shows callus growth on MS media containing 0.2mg/L IBA with 0.1 mg/L cytokinin, the combination of which can be seen to have induced root growth. Figure 5-6 shows compact callus growth from explants incubated on 0.1mg/L IBA plus 0.1mg/L BAP supplemented MS media.

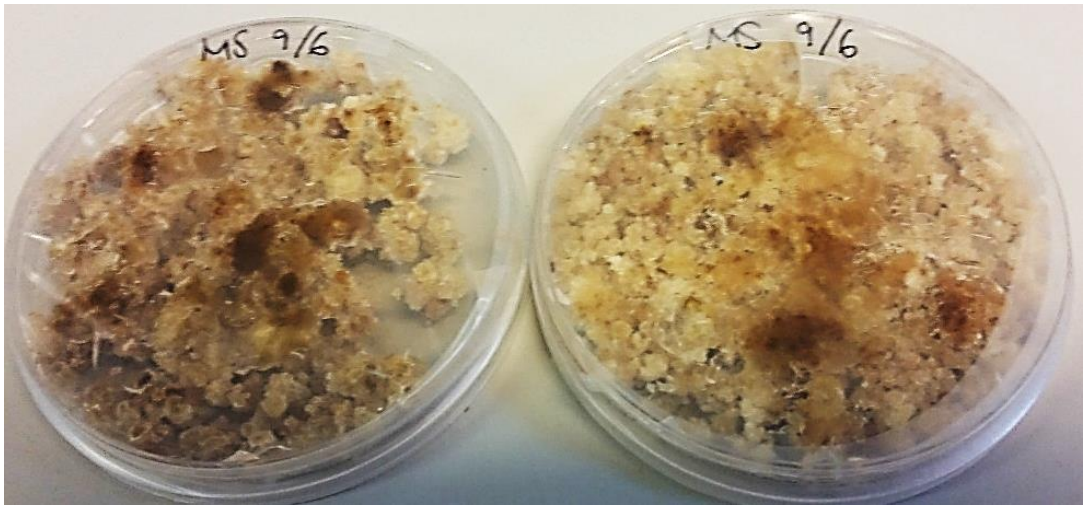

Figure 5-7 Friable callus used for initiation of suspension cultures

Figure 5-7 shows an image of the friable callus type which was used to initiate suspension cultures. This callus had been subcultured several times from callus such as that observed in Figure 5-4 and incubated in the dark at 22℃ - under the same conditions which the suspension cultures were held, as described in section 5.5. The differing colouration of the callus is due to the fact that the callus is incubated in the dark and would therefore contain very low chlorophyll and chloroplast levels.

5.4.1.3 Use of alternative growth regulators

In a similar fashion to that displayed in Table 5-1. 2,4-D and Kinetin were tested for their functionality within the media for explant growth. They were initially paired together and then tested with the parallel regulator to determine which partnership and which concentrations were optimal for *F. japonica* callus growth.

- 2,4-D has a differing and lower range of working concentration as its auxin counterpart IBA: 0.01-6.0 mg/L
- Kinetin has the same working concentration range as its cytokinin counterpart BAP: 0.1-5.0 mg/L

Figure 5-8 is one example of the several IBA & Kin combination trials. As seen in this figure, many of the explants on this regulator combination plate showed

root development – in this case fine roots – hence this combination was not considered for further development. The 2,4-D & BAP regulator combination plates were visibly slow to develop callus from explants compared to the original IBA & BAP combination and was therefore not investigated further. Figure 5-9 shows some of the 2,4-D & Kin trial plates. This regulator combination in general exhibited rapid and friable callus development in comparison to all other plate types. This combination was consequently deemed to be successful and was used extensively throughout the callus development stages in conjunction with the original IBA & BAP regulator combination.

Figure 5-8 An example of IBA & Kinetin test plate – displaying the growth of fine roots from explant material.

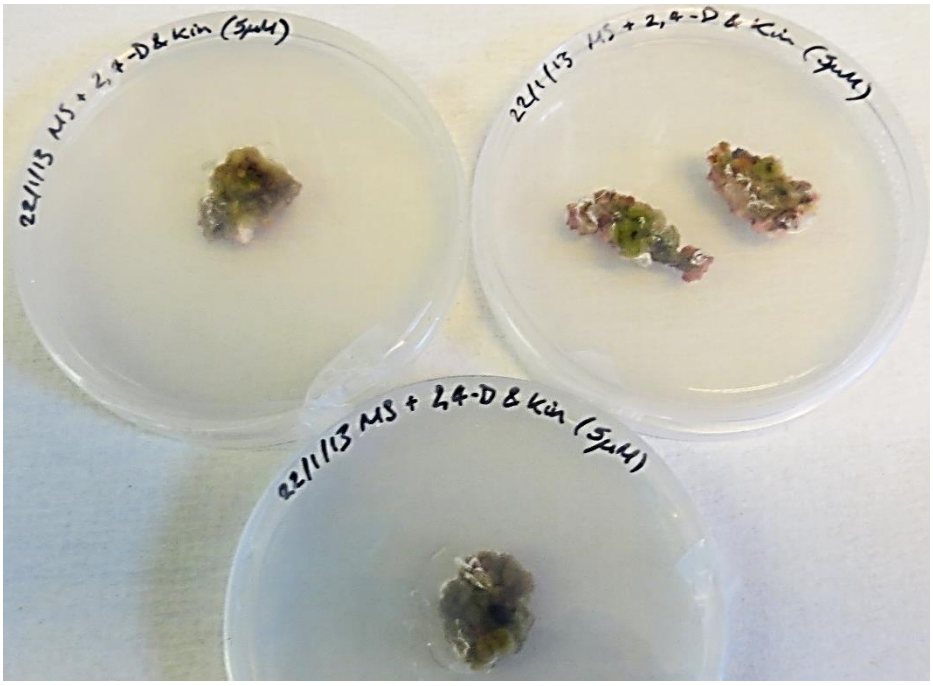

Figure 5-9 2,4-D & kinetin trial plate - rapid callus generation from explants.

5.5 Suspension culture

Suspension culture is an extremely useful tool when working with cells, and has been used extensively within mammalian [184, 185], plant [163, 186] and insect species [187, 188]. It allows dedifferentiated cells to be grown *en masse* and under controlled conditions *in vitro*, thereby allowing an investigator to vary conditions to assay their effects on the cells, promote the production of secondary substances, characterise the growth of a certain cell line and test various drugs such as inhibitors on the cell line to determine their effects.

The impetus for creating suspension cultures from the *F. japonica* species was to increase the amount of plant material available for various assays, including mitochondrial based investigations, to characterise the growth of the culture *in vitro* and to assay the effect of inhibitors upon whole cells and cell extracts.

Friable callus material obtained from plates which was considered to be free from contamination and growing independently from the initial explant was considered for transfer into liquid media for initiation of suspension culture.

5.5.1 Media & growth regulator considerations for suspensions

Initially, liquid media of the same composition as that of the callus solid media (minus the agar or solidification element) was used when transferring the callus into liquid media, as this was thought to be the most stable and least stressful change in environment for the callus cells. The concentration of the growth regulators were also kept constant to the individual callus previous solid media.

This procedure was performed for 3-4 suspension refreshment cycles and reviewed as to its efficiency – which was measured by the visible growth of cells in the media and also the visible viability of the culture, taking into consideration browning or contamination of the cultures. Further research into conditions for suspension culture growth provided various different conditions which were known to be optimal in other plant species – such as *Nicotiana tabacum* (tobacco) [159], *Petunia hybrida* [160], *Stevia rebaudiana* [161], *Coffea arabica* (coffee) [162] and *A. thaliana* [163]. Therefore conditions were altered with a view to optimising growth, both speed and viability within the cultures.

The callus was judged to have become habituated to the suspension when most of the original mass of callus had either broken up or had been filtered from the suspension, and cells are visible and numerous in suspension. The aggregates are removed either by pouring off the suspended cells from the top of the mass in the culture or via sterile filtration. The optimal conditions for the continuing growth of the *F. japonica* cells in suspension were as follows:

- Gamborg B5 media, supplemented with 3% sucrose
- 1mg/ml 2,4-D without addition of cytokinin.

The decision to swap media from MS to GB5 was made as GB5 media is widely recommended as the media in which to grow suspension cells as it contains lower concentrations of inorganic nutrients, which is preferable once cells are growing freely in suspension. These conditions are able to maintain a stable and actively growing suspension culture of *F. japonica* for a minimum of 6 months.

5.5.2 Growth characterisation of suspension cultures

Growth characterisation was achieved using multiple techniques which are detailed in this section. Eighteen samples were set up, 45ml of GB-5 media with 1 mg/ml 2,4-D made up to 50ml total with 5ml of established culture. Three of these cultures were taken to be measured every three days over a period of fifteen days.

5.5.2.1 Contamination testing of suspension cultures

PDA & L-Agar plates were poured and 100µl from each of the three cultures, was plated out in order to test for contamination in the suspension. 100µl of sterile water was also plated onto PDA & L-Agar under the same sterile conditions in a flow hood to act as a control. Details of the plates are discussed in chapter 2. This step was necessary to ensure that the suspension was free from contamination due to bacterial or fungal presence. Any cultures which showed contamination on corresponding plates were disposed of and any assay results from contaminated cultures were not taken into account when analysis took place.

5.5.2.2 Cell counts

Cell counts were performed using a haemocytometer and a light microscope from samples and were analysed to determine the cell density per ml of culture. Details of the method are described in chapter 2 section 2.3.3.

This method proved to be inaccurate due to the nature of the cultures – many of the cultures contained aggregates which were too large to be drawn under the cover slip by the capillary action of the liquid media. This caused the counts to be substantially lower and not fitting with data generated from other methods of culture characterisation. For these reasons, this method was not used in any of the growth characterisation analysis.

5.5.2.3 Cell density

Cell density from each of the cultures was performed as described in chapter 2 section 2.3.3. Each characterisation assay was performed in its entirety at least 3

times with averages taken from each of the three repeats for each point, with sample number representing 3 day increments.

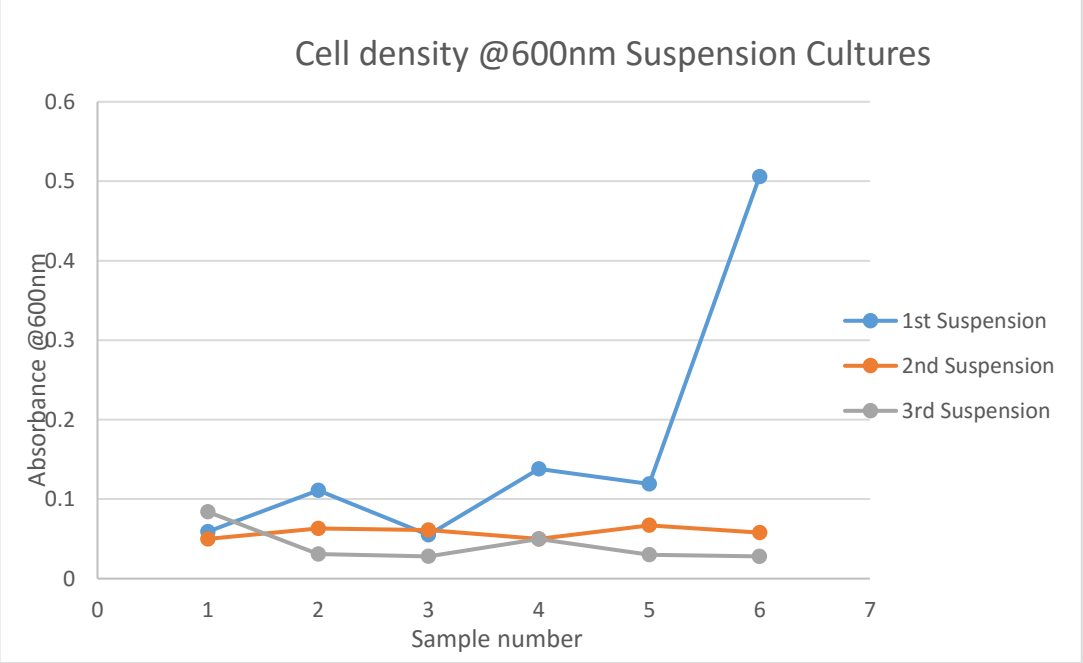

Figure 5-10 Graph showing average cell density @600 nm over three suspension culture experiments. 1st suspension data set shown in blue, 2nd in orange and 3rd in grey.

As can be seen in Figure 5-10 the average density of each of the cultures was variable throughout. The first suspension increased in density, indicating an increase in cell number; the second stayed relatively flat, indicating a stable cell number; the third with a decrease in density, indicating a loss of cells. This may be a factor of the initial culture from which each of the suspensions was set up, as they may have been subcultured at different stages in the cell cycle, effecting the ability of the cells to cope with and grow in the fresh media environment.

5.5.2.4 TTC testing

The triphenyltetrazolium chloride (TTC) assay was used to determine cell viability of the *F. japonica* cell suspensions. Details of this method can be found in chapter 2 section 2.3.3. The viability of each of the cultures was expressed as an absorbance value @492 nm against a blank of fresh media containing the same

additions to that of the cultures. As with the density testing, each assay was repeated a minimum of three times, with three repeats per run.

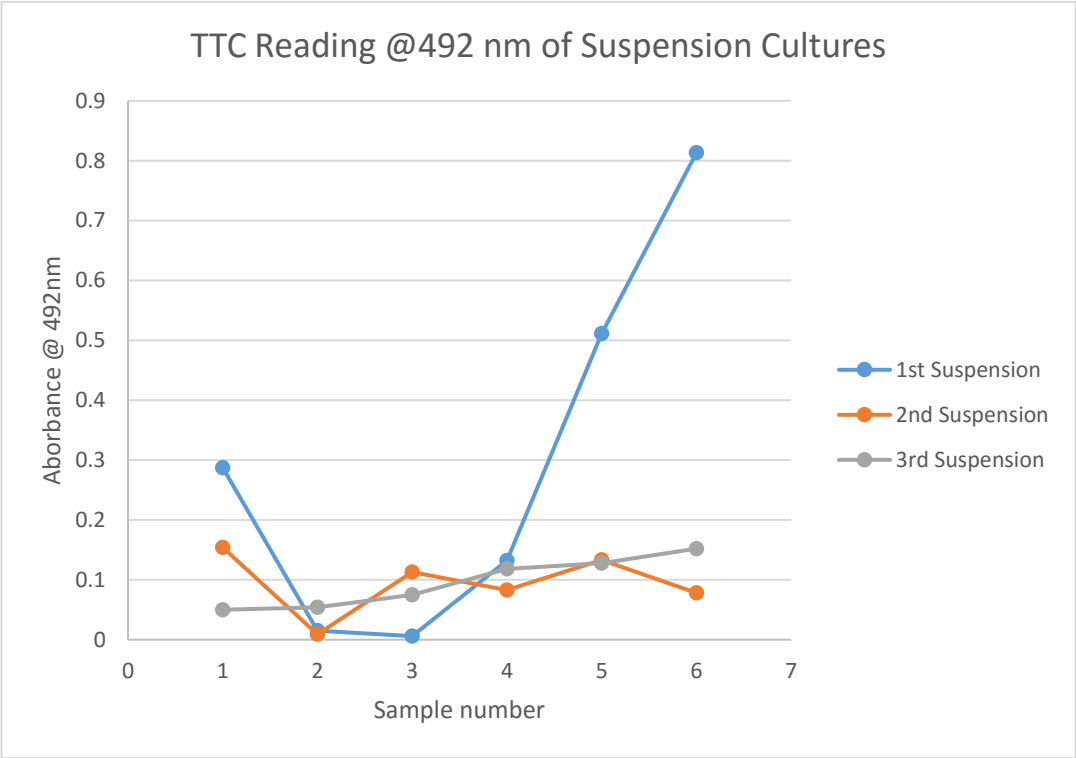

Figure 5-11 Graph showing average cell viability measured by TTC assay over a three suspension experiment series. 1st suspension data set shown in blue, 2nd in orange and 3rd in grey.

Graphs showing the average TTC reading of each suspension are shown in Figure 5-11. The first suspension shows that viability increases over time, which correlates with the first suspension density reading in Figure 5-10, which indicates increasing density. This would be compatible with the idea that more cells would increase the viability reading. The second suspension shows a relatively flat trend, indicating that the viability of the culture does not change. This also correlates with the density readings for the second suspension in Figure 5-10 as this graph also shows a relatively stable density. Finally, the third suspension shows a positive trend of viability, which is at odds with the density readings for this suspension, shown to have a negative trend in Figure 5-10. These results taken together would indicate overall that a smaller amount of cells had an increasing viability in this culture.

5.5.2.5 Dry weights of *F. japonica* cell suspension cultures

Another method of characterisation of *F. japonica* cell suspensions was performed - a measure of the total cell mass within the suspension. The details of the method are seen in chapter 2 section 2.3.3. This method was, as with cell density measurements and TTC assays performed three times, with three repeats per run.

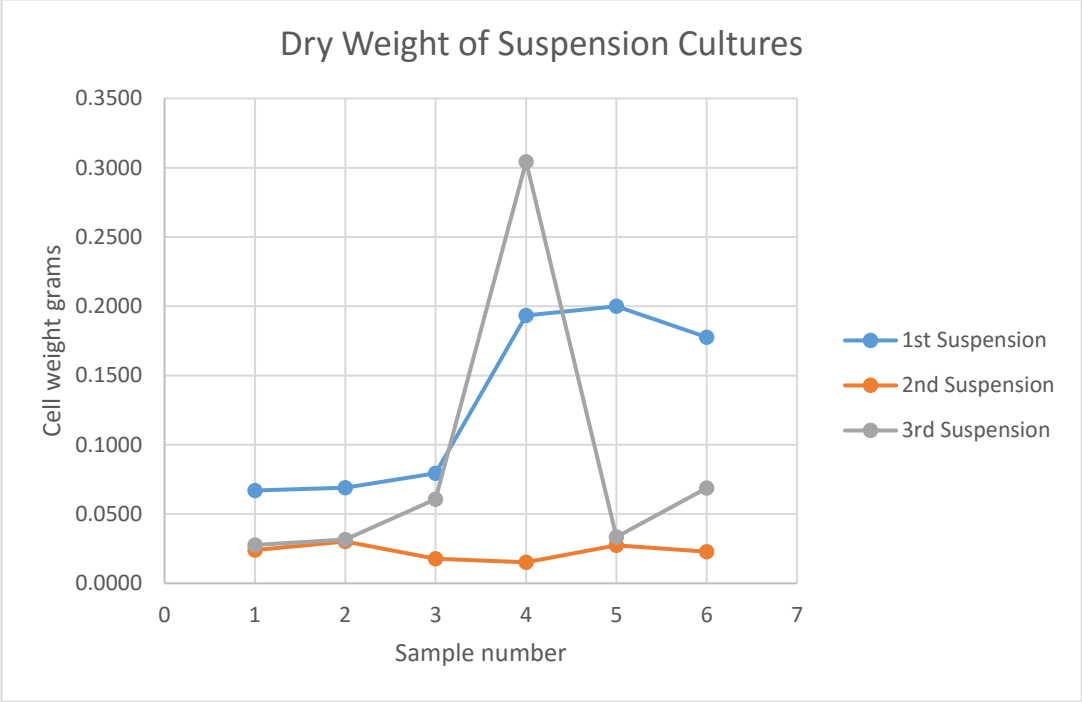

Figure 5-12 Graph showing average dry cell weight in grams of three suspension culture experiments. 1st suspension data set shown in blue, 2nd in orange and 3rd in grey.

Figure 5-12 show the graphs of average dry cell weight of each of the three suspensions. The first suspension shows an increase in dry cell weight. This correlates well with the cell density and viability readings from this culture; all show a positive trend. The data for the second suspension also correlates with the density and viability data from this suspension; all show a relatively flat trend. The third suspension data shown bucks the trend of the density and viability data for this suspension – there is a density decrease, viability remains positive and as shown, there is only a small increase in dry cell weight.

5.6 Summary

This chapter details the stages of initiating and optimisation of *F. japonica* cell culture, from callus generation to cell suspension. This study provides a solid basic protocol for the generation of *F. japonica* cell suspension culture using common laboratory chemicals and equipment.

Optimisation of media, conditions and growth regulators are described, alongside troubleshooting for contamination issues when setting up and subculturing both callus and suspension cultures. Types of callus with regulator conditions which will provide each type, for example rooting callus, friable and dense callus conditions are all described, with friable callus proving the most effective at generation of an actively growing and viable suspension culture.

Three different methods for growth characterisation of suspension cultures are presented; TTC viability testing, density measurements and dry weight determination. Each of these methods has imperfections, due to the inherent variability of the independent growth of each culture. In this case, the all of the methods used to attempt to measure growth are extremely variable, and overall are not consistent enough for a scientific conclusion to be drawn from them. Batch growth of cell suspension would negate these variations as this method provides balanced growth with completely controlled conditions, presenting a homogeneous culture for growth kinetic studies [189]. Batch culture would also be beneficial when testing inhibitors on a cell suspension population, as well as testing for generation of secondary metabolites such as resveratrol – which is discussed in detail in chapter 7.

6 Mass Spectroscopy

6.1 Introduction

Mass spectroscopy measures the mass to charge ratio and abundances of components within a sample [190]. The technique itself was discovered by accident by English physicist J. J. Thomson in 1897 whilst researching the transmission of electricity through gases [191]. Over a hundred years later, the applications of mass spectroscopy have expanded through the worlds of physics to chemistry and biology. Chemists use mass spectroscopy in drug discovery to analyse metabolite reactions and define purity levels in synthesised compounds. In biology and biochemistry, mass spectroscopy has been used in recent years to analyse non-volatile compounds such as peptides and oligosaccharides, allowing the study of the composition of proteins and identification via linked database searching with generated spectra [118].

The basic steps for mass spectroscopy are ionization, acceleration and detection. The mass spectrometer used in the following study was an LQT Orbitrap XL, which ionizes the sample to be analysed via electrospray – effectively creating an aerosol of the sample which passes into the mass analyser. This is achieved via the dispersal of a fine spray of droplets of the sample by forcing the liquid through a tiny capillary (around 1μm tip diameter) under a high voltage [192]. The solvent evaporates and ejects the highly charged ions into the mass analyser at a critical point in the electrical field strength [193]. Nano-flow electrosprays are used, enabling very small amounts of sample (down to the pictogram region [194]) to be analysed, generating multiply charged ions to largely structurally intact biomolecules [195].

In this instrument a linear quadrupole mass analyser is utilised which consists of four parallel metal rods with opposite rods connected electrically, with AC and DC voltage superimposed with a radio frequency. This generates an electrical field through which the ions pass with an oscillation motion, which is unique to each mass

to charge ratio. If the mass to charge ratio is within the pre-set boundaries, the ions will eventually hit the detector and provide a graphical display of the sample composition [193].

Tandem mass spectroscopy is utilized with collision-induced dissociation. This causes fractionation of the peptides by collisions with a neutral gas in the mass analyser instrument [196]. The collisions cause an increase in kinetic energy within the molecule and result in breaking of internal bonds, resulting in fragmentation. The ions are then passed through the analyser to the detector for structural determination in tandem to the first mass detection, increasing specificity and sensitivity in sample identification [197].

In this study, samples containing mitochondrial proteins from both *A. maculatum* and *F. japonica* sources had been separated via SDS-PAGE and BN-PAGE. Prominent bands were excised and digested using trypsin, which is a serine protease most commonly used for the digestion of proteins for mass spectroscopy analysis. Trypsin specifically cleaves protein at the C-terminal side of arginine or lysine residues which results in peptides of varying length sufficient for the generation of a peptide map which is used to identify the protein from a database of theoretical or defined maps [198]. The process of the digestion is described in detail in chapter 2 section 2.10. Each mitochondrial sample was analysed and the constituent proteins identified along with an approximate quantification of each within the sample. *A. maculatum* and *F. japonica* samples are compared in an attempt to explore the protein complement of each of these species mitochondria.

6.2 SDS-PAGE sample preparation for *F. japonica*

The first stage in the mass spectroscopy process was to prepare the samples of interest to be analysed. The separation of the complexes and peptides within the crude mitochondrial samples was achieved using SDS and BN-PAGE, the techniques and advantages of which, along with information relating to processing of the peptides, have been discussed in detail in chapter 2 section 2.6.

Initially, *F. japonica* samples were prepared from an SDS-PAGE gel, the highlighted sections seen in Figure 6-1 excised and processed. These are indicated by the roman numerals I, II & III in the figure. Section I represents at prominent band present at approximately 40 kDa in the *F. japonica* bud mitochondrial preparation, II the equivalent band in the *F. japonica* leaf mitochondrial preparation and III represents the same band from suspension grown *F. japonica*.

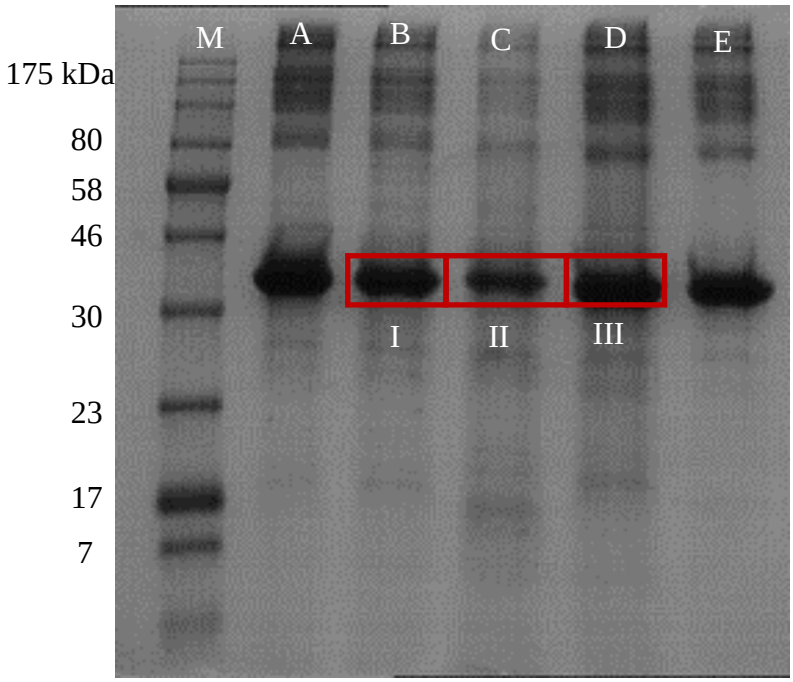

Figure 6-1 10% SDS-PAGE gel with highlighted areas processed for mass spectroscopy. M – protein markers in kDa, A – late bud preparation of *F. japonica* crude mitochondria. B – second preparation of late bud crude mitochondria from *F. japonica*. C – crude mitochondria isolated from *F. japonica* leaves. D – crude mitochondria isolated from suspension culture of *F. japonica* . E – crude mitochondria isolated from a second suspension culture of *F. japonica*.

6.3 Initial mass spectroscopy results for *F. japonica*

The results from sample I of the crude *F. japonica* mitochondria are displayed in Table 6-1. As the *F. japonica* genome has not been sequenced, the information in the table relates to proteins or peptides which are present in the sample that share some homology with other species. Many of the samples contained serum albumin proteins, in this sample both bovine (P02769) and human (P02768) albumin are represented. This is due to residual albumin present in the samples from

the isolation and purification procedures, therefore these albumin results are excluded from Table 6-4 through to Table 6-10. The albumin samples are included in the first three tables to demonstrate the dominance of this protein in the samples. In all samples, various human keratin proteins were also identified. This is due to dust and hair contamination during the sample preparation for mass spectroscopy and have therefore been excluded from all tables in this analysis.

Accession number	Score	Sequence coverage (%)	emPAI
P02769|ALBU_BOVIN	3617	48	9.62
P05493|ATPAM_PEA	693	35	1.25
P02768|ALBU_HUMAN	633	8	0.45
P92549|ATPAM_ARATH	291	23	0.69
A8ACN8|ATPA_CITK8	194	14	0.26

Table 6-1 Top peptide matches from sample I mass spectroscopy.

The data gained from sample I is displayed in Table 6-1. The score column in this table indicates the probability that the observed match is a random event, with 'high' scores representing 'low' probability that the event is random. In this case, and for each of samples I, I and III, an individual ion score of greater than 34 indicates identity or extensive homology to the predicted peptide, as indicated by the peptide score distribution graph seen in Figure 6-2. All of the data presented in this chapter is generated by the Mascot program developed by Matrix Science [199].

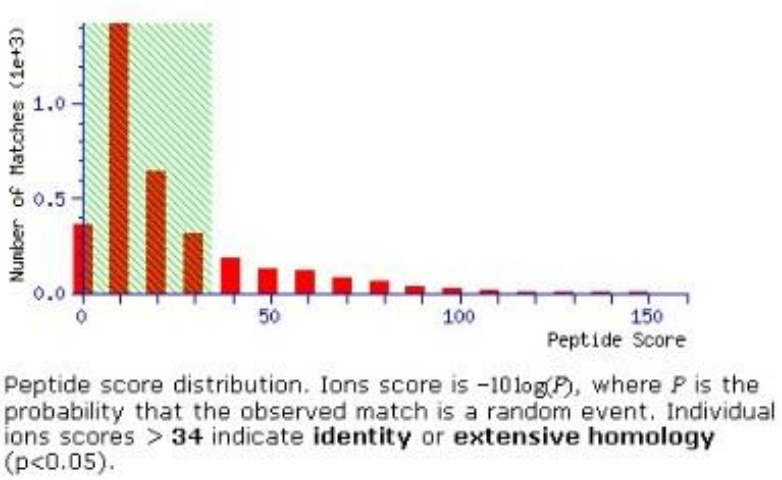

Figure 6-2 Peptide score distribution graph for samples I, II and III.

The sequence coverage column indicates the amount of coverage, in percentage, which the peptide sequence identified in the sample matches the sequenced protein identified from the database searched. Again, the higher this number, the greater coverage of the protein and the higher likelihood that the identification is correct. The emPAI column represents the exponentially modified protein abundance index, which gives an approximate relative quantitation of the identified protein in the sample. The higher the number, the greater the amount of the specific protein in the initial sample. This is a label-free method and quantifies the proteins based on the sequence coverage from the peptide matches in the database result [200]. Much more information is available through the Mascot program for thorough analysis of each peptide identified, however the results presented here are sufficient for an overview of the protein content of each of the excised bands represented in this chapter.

Each table of results is representative of one of the hierarchical clustered ‘families’ of proteins in the Mascot generated report, which attempts to cluster together protein hits into ‘families’ ordered by protein score. The family presented is not necessarily the first protein family in this list for each sample, due to the fact that in many samples, keratin and albumin samples are dominant and therefore are the highest ranking family for that sample. When the presented results are not

representative of the highest ranking family, the family ‘order’ is provided for the sample.

As aforementioned, the albumin samples in Table 6-1 are representative of contamination from the isolation and purification procedure of the mitochondria in this sample and will be disregarded from analysis. The highest scoring predicted protein other than the bovine albumin is the ATPAM_PEA, which is identified as mitochondrial ATP synthase subunit alpha from *Pisum sativum* (garden pea). This is followed by ATPAM_ARATH which is also identified as mitochondrial ATP synthase subunit alpha from the *A. thaliana* plant species. The final potential match is ATPA_CITK8, another ATP synthase subunit alpha protein isolated from the bacteria *Citrobacter koseri*. This bacteria is part of the normal digestive flora in humans [201] and is potentially present in these results due to contamination of the sample. The fact that the mitochondrial ATP synthase subunit alpha is identified from two different plant species from the peptides in this sample is indicative of a high possibility that the *F. japonica* sample I contains a homologous version of this protein.

Accession number	Score	Sequence coverage (%)	emPAI
P02769|ALU_BOVIN	2592	49	9.62
A1XFU0|ATPA_NUPAD	1184	33	2.35
Q01915|ATPM_SOYB	1132	48	3.01
P05492|ATPM_OENBI	1014	45	2.54
P26854|ATPAM_MARPO	669	23	1.24
P92549|ATPAM_ARATH	572	26	1.68
Q85X67|ATPA_PINKO	412	18	0.72
Q9MUT2|ATPA_MESVI	316	10	0.51
A5CQ58|ATPA_CLAM3	241	9	0.39
B3CN53|ATPA_WOLPP	108	6	0.33

Table 6-2 Top peptide matches for sample II mass spectroscopy

The predicted protein data from sample II, which represents the band excised from the leaf isolated mitochondrial sample run on the SDS-PAGE gel in Figure 6-1, is represented in Table 6-2. Disregarding the albumin sample, the highest scoring peptide match is that of ATPA_NUPAD, representing chloroplastic ATP synthase subunit alpha from *Nuphar advena* (yellow pond-lily). This could be indicative that the isolation of mitochondria from the *F. japonica* leaves contained some chloroplast

contamination, therefore containing the chloroplastic version of the ATP synthase subunit alpha which would be present in the thylakoid membranes of the organelle.

The following four peptide matches, ATPM_SOYB from *Glycine hispida* (soybean), ATPM_OENBI from *Onagra biennis* (evening primrose), ATPAM_MARPO from *Marchantia aquatica* (liverwort) and ATPAM_ARATH from *A. thaliana* are all of mitochondrial ATP synthase subunit alpha, which is in accord with the samples from sample I presented in this section. ATPA_PINKO, from *Pinus koraiensis* (Korean pine) and ATPA_MESVI, from *Mesostigma viride* (green algae) are the next matches, both of chloroplastic ATP synthase subunit alpha proteins. This gives a further indication of chloroplastic contamination of this mitochondrial sample. The final two matches are of ATP synthase subunit alpha from bacteria ATPA_CLAM3, *Clavibacter michiganensis* and ATPA_WOLPP, *Wolbachia pipientis* which both have a low sequence coverage score, possibly indicating a high level of sequence homology of the ATP synthase subunit alpha protein throughout taxonomic domains.

Accession number	Score	Sequence coverage (%)	emPAI
P02769|ALBU_BOVIN	4640	53	16.67
P08835|ALBU_PIG	1657	12	0.91
Q01915|ATPAM_SOYB	1025	45	2.37
P05492|ATPAM_OENBI	888	41	1.98
P26854|ATPAM_MARPO	517	24	1.00
P92549|ATPAM_ARATH	457	31	1.25
Q5XLE4|ALBU_EQUAS	162	10	0.60
A4WGF3|ATPA_ENT38	94	14	0.19
Q6V9I6|HDT1_SOLCH	51	2	0.11

Table 6-3 Mass spectroscopy data for sample III

Table 6-3 contains the data generated from the mass spectroscopy of sample III which represents the mitochondrial samples isolated from suspension grown *F. japonica* cells. This sample contained predicted proteins also seen in sample I and II. This is a positive indication that the three methods of mitochondrial isolation from the different *F. japonica* sources are consistent and that the characteristics of the mitochondria do not differ vastly in the leaves, buds and the suspension cells. ATPAM_ARATH is present in all three samples, with ATPAM_SOYBN, ATPAM_OENBI and ATPAM_MARPO, which are all ATP synthase subunit alpha mitochondrial proteins, predicted to be present in sample II and III. The

HDT1_SOLCH predicted peptide is the first indication of a histone deacetylase present in these samples. This has a score of 51 and is predicted from *Solanum chacoense* (wild potato).

6.4 Mass spectroscopy comparison of *F. japonica* & *A. maculatum*

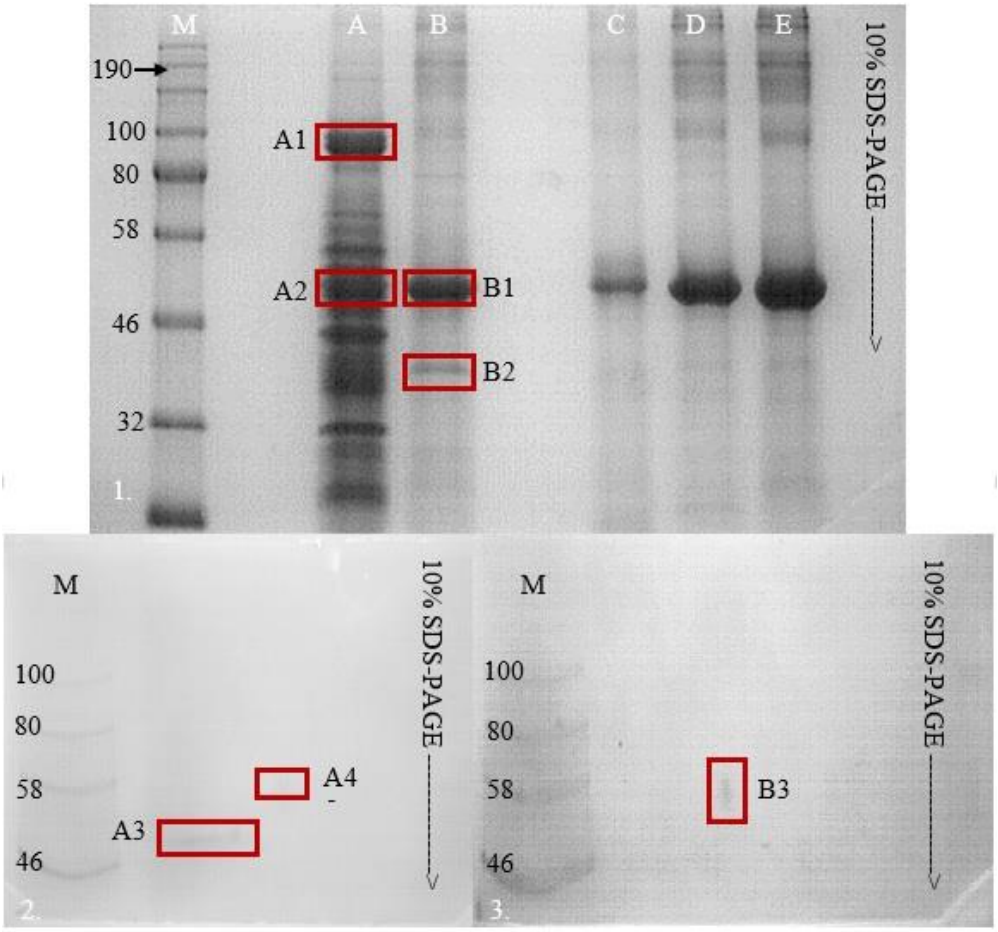

Figure 6-3 Samples taken for mass spectroscopy analysis are highlighted over three gels. GEL 1 (top) – 10% SDS-PAGE gel, M – protein marker, A – *A. maculatum* purified mitochondrial samples, B – *F. japonica* crude mitochondrial preparation, C – crude *F. japonica* mitochondrial sample, D – crude mitochondrial preparation from *F. japonica*. E – crude mitochondrial sample from suspension culture of *F. japonica*. Red boxes indicate bands of gel which were excised and prepared for mass spectroscopy. GEL 2 (BOTTOM LEFT) – BN/SDS- PAGE second dimension gel of *A. maculatum* purified mitochondrial sample. Boxes indicate areas excised for mass spectroscopy and the data labels assigned to them. GEL 3 (BOTTOM RIGHT) - BN/SDS- PAGE second dimension gel of *F. japonica*, with box indicating area excised and prepared for mass spectroscopy. All marker proteins weights are indicated in kDa.

To determine if the data generated for the *F. japonica* mitochondrial samples was in any way comparable to *A. maculatum* data, mitochondrial samples from both species were prepared and electrophoresed on SDS-PAGE and BN/SDS-PAGE gels as described previously (chapter 2 section 2.6). The resulting gels are presented in Figure 6-3, with boxes highlighting areas excised and prepared for mass spectroscopy analysis. For the following samples, all albumin results have been excluded for conciseness. *A. maculatum* has not had its genome sequenced to date, therefore the results are given as closest scoring predicted proteins rather than exact matches. Figure 6-4 shows the peptide score distribution for samples A1-A4 and B1–B3, with a score greater than 42 indicating extensive homology to the identified putative protein.

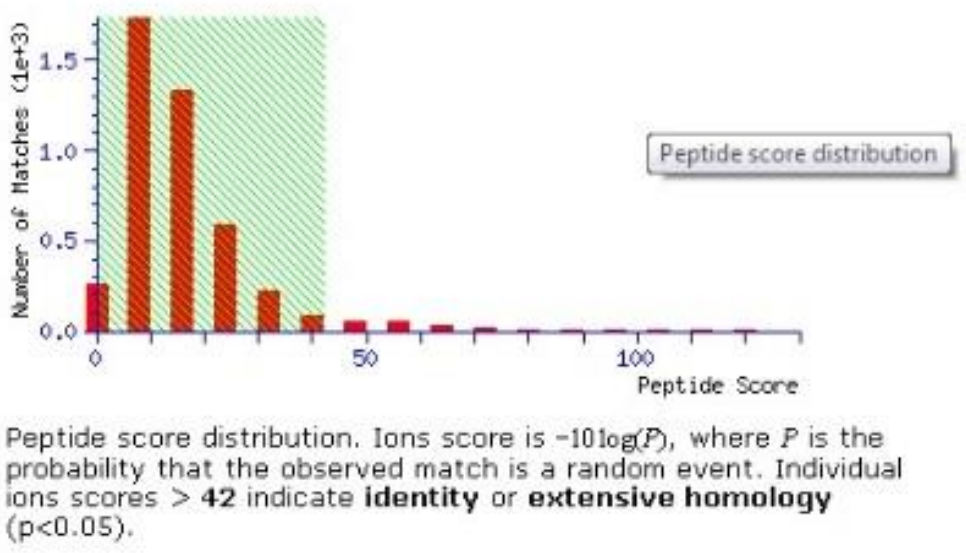

Figure 6-4 Peptide score distribution for second set of mass spectroscopy

Accession number	Score	Sequence coverage (%)	emPAI
Q9SIB9|ACO2M_ARATH	945	48	1.17
P49608|ACOC_CUCMA	660	34	1.13
Q42669|ACOC_CUCMC	483	24	0.42
Q6YZX6|ACOC_ORYSJ	389	26	0.58
Q42560|ACO1_ARATH	369	17	0.75
Q94A28|ACO3M_ARATH	309	5	0.27
O04916|ACOC_SOLTU	247	5	0.61
P09339|ACON_BACSU	53	4	0.07

Table 6-4 Mass spectroscopy data for Arum 1 sample

Table 6-4 represents the data generated from the sample marked A1 in Figure 6-3. This is a prominent band in the *A. maculatum* mitochondrial lane in the figure, whereas the *F. japonica* sample does not show a significant band in this area. As can be seen in Table 6-4, all of the putative identifications in this family are proteins with the designated name starting with 'ACO'. This code refers to the protein being a member of the aconitate hydratase family of enzymes which have an important role as part of the tricarboxylic acid (TCA) pathway during carbohydrate metabolism. All three *A. thaliana* ACO2M, ACO1 and ACO3M proteins are predicted to be present in this sample which comprise the entire second stage of the subpathway – converting oxaloacetate to isocitrate. Also present are the putative ACO proteins from *Cucumis melo*, an oriental melon species, *Oryza sativa*, rice and *Solanum tuberosum*, potato.

Accession number	Score	Sequence coverage (%)	emPAI
Q01859|ATPBM_ORYS	751	35	1.66
P83483|ATPBM_ARATH	642	27	1.01
A1ALL7|ATPB1_PELPD	69	9	0.21
Q8MBQ4|ATPB_IPOCC	58	9	0.13

Table 6-5 Mass spectroscopy data for Arum 2 sample

Table 6-5 represents the data generated from the sample marked A1. All of the predicted peptides in this family are versions of ATP synthase subunit beta. ATPBM_ORYS is a mitochondrial version from *O. sativa*, ATPBM_ARATH, a mitochondrial version from *A. thaliana*, ATPB_IPOCC a chloroplastic version from *Ipomoea coccinea* (flowering plant, scarlet morning glory). The final version is ATPB1_PELPD, which is a bacterial version of the same protein. This band is the equivalent of the *F. japonica* bands excised from Figure 6-3. Interestingly, the subunit identified in the *F. japonica* data in Table 6-1 through Table 6-3 at this location is ATP synthase subunit alpha, whereas in the *A. maculatum* sample, ATP synthase subunit beta is dominant.

Accession number	Score	Sequence coverage (%)	emPAI
Q6YZX6|ACOC_ORYSJ	554	18	0.87
Q9SIB9|ACO2M_ARATH	530	19	0.76
P49608|ACOC_CUCMA	295	19	0.69
Q94A28|ACO3M_ARATH	277	11	0.31
Q42669|ACOC_CUCMC	162	10	0.26

Table 6-6 Mass spectroscopy data for Arum 3 sample.

Table 6-6 represents the data generated from the *A. maculatum* mitochondrial sample A3 as seen in Figure 6-3. This sample was excised from a BN/SDS-PAGE gel, the significance of which was that the sample had gone through another separation process, meaning that hypothetically the sample should be of a greater purity. In this sample once again the 'ACO' identifier is present on all of the predicted proteins, as with the data from the *Arum* 1 sample seen in Table 6-4. This indicates the presence of aconitate hydratase protein, and as with the *Arum* 1 sample, several different versions are identified, ACO2M_ARTAH and ACO3M_ARATH both predicted from *A. thaliana* alone.

Accession number	Score	Sequence coverage (%)	emPAI
Q01859|ATPBM_ORYS	91	8	0.18

Table 6-7 Mass spectroscopy data for Arum 4 sample

Table 6-7 represents the data generated from the *A. maculatum* mitochondrial sample A4 as seen in Figure 6-3, also generated from the second dimension BN/SDS-PAGE gel. The only result generated was of ATPBM_ORYS, a mitochondrial ATP synthase beta subunit from *O. sativa*. This is the same predicted protein which was identified in the *Arum* 2 sample in Table 6-5 and it appears that the second dimension separation of the mitochondrial sample has acted as a purification method, resulting in the single result in this case.

Accession number	Score	Sequence coverage (%)	emPAI
P17614|ATPBM_NICPL	632	31	1.23
B6JD09|ATPB_OLICO	107	7	0.29

Table 6-8 Mass spectroscopy data *F. japonica* B1 sample.

Table 6-8 represents the data generated from the *F. japonica* mitochondrial sample B1 as seen in Figure 6-3. ATPBM_NICPL is an ATP synthase beta mitochondrial subunit from *Nicotiana plumbaginifolia* (Mexican tobacco), ATPB_OLICO another ATP synthase beta subunit from a bacterium, *Oligotropha carboxidovorans*. This excised sample should be essentially the same as sample II in Figure 6-1. Interestingly, the subunit identified in the sample II data in Table 6-2 at this location is ATP synthase subunit alpha, whereas in the B1 sample, ATP synthase subunit beta is dominant. The size difference between the alpha and beta subunits is relatively small: the alpha being approximately 55kDa and the beta approximately

59kDa [202], making it a possibility that excising a few millimetres away from the band in the sample gel and extracting the proteins would give a different result when assayed. It does, however, fit with the *A. maculatum* A2 sample which is taken from the same region of the gel and contains a majority of ATP synthase beta mitochondrial subunit.

Accession number	Score	Sequence coverage (%)	emPAI
P29409|PGKH_SPIOL	200	15	0.42

Table 6-9 Mass spectroscopy data *F. japonica* sample B2

Table 6-9 represents the data generated from the *F. japonica* mitochondrial sample B2 as seen in Figure 6-3. PGKH_SPIOL is a phosphoglycerate kinase putative protein match from *S. oleracea*. This is an enzyme involved in the Calvin cycle, a part of carbohydrate biosynthesis. As can be seen in Figure 6-3, this is the second most prominent band in the *F. japonica* mitochondrial sample when run on 10% SDS-PAGE. It appears to also be present in the *A. maculatum* sample, however there are many more bands of the same or very similar prominence in this region of the *A. maculatum* lane.

Accession number	Score	Sequence coverage (%)	emPAI
Q9SIB9|ACO2M_ARATH	73	7	0.16

Table 6-10 Mass spectroscopy data *F. japonica* B3 sample. Representative of family rank 16

Table 6-10 represents the data generated from the *F. japonica* mitochondrial sample B3 as seen in Figure 6-3. This sample is excised from a second dimension gel BN/SDS-PAGE and contains ACO2M_ARATH, which is also present in the *Arum* 1 and *Arum* 3 samples. This is a member of the aconitate hydratase family of enzymes, which as mentioned previously, has an important role in the TCA pathway during carbohydrate metabolism.

6.5 Conclusion

This chapter contains the details of the mass spectroscopy performed on the peptide samples excised from both SDS-PAGE and 2D BN/SDS-PAGE gels. The aim of these experiments was to determine the major constituents of the prominent bands isolated from the gels representing the mitochondrial samples isolated from both the *F. japonica* and *A. maculatum* plant species. As neither of these plants have had their full genome - or that of their mitochondria - sequenced, the results gained were to be based on homology to other proteins identified within databases of other plant species. As both samples were of mitochondrial source, the expected results were to be that of proteins and enzymes associated with the organelle.

As discussed earlier in the chapter, many of the results contained high levels of albumin and keratin contamination, from the isolation process and hair or dust contamination, respectively. These results were largely excluded from the presented results, however, they were likely to have contributed to the lower emPAI results of the predicted proteins presented within the tables. The proportion of the proteins is based on the entire complement of proteins in the sample, making the overall ratio of the predicted proteins lower when high levels of contamination proteins are present. Improvements to the purification process would lower the amount of albumin contamination and careful handling of isolated protein samples would reduce the keratin levels in the samples.

The first three samples (samples I, II and III) were isolated from 10% SDS-PAGE gels containing mitochondrial samples from three different sources of *F. japonica*. All three samples contained putative ATP synthase alpha subunits of mitochondrial source and ATP synthase alpha subunit of chloroplastic source was identified in sample II, representing the leaf mitochondrial isolation. ATP synthase uses the chemiosmotic proton gradient within membranes to catalyse the formation of ATP from ADP during oxidative phosphorylation [203]. This can be within the mitochondrial membrane, thylakoid membrane in chloroplasts or the cell membrane of bacteria. That this is the prominent protein in all three of the samples it suggests high levels of ATP synthase in the *F. japonica* mitochondrial samples.

In order to compare the *F. japonica* mitochondrial samples, *A. maculatum* mitochondrial samples were prepared for analysis using the same protocol. The *Arum* 2 sample and the B1 sample representing the *F. japonica*, which was isolated from the same region of the SDS-PAGE gel as samples I, II and III of the previous *F. japonica* samples showed a dominance of putative ATP synthase beta subunit. As discussed earlier in the chapter, it could be hypothesised that the samples would concur and both contain the same subunit. The disparity could be due to the small size difference of the alpha and beta subunits in ATP synthase and the likelihood that a small change in the area excised from the gel could result in a different protein being identified. This result, however, confirms that a large proportion of the bands in this region of both species contain some form of ATP synthase protein.

Of the putative proteins isolated from the 2D gels, *Arum* 3 and the *F. japonica* B3 sample both contain versions of aconitate hydratase protein, which is involved in the TCA pathway of carbohydrate metabolism. This is an indication that the *F. japonica* mitochondria contain a large amount of this protein, which may have an indication as to how they generate such a large amount of energy during the initial stages of growth. The consequences of both the aconitate hydratase and ATP synthase presence in the samples will be discussed in further detail in chapter 7.

7 Discussion

7.1 Aim and hypothesis of the project

The aim of this project was to investigate the rapid growth of *F. japonica* at the early stages of growth. It has focused on mitochondria, as they are the main energy producing (in the form of ATP and reducing equivalents) organelle within most eukaryotic cells [202]. The hypothesis was that *F. japonica* bud cells would contain a large amount of mitochondria in order to provide for the huge amount of energy which would be needed for the plant to grow at such a rapid rate, as mitochondrial division and biogenesis within cells is stimulated by energy demand [203].

7.2 Isolated mitochondria from *F. japonica* bud tissue

The first stages of the investigation focused on the isolation of mitochondria from the early plant material; the early emergent buds of *F. japonica*. This process was optimised as much as was possible through the duration of the project, and yet purification of the mitochondria from the plant material was not greatly successful due to lack of overall numbers of mitochondria within the cells, as discussed throughout chapter 2. When assayed using the oxygen electrode, the mitochondrial samples showed very little oxygen reducing activity, which indicated a lack of functional mitochondria within the sample. For comparison, *A. maculatum* spadices were also used for mitochondrial isolation using an established protocol. The *A. maculatum* were used as a comparative sample as the spadices are known to contain a large amount of mitochondria during the thermogenic stage in their growth at which they were harvested. The purification of mitochondria from the *A. maculatum* samples was a great deal more efficacious, with the purified samples displaying much higher oxygen reduction activity when assayed using the oxygen electrode. This gave an indication that the *F. japonica* samples which were isolated from the early buds were not mitochondria rich, which led to further investigation into the cell structure and ultra-structure.

In order to study the *F. japonica* cells, samples were prepared for TEM. After optimising the process of fixation and staining for all of the *F. japonica* samples they were imaged. The TEM pictures clearly show a lack of mitochondria in the sections investigated. Especially, again, in comparison to *A. maculatum* spadix sections which were prepared using the same technique. This information was in agreement with the data gained from the initial mitochondrial isolation from the *F. japonica* buds – there were very few mitochondria within the buds to be purified and the low levels of activity could be due to the overall lack of mitochondria within the samples.

7.3 ***F. japonica* cell culture**

Cell suspension culture was set up using explants taken from *F. japonica* leaves. To the best of our knowledge this had not been attempted before with this species, providing an opportunity for optimisation of the whole cell culture technique based on established protocols designed for different plant species. Once the most fruitful plant growth regulator combination had been discovered and conditions optimised, the *F. japonica* explants were grown successfully on solid media and eventually dedifferentiated friable callus growth was transferred to liquid media as described in section 2.3.2. These cells were grown in incubators until a suspension was created containing free cells and small aggregates. Contamination was a major issue encountered in this process, with initial set up cultures containing both bacterial and fungal contamination. After a complete overhaul of sterile procedure for the whole of the protocol, much of this contamination was eliminated, although not completely eradicated. The cell culture allowed constant access to *F. japonica* cells, and although attempts to characterise the growth and viability were not overtly successful, the basis of creating a cell suspension from *F. japonica* is established in this project.

The mitochondrial isolations attempted on the cell suspensions were subject to the same difficulties as that of the isolation from plant material. The initial purification provided crude mitochondrial fractions, but any further attempt at purification was ineffective. The samples gained showed approximately the same

levels of respiration activity as that of the mitochondria isolated from the *F. japonica* bud mitochondria – the levels of oxygen reduction were very low. Due to the crude nature of the samples, many proteins which are not mitochondrial could potentially be present in the samples, which would increase the level of total protein detected within the sample and decrease the specific activity as a result. Using TEM to visualise the cells from the suspension made clear that very few mitochondria were present in these cells, which concurs with the oxygen electrode assays and all of the results gained from the analysis of *F. japonica* bud mitochondria.

7.2 Mass spectroscopy data

Mass spectroscopy was performed after separation of the crude mitochondrial samples on a variety of gels. The SDS-PAGE gels gave a more general band of peptides in comparison to that of the 2D-BN/SDS-PAGE, which gave a smaller spot of peptides. The excised bands/spots in question are shown again in section 6.4. The bands in the SDS-PAGE gels contained a majority of ATP synthase subunits, as well as some putative aconitate hydratase enzyme. This was true of both the *F. japonica* and the *A. maculatum* samples. The spots excised from the 2D gels again contained a mixture of aconitate hydratase and ATP synthase peptides, with the only *F. japonica* spot visible on the 2D gel containing putative aconitate hydratase. As previously mentioned, neither of these species has a complete sequenced genome – therefore the potential matches are all based upon similarity to other species. The most common sequence homology hits were based on *A. thaliana* peptides and proteins. As discussed in section 6.5, all of the ATP synthase homology was related to the mitochondrial form ATP synthase.

7.2.1 ATP synthase

The mass spectroscopy data gained from the *F. japonica* samples indicate that ATP synthase beta subunit is a very large contributing fraction of the mitochondrial sample. The band marked B1 in Figure 6-3 represents the most dominant band on the SDS-PAGE gel, and as shown in chapter 6, it contains a putative ATP synthase beta subunit - as homologous to that of the sequenced plant

species *Nicotiana plumbaginifolia* (Mexican tobacco). The overall score of 632 and emPAI of 1.23 are very high for this match, where a score over 42 indicates 'identity or extensive homology', this indicates a high degree of confidence that the match is accurate.

ATP synthase is one of the most prevalent proteins on Earth [204], as the generation of ATP is extremely important in providing fuel for almost all cellular energetic cellular activities. Over 60% of the amino acid residues from ATP synthase beta subunit are conserved across kingdoms - bacterial, plants and mammalian [205]. The protein itself is made of two portions, F_O and F_1. F_O is a transmembranous protein located in the inner mitochondrial membrane, the F_1 portion is water soluble and present in the mitochondrial matrix. Together, these portions of ATP synthase use the energy generated by the electrochemical proton gradient to form ATP from ADP and inorganic phosphate [206]. The beta subunit of ATP synthase is part of the F_1 portion of the protein, and contributes to the catalytic site [207]. Unlike the mammalian and bacterial forms of ATP synthase, the plant enzyme is poorly characterised [208]. The ATP synthase complex is discussed in detail in chapter 1. The catalytic site of ATP synthesis is present on the beta subunit in the F_1 complex, which has been shown to be present in large amounts in the *F. japonica* samples when assayed using mass spectroscopy.

As the F_1 subunit of ATP synthase is water soluble, if solublisation of the mitochondrial sample was not thorough, the water soluble proteins present in the F_1 subunit would be dominant in the solublised sample compared to any proteins which would still be membrane bound. This could be a contributing factor to the dominance of the ATP synthase beta subunit found in the *F. japonica* sample – however further solublisation experiments would have to be performed to confirm this hypothesis. This could also be partially responsible for the underrepresentation of other mitochondrial complexes within the sample assayed. If the solublisation was incomplete, the potential of loss of matrix bound complexes would be high and the proteins still bound in the mitochondrial membrane would likely be lost during the solublisation process [209].

7.2.2 Aconitate hydratase

Aconitate hydratase was the second major protein factor found in the mass spectroscopy data. This enzyme catalyses the second step in the tricarboxylic acid (TCA) - the interconversion of citrate isocitrate and cis-aconitate in the mitochondria and cytosol [210]. It is also known to be a mitochondrial oxidative stress sensor [211], due to its high sensitivity to reactive oxygen species in its mitochondrial form [212]. The TCA cycle 'moves' electrons from organic acids to redox cofactors, forming NADH, $FADH_2$, carbon dioxide and one molecule of ATP [144]. The TCA cycle is linked with the electron transport chain, in that succinate dehydrogenase (complex II) participates in both reactions. In this way, the TCA cycle provides ATP and reducing equivalents to be used for further ADP phosphorylation and therefore energy production in the form of additional ATP [213]. As pyruvate is the main substrate for the TCA cycle and is also the major product from glycolysis, this is a link between the two processes [144]. Given the mass spectroscopy results in this project, it may indicate an increase in these two linked pathways as a source of ATP production which is independent from the electron transport chain, providing the plant with energy even when mitochondrial levels are low.

With a score of 73, the presence of this enzyme in the B3 peptide spot excised from the BN/SDS-PAGE gel seen Figure 6-3 is highly likely, as a score of over 42 indicates 'identity or extensive homology'. This is a suggestion that the levels of aconitate hydratase enzyme in the crude mitochondrial samples are high as this is the most dominant spot on the 2D gel. In turn, this gives an indication that the TCA cycle may play a bigger part in the generation of energy within the *F. japonica* cells – perhaps a more efficient TCA cycle within the mitochondria would go some way make up for the lack of overall numbers of the organelle. In order to test this hypothesis, a comparison of TCA cycle levels with other species of plant would need to be drawn and a quantitative measure of the efficiency of the TCA cycle in both *F. japonica* and the chosen comparative species would be essential.

7.3 Summary and future research

This project has explored the invasive plant species *Fallopia japonica*, attempting to discern the mechanism behind the extraordinarily rapid growth it exhibits. It has focused on mitochondria, as the main energy (in the form of ATP) producing organelle within cells.

Isolation of mitochondria was achieved from 'wild grown' plant tissue, as well as suspension grown cells. Purification of the mitochondrial samples was attempted, but proved to require a large amount of resources and plant cells to optimise the procedure; it was therefore not considered to be a viable route for this project.

In order to provide *F. japonica* material year-round, which was not reliant on the species growth season, cell culture was set up from leaf explants of *F. japonica*. This was a novel protocol which was optimised from various successful protocols for different plant species in the literature [153, 159-161, 163, 165, 168]. This project contains an optimised protocol for the generation of cell culture from *F. japonica* leaf explants, through callus and callus optimisation to transfer and maintenance of suspension cell culture.

The TEM images acquired from various *F. japonica* sources indicate that very few mitochondria are present in the plant cells, in comparison to other high energy demanding plant cells – as shown with the comparison to *A. maculatum*. This data concurs with the mitochondrial isolation results and the data gained from the assays performed on these samples. Many previous studies have shown the correlation between increased mitochondrial numbers and fast growing plant tissues, some examples of these studies can be seen in Table 7-1.

Author and year	Major findings
Griffin et al. 2000 [224]	Increase in mitochondrial numbers in fast growing cells in an elevated CO_2 environment.
Colaço et al. 2012 [225]	Mitochondrial numbers increase in fast growing pollen tubes in various plant species.
Robertson et al. 1995 [226]	Mitochondrial levels increase three-fold in young wheat leaves grown in elevated CO_2.
Tissue et al. 2002 [227]	Increase of mitochondrial levels in sweetgum (*Liquidambar styraciflua*) high canopy leaves
Welchen 2013 [228]	Actively growing plant cells display increased numbers of mitochondria.

Table 7-1 Examples in the literature of evidence of increased mitochondrial number in growing plant tissues.

The hypothesis throughout this project was that *Fallopia japonica* would require huge amounts of energy in order to grow at the explosive rates observed both in the wild and when grown under controlled conditions. It is generally recognised that cells with high energy demands have an increased number of mitochondria, as the majority of ATP is synthesised by mitochondria in not only plants but also animals and fungi [144]. Overall, the initial hypothesis that mitochondria would be numerous in the *F. japonica* cells has proved to be false, confirmed by the combination of the oxygen electrode results, TEM and attempts to isolate mitochondria from both wild grown plant material and cell culture. Some alternative hypotheses are explored briefly below.

The mass spectroscopy data has provided another potential hypothesis – if proteins such as ATP synthase and aconitate hydratase are upregulated within *F. japonica*, it could be possible that the mitochondria within the plant are more efficient due to a higher level of ATP generation per unit, if they were to contain more of the enzymes required in the generation of ATP. This does not however,

explain the low levels of activity found when the mitochondria are isolated from the plant material or suspension cells. As eluded to earlier in this chapter, a comparison of levels of enzymes would be required to determine if these proteins are indeed upregulated in *F. japonica*. This could be achieved using the Northern blotting technique. For example; to detect the presence of ATP synthase beta subunit mRNA, isolated total sample RNA would be run on a SDS-PAGE (or other denaturing) [214] gel before hybridisation probing using a cDNA of the protein sequence – potentially using the *A. thaliana* ATP synthase beta subunit as a homology match [215]. As the beta subunit is nuclear encoded and the alpha is synthesised in the mitochondria [216], using different probes for each subunit could provide data on mitochondrial and nuclear levels of gene expression and protein synthesis. This technique could also allow analysis of differential gene expression throughout time and growth stages of the plant or cell culture [217]. Northern blotting, again, could potentially be used for this investigation into energy production.

Another potential route of investigation would be that of glycolysis levels within the plant cells. As the mitochondria do not seem to be numerous within the cells, and are not active when isolated, potential cytosolic enzymes, such as enzymes involved in glycolysis could be upregulated and providing a large amount of energy for plant growth. In cancer cells, energy production is preferentially derived from glycolysis rather than the respiratory pathway [218]. This phenomenon is known as the Walberg effect [219]. Measurement of glycolytic levels and inhibiting key enzymes in the pathway such as phosphofructokinase (PFK) [220] would allow analysis of the levels of glycolysis within the cells. PFK catalyses the first committed step of glycolysis, the conversion of fructose-6-phosphate to fructose-1,6- bisphosphate [213]. The use of equipment, such as a Seahorse (Seahorse Bioscience) using kits to measure mitochondrial respiration and glycolytic levels in real time in micro volumes would be invaluable for future research into this area.

As discussed in Chapter 1, the most popular and commonly used herbicides rely on disruption of protein synthesis within plants. This project provides an alternative way of looking at control of growth of *F. japonica*, as by determining how the plant generates energy for growth, it provides new potential targets for inhibition. Generation of *F. japonica* knockout mutants for either ATP synthase subunit beta or PFK, or indeed using RNA interference to silence these genes [208] could provide a wealth of information as to the effects of knocking out these enzymes on the growth and survival of *F. japonica*. These results could lead to novel inhibitor design, based on a fundamentally different system of preventing energy production within the plant. As the herbicide market is estimated to be worth $30 billion dollars worldwide by the year 2019 [221] and current herbicide resistance is increasing across the world to levels that threaten agriculture viability [222], the generation of new herbicides with different mode of actions are required and would be extremely valuable to agricultural productivity [223].

8 References

1. His Majesty The Emperor of, J., *Linnaeus and taxonomy in Japan.* Nature, 2007. **448**(7150): p. 139-140.

2. Jokl, D.H.K., Hiyama, F., *Philipp Franz von Siebold A Medical Pioneer of the 250- Year Holland-Japan Legacy.* Arch ophthalmol, 2003. **121**: p. 562-565.

3. Bailey, J.P., Conolly, A.P., *Prize-winners to pariahs - A history of Japanese Knotweed s.l. (Polygonaceae) in the British Isles.* Watsonia, 2000. **23**: p. 93-110.

4. Makino, T., *Polygonum reynoutria (Houtt.) Makino.* . Botanical Magazine Tokyo, 1901. **15**(84).

5. Ronse Decraene, L.P., Akeroyd, J. R., *Generic limits in Polygonum and related genera (Polygonaceae) on the basis of floral character.* Botanical Journal of the Linnean Society, 1988. **98**: p. 921-971.

6. Stace, C.A., *New Flora of the British Isles*. 1991, Cambridge: Press Syndicate of the University of Cambridge.

7. Bailey, J.P., Stace, C.A., *Chromosome number, morphology, pairing, and DNA values of species and hybrids in the genus Fallopia (Polygonaceae).* Plant Systematics and Evolution, 1992. **180**: p. 29-52.

8. Bram, M.R., McNair, J.N., *Seed Germinability and Its Seasonal Onset of Japanese Knotweed (Polygonum cuspidatum).* Weed Science, 2004. **52**(5): p. 759-767.

9. Child, L., Wade, M., *The Japanese Knotweed Manual*. 2000, Chichester: Packard Publishing

10. Conolly, A.P., *The distribution and history in the British Isles of some alien species of Polygonum and Reynoutria.* Watsonia, 1977. **11**: p. 291-311.

11. Synge, P., M., *The R.H.S. Suppliment to the Dictionary of Gardening*. 1956, Oxford: Oxford University Press.

12. Siebold, P.F., *Extrait du catalogue et du prix-courant des plantes du Japon et des Indes-Orientales et Occidentales Neerlandaises.* Jaarbook Van de Koninklijke Nederlandsche Maatschappij tot Aanmoediging van den Tuinbouw, 1848: p. 38-49.

13. Storrie, J., *The Flora of Cardiff*. 1886, Cardiff.

14. Walters, C., *The Park Flora.* J. Oldham microsc. Soc. Fld Club, 1887. **1**(4).

15. Anon., *Polygonum cuspidatum.* Journal of the Royal Horticultural Society, 1905.
29(180).

16. Davey, F.H., *Flora of Cornwall*. 1909, Penryn.

17. Hollingsworth, M.L., Bailey, J.P., *Evidence for massive clonal growth in the invasive weed Fallopia japonica (Japanese Knotweed).* Botanical Journal of the Linnean Society, 2000. **133**: p. 463-472.

18. Kurose, D., Renals, T., Shaw, R., Furuya, N., Takagi, M., Evans, H., *Fallopia japonica, an increasingly intractable weed problem in the UK: Can fungi help cut through this Gordian knot?* Mycologist, 2006. **20**(4): p. 126-129.

19. Council, C. *Japanese Knotweed*. 2012 [cited 2012 26/01];
Available from:
http://www.cornwall.gov.uk/default.aspx?page=13789.

20. Council, D. *Biodiversity - Japanese Knotweed*. 2012 [cited 2012 26/01];
Available from:
http://www.devon.gov.uk/environment/natural_environment/biodiversity/japanese_kn otweed.htm.

21. *Wildlife and Countryside Act 1981*. [cited 2012 26/01];
Available from:
http://www.legislation.gov.uk/ukpga/1981/69.

22. *Environmental Protection Act 1990*. 1990 [cited 2012 30/01];
Available from:
http://www.legislation.gov.uk/ukpga/1990/43/section/34.

23. *Japanese Knotweed Alliance*. [cited 2012 30/01/2012]; Available from:
http://www.cabi.org/japaneseknotweedalliance/default.aspx?site=139&page=355.

24. F. Williams, R.E., A. Harris, D. Djeddour, C. Pratt, R.S. Shaw, S. Varia, J. Lamontagne-Godwin, S.E. Thomas, S.T. Murphy, *The Economic Cost of Invasive Non-Native Species on Great Britain*, in *Knowledge for life*. 2010, Centre for Agriculture and Biosciences International.

25. Species, N.-E.N.o.I.A., *European Network on Invasive Alien Species*

26. Agency, E.E., *The impacts of invasive alien species in Europe.* Technical reports 2012. **16**.

27. Celesti-Grapow, L., et al., *Inventory of the non-native flora of Italy.* Plant Biosystems

- An International Journal Dealing with all Aspects of Plant Biology, 2009. **143**(2): p. 386-430.

28. Nobanis, S.o., *Risk-mapping for 100 non-native species in Europe*. 2012, NOBANIS - European Network on Invasive Alien Species: Copenhagen.

29. Bailey, J.P., Bímová, Kateřina., Mandák, Bohumil., *The potential role of polyploidy and hybridisation in the further evolution of the highly invasive Fallopia taxa in Europe.* Ecological Research, 2007. **22**(6): p. 920-928.

30. Engler, J., K. Abt, and C. Buhk, *Seed characteristics and germination limitations in the highly invasive Fallopia japonica s.l. (Polygonaceae).* Ecological Research, 2011. **26**(3): p. 555-562.

31. Shiosaka H, S.O., *Morphological changes in Polygonum cuspidatum Sieb. et Zucc. Reciprocally transplanted among different altitudes.* Japanese Journal of Ecology, 1993. **43**: p. 31-37.

32. Bailey, J.P., K. Bímová, and B. Mandák, *Asexual spread versus sexual reproduction and evolution in Japanese Knotweed s.l. sets the stage for the "Battle of the Clones".* Biological Invasions, 2008. **11**(5): p. 1189-1203.

33. Adachi, N., Terashima, I., Takahashi, M., *Central Die-back of Monoclonal Stands of Reynoutria japonica in an Early Stage of Primary Succession on Mount Fuji.* Annuals of Botany, 1996. **77**(477-486).

34. Adachi, N., Terashima, I., Takahashi, M., *Mechanisms of Central Die-back of Reynoutria japonica in the Volcanic Desert on Mt. Fuji. A Stochastic Model Analysis of Rhizome Growth.* Annals of Botany, 1996. **78**: p. 169-179.

35. Adachi, N.T., Takahashi, I., M., *Nitrogen translocation via rhizome systems in monoclonal stands of Reynoutria japonica in anoligotrophic desert on Mt Fuji: Field experiments.* Ecological Research, 1996. **11**: p. 175-186.

36. Chiba, N., Hirose, T. *Nitrogen acquisition and use in three perennials in the early stage of primary succession.* Functional Ecology, 1993. **7**: p. 287-292.

37. Hirose, T., Tateno, M., *Soil nitrogen patterns induced by colonization of Polygonum cuspidatum on Mt. Fuji.* Oecologia, 1984. **61**: p. 218-223.

38. Suzuki, J.I., *Growth Dynamics of Shoot Height and Foliage Structure of a Rhizomatous Perennial Herb, Polygonum cuspidatum.* Annals of Botany, 1994. **73**: p. 629-638.

39. Zhou, Z., et al., *Patch establishment and development of a clonal plant,*

Polygonum cuspidatum, on Mount Fuji. Molecular Ecology, 2003. **12**(6): p. 1361-1373.

40. Yamamoto, T., et al., *Basaltic pyroclastic flows of Fuji volcano, Japan: characteristics of the deposits and their origin.* Bulletin of Volcanology, 2005. **67**(7): p. 622-633.

41. Bashtanova, U.B., K.P. Beckett, and T.J. Flowers, *Review: Physiological Approaches to the Improvement of Chemical Control of Japanese Knotweed (Fallopia japonica).* Weed Science, 2009. **57**(6): p. 584-592.

42. Bailey, J.P., *Japanese Knotweed s.l. at home and abroad*. Plant Invasions: Ecological Threats and Management Solutions 2003, Leiden Backhuys Publishers.

43. David J. Beerling, J.P.B., Ann P. Conolly, *Fallopia japonica (Houtt.) Ronse Decraene*. Journal of Ecology, 1994. **82**(4): p. 959-979.

44. Smith, J.M.D., et al., *A simulation model of rhizome networks for Fallopia japonica (Japanese knotweed) in the United Kingdom.* Ecological Modelling, 2007. **200**(3-4): p. 421-432.

45. Brock J.H., W.M. *Regeneration of Japanes knotweed (Fallopia japonica) from rhizome and stems: Observation from greenhouse trials.* in *Proc. IXth Intern. Symp. on the Biology of Weeds.* 1992. Dijon.

46. Brock J.H., C.L.E., de Waal L.C. and Wade P.M., *The invasive nature of Fallopia japonica is enhanced by vegetative regeneration from stem tissues.* Plant Invasion– General Aspects and Special Problems., ed. P.K. Pyšek P., Rejmánek M. and Wade M. 1995, Amsterdam: SPB Academic Publishing.

47. Brock, J.H., *Vegetative Regeneration of Japanese Knotweed*. 2007, Arizona State University.

48. Moravcová, L., et al., *Potential phytotoxic and shading effects of invasive Fallopia (Polygonaceae) taxa on the germination of native dominant species.* NeoBiota, 2011. **9**(0): p. 31.

49. Reinhardt, F., Herle, M., Bastiansen, F., Streit, B. , *Economic Impact of the Spread of Alien Species in Germany* 2003, Federal Environmental Agency: Berlin.

50. Authority, O.D., *Learning Legacy* in *Treating Japanese Knotweed on the Olympic Park.* 2011, London Organising Committee of the Olympic Games and Paralympic Games Limited (LOCOG) London.

51. Agency, E. *Japanese Knotweed Code of Practice*. 2006 [cited 2012 3/02]; Available from: http://www.environment-agency.gov.uk/static/documents/Leisure/Knotweed_CoP.pdf.

52. Surveyors, R.I.o.C., *Japanese knotweed and residential property,*

R.I.o.C. Surveyors, Editor. 2012: Coventry, UK.

53. Awford, J., *Homeowner discovers house has lost half its value after Japanese knotweed invaded her back garden and started taking it over*, in *The Daily Mail*. 2014.

54. *Lancashire Invasive Species Project*. 2010 [cited 2012 03/02]; Available from: http://www.lancashireinvasives.org/pages/8_japanese_knotweed.

55. Shaw, R.H., S. Bryner, and R. Tanner, *The life history and host range of the Japanese knotweed psyllid, Aphalara itadori Shinji: Potentially the first classical biological weed control agent for the European Union.* Biological Control, 2009. **49**(2): p. 105- 113.

56. *The Potential Agents*. 2010 [cited 2012 06/02]; Available from: http://www.cabi.org/japaneseknotweedalliance/?site=139&page=356.

57. Beckett, K.P., *Response to Consultation on the Release of a non-native Biocontrol Agent for the Control of Japanese Knotweed*. 2009, Phlorum.

58. Shaw, R., *Progress with weed biocontrol projects*, in *Knowledge for life*, C.i.t. UK, Editor. 2013, CABI.

59. Duke, S.O. and S.B. Powles, *Glyphosate: a once-in-a-century herbicide.* Pest Management Science, 2008. **64**(4): p. 319-325.

60. Briggs, J.A., T. Whitwell, and M.B. Riley, *Remediation of Herbicides in Runoff Water from Container Plant Nurseries Utilizing Grassed Waterways.* Weed Technology, 1999. **13**(1): p. 157-164.

61. Barney, J.N., Nishanth, T., DiTommaso, A., Bhowmik, P.C., *The Biology of Invasive Alien Plants in Canada. 5. Polygonum cuspidatum Sieb. & Zucc. [= Fallopia japonica (Houtt.) Ronse Decr.]*. CANADIAN JOURNAL OF PLANT SCIENCE, 2006. **86**(887-905).

62. Beerling, *The use of non-persistent herbicides, glyphosate and 2,4-D amine to control riparian stands of japanese knotweed (Reynoutria japonica Houtt.).* Regulated Rivers: Research & Management, 1990. **5**: p. 413-417.

63. Soll, J. *Controlling Knotweed (Polygonum cuspidatum, P. sachalinense, P. polystachyum and hybrids) in the Pacific Northwest*. The Global Invasive Species Initiative, 2004.

64. McCourt, J.A. and R.G. Duggleby, *Acetohydroxyacid synthase and its role in the biosynthetic pathway for branched-chain amino acids.* Amino Acids, 2006. **31**(2): p. 173-210.

65. Pue, N. and L.W. Guddat, *Acetohydroxyacid synthase: a target for antimicrobial drug discovery.* Curr Pharm Des, 2014. **20**(5): p. 740-53.

66. Figueroa, P., *Japanese knotweed herbicide screening trial applied as a roadside spray*. Proc. West. Soc. Weed Sci., 1989. **42**: p. 288-298.

67. Mandy Tu, C.H., John M. Randall, *Weed Control Methods Handbook: Tools and Techniques for Use in Natural Areas*. 2001, The Nature Conservancy: California, USA.

68. Flasiński, M. and K. Hąc-Wydro, *Natural vs synthetic auxin: Studies on the interactions between plant hormones and biological membrane lipids.* Environmental Research, 2014. **133**: p. 123-134.

69. Grossmann, K., *Auxin Herbicide Action: Lifting the Veil Step by Step.* Plant Signaling & Behavior, 2007. **2**(5): p. 421-423.

70. Grossmann, K., *Auxin herbicides: current status of mechanism and mode of action.*
Pest Manag Sci, 2010. **66**(2): p. 113-20.

71. Borzenkova, R., Sobyanina, E., Pozdeeva, A., Yashkov, M., *Effect of phytohormones on starch-synthesizing capacity in growing potato tubers.* Russ. J. Plant Physiol., 1998. **45**: p. 472-480.

72. Simko, I., *Sucrose application causes hormonal changes associated with potato tuber induction.* J. Plant Growth Regul., 1994. **13**: p. 73-77.

73. Drozdova, I., Bondar, V., Bukhov, N., Kotov, A., Kotova, L., Maevskaya, S., Mokronosov, A., *Effects of light spectral quality on morphogenesis and source-sink relations in radish plants.* Russ. J. Plant Physiol., 2001. **48**: p. 415-420.

74. Dauer, J.T. and E. Jongejans, *Elucidating the Population Dynamics of Japanese Knotweed Using Integral Projection Models.* PLoS ONE, 2013. **8**(9): p. e75181.

75. Schnitzler, A., Muller, S., *Ecology and biogeography of highly invasive plants in Europe: giant knotweeds from Japan (Fallopia japonica and F. sachalinensis).* Revue d'Ecologie, 1998. **53**(1).

76. Bailey, J.P., Waal,L.C. de, Child, L.E., Wade P.M. and Brock, J.H., *The reproductive biology and fertility of Fallopia japonica (Japanese Knotweed) and its hybrids in the British Isles.*, in *Ecology and management of invasive riparian plants*. 1994, John Wiley and Sons: Chichester. p. 141-158.

77. Hrušková, H.H., J., *Regeneration of knotweed (Reynoutria spp.) from stem cuttings.* Acta Universitatis Agriculturae et Silviculturae

Mendelianae Brunensis 1999. **47**(3): p. 73-76.

78. Dassonville, N., et al., *Invasion by Fallopia japonica increases topsoil mineral nutrient concentrations.* Ecoscience, 2007. **14**(2): p. 230-240.

79. Ungvari, Z., et al., *Mitochondrial protection by resveratrol.* Exercise and sport sciences reviews, 2011. **39**(3): p. 128-32.

80. Lyons, M.M., et al., *Resveratrol in raw and baked blueberries and bilberries.* J Agric Food Chem, 2003. **51**(20): p. 5867-70.

81. Smoliga, J.M., J.A. Baur, and H.A. Hausenblas, *Resveratrol and health - A comprehensive review of human clinical trials.* Molecular Nutrition & Food Research, 2011. **55**(8): p. 1129-1141.

82. Jang, M., *Cancer Chemopreventive Activity of Resveratrol, a Natural Product Derived from Grapes.* Science, 1997. **275**(5297): p. 218-220.

83. Hain, R., Bieseler, B., Kindl, H., Schroder, G., Stocker, R., *Expression of a stilbene synthase gene in Nicotiana tabacum results in synthesis of the phytoalexin resveratrol.* Plant Molecular Biology, 1990. **15**: p. 325-335.

84. Yu, C.K., et al., *Constitutive accumulation of cis-piceid in transgenic Arabidopsis overexpressing a sorghum stilbene synthase gene.* Plant & cell physiology, 2006. **47**(7): p. 1017-21.

85. Kiselev, K.V., *Perspectives for production and application of resveratrol.* Applied microbiology and biotechnology, 2011. **90**(2): p. 417-25.

86. Vastano, B.C., et al., *Isolation and Identification of Stilbenes in Two Varieties of Polygonum cuspidatum.* Journal of Agricultural and Food Chemistry, 2000. **48**(2): p. 253-256.

87. Information, N.C.f.B., U.S.N.L.o. Medicine, Editor. 2015, U.S. National Library of Medicine: Bethesda, MD.

88. de la Lastra, C.A., Villegas, I., *Resveratrol as an antioxidant and pro-oxidant agent: mechanisms and clinical implications.* Biochemical Society Transactions, 2007. **35**(5): p. 1156-1160.

89. Yen, G.-C., P.-D. Duh, and C.-W. Lin, *Effects of Resveratrol and 4-hexylresorcinol on Hydrogen Peroxide-induced Oxidative DNA Damage in Human Lymphocytes.* Free Radical Research, 2003. **37**(5): p. 509-514.

90. Ungvari, Z., et al., *Resveratrol increases vascular oxidative stress resistance.* American journal of physiology. Heart and circulatory physiology, 2007. **292**(5): p. H2417-24.

91. Smoliga, J.M., O. Vang, and J.A. Baur, *Challenges of translating basic research into therapeutics: resveratrol as an example.* The journals of gerontology. Series A, Biological sciences and medical sciences, 2012. **67**(2): p. 158-67.

92. Chen, H., et al., *Quality assessment of Japanese knotweed (Fallopia japonica) grown on Prince Edward Island as a source of resveratrol.* J Agric Food Chem, 2013. **61**(26): p. 6383-92.

93. Masakapalli, S.K., et al., *Subcellular Flux Analysis of Central Metabolism in a Heterotrophic Arabidopsis Cell Suspension Using Steady-State Stable Isotope Labeling.* Plant Physiology, 2009. **152**(2): p. 602-619.

94. Segui-Simarro, J.M., M.J. Coronado, and L.A. Staehelin, *The Mitochondrial Cycle of Arabidopsis Shoot Apical Meristem and Leaf Primordium Meristematic Cells Is Defined by a Perinuclear Tentaculate/Cage-Like Mitochondrion.* Plant Physiology, 2008. **148**(3): p. 1380-1393.

95. Bereiter-Hahn, J., Voth, M. *Dynamics of Mitochondria in Living Cells: Shape Changes, Dislocations, Fusion, and Fission of Mitochondria.* Microscopy Research and Technique, 1994. **27**: p. 198-219.

96. Havelund, J.F., Salvato, F., Chen, M., Rao, R., Rogowska-Wrzesinska, A., Jensen, O. N., Gang, D. R., Thelen, J. J. and Møller, I. M., *Isolation of Mitochondria from Potato Tubers.* Bio-protocol 2014. **4**(17).

97. Keech, O., P. Dizengremel, and P. Gardeström, *Preparation of leaf mitochondria fromArabidopsis thaliana.* Physiologia Plantarum, 2005. **124**(4): p. 403-409.

98. Dixon, R.A., Gonzales, R.A., ed. *Plant Cell Culture - A Practical Approach*. Second edition ed. The Practical Approach Series, ed. D. Rickwood, Hames, B.D. 1994, Oxford University Press: Oxford.

99. Evans, D.E., Coleman, J.O.D., Kearns, A., *Plant Cell Culture - The Basics*. 2003, London: BIOS Scientific Publishers.

100. Razdan, M.K., *Introduction to Plant Tissue Culture*. Second edition ed. 2003, Enfield: Science Publishers, Inc.

101. Torre, F., Fernandez, R., Saporta, L., Sanjurjo, L., Segura, A., Vidal, J.R., *Relationship among growth curve, nutrient consumption and genetic transformation efficiency of 'Albarino' (Vitis vinifera) cell suspensions.* Vitis, 2012. **51**(2): p. 73-78.

102. Steponkus, P.L. and F.O. Lanphear, *Refinement of the triphenyl tetrazolium chloride method of determining cold injury.* Plant Physiol, 1967. **42**(10): p. 1423-6.

103. Arabidopsis Genome, I., *Analysis of the genome sequence of the flowering plant Arabidopsis thaliana.* Nature, 2000. **408**(6814): p. 796-815.

104. May, M.J. and C.J. Leaver, *Oxidative Stimulation of Glutathione Synthesis in Arabidopsis thaliana Suspension Cultures.* Plant Physiol, 1993. **103**(2): p. 621-627.

105. Christie, J.M. and G.I. Jenkins, *Distinct UV-B and UV-A/blue light signal transduction pathways induce chalcone synthase gene expression in Arabidopsis cells.* Plant Cell, 1996. **8**(9): p. 1555-67.

106. Clarke, A., et al., *NO way back: nitric oxide and programmed cell death in Arabidopsis thaliana suspension cultures.* Plant J, 2000. **24**(5): p. 667-77.

107. Schagger, H. and G. von Jagow, *Tricine-sodium dodecyl sulfate-polyacrylamide gel electrophoresis for the separation of proteins in the range from 1 to 100 kDa.* Anal Biochem, 1987. **166**(2): p. 368-79.

108. Rabilloud, T., *A comparison between low background silver diammine and silver nitrate protein stains.* Electrophoresis, 1992. **13**(7): p. 429-39.

109. Schägger, H., *Tricine–SDS-PAGE.* Nature Protocols, 2006. **1**(1): p. 16-22.

110. Swamy, M., et al., *Blue native polyacrylamide gel electrophoresis (BN-PAGE) for the identification and analysis of multiprotein complexes.* Sci STKE, 2006. **2006**(345): p. pl4.

111. Wittig, I., H.P. Braun, and H. Schagger, *Blue native PAGE.* Nat Protoc, 2006. **1**(1): p. 418-28.

112. Mahmood, T. and P.C. Yang, *Western blot: technique, theory, and trouble shooting.*
N Am J Med Sci, 2012. **4**(9): p. 429-34.

113. Sabar, M., J. Balk, and C.J. Leaver, *Histochemical staining and quantification of plant mitochondrial respiratory chain complexes using blue-native polyacrylamide gel electrophoresis.* The Plant journal : for cell and molecular biology, 2005. **44**(5): p. 893-901.

114. Lee, Y. and G. Tsao, *Dissolved oxygen electrodes*, in *Advances in Biochemical Engineering, Volume 13*, T.K. Ghose, N. Blakebrough, and A. Fiechter, Editors. 1979, Springer Berlin Heidelberg. p. 35-86.

115. Ltd., R.B., *The Rank Brothers Oxygen Electrode Operating Manual*. 2002: Cambridge.

116. Hoffmann, E., *Mass spectrometry*. 1996: Wiley Online Library.

117. Gundry, R.L., et al., *Preparation of proteins and peptides for mass spectrometry analysis in a bottom-up proteomics workflow.* Curr Protoc Mol Biol, 2009. **Chapter 10**: p. Unit10 25.

118. Mendoza, V.L. and R.W. Vachet, *Probing protein structure by amino acid-specific covalent labeling and mass spectrometry.* Mass Spectrom Rev, 2009. **28**(5): p. 785- 815.

119. Karageorgou, P. and Y. Manetas, *The importance of being red when young: anthocyanins and the protection of young leaves of Quercus coccifera from insect herbivory and excess light.* Tree Physiol, 2006. **26**(5): p. 613-21.

120. Karageorgou, P. and Y. Manetas, *The importance of being red when young: anthocyanins and the protection of young leaves of Quercus coccifera from insect herbivory and excess light.* Tree Physiology, 2006. **26**(5): p. 613-621.

121. Douce, R., A.L. Moore, and M. Neuburger, *Isolation and oxidative properties of intact mitochondria isolated from spinach leaves.* Plant Physiol, 1977. **60**(4): p. 625- 8.

122. Chien, L.-F., Y.-C. Wu, and H.-P. Chen, *Mitochondrial energy metabolism in young bamboo rhizomes from Bambusa oldhamii and Phyllostachys edulis during shooting stage.* Plant Physiology and Biochemistry, 2011. **49**(4): p. 449-457.

123. Verleur, J.D., *Studies on the Isolation of Mitochondria from Potato Tuber Tissue.*
Plant Physiology, 1965. **40**(6): p. 1003-1007.

124. Affourtit, C. and A.L. Moore, *Purification of the plant alternative oxidase from Arum maculatum: measurement, stability and metal requirement.* Biochimica et Biophysica Acta (BBA) - Bioenergetics, 2004. **1608**(2–3): p. 181-189.

125. Lang, E.G.E., et al., *Simultaneous isolation of pure and intact chloroplasts and mitochondria from moss as the basis for sub-cellular proteomics.* Plant Cell Reports, 2011. **30**(2): p. 205-215.

126. Millar, A.H., A. Liddell, and C.J. Leaver, *Isolation and Subfractionation of Mitochondria from Plants.* 2007. **80**: p. 65-90.

127. Hrubec, T.C., J.M. Robinson, and R.P. Donaldson, *Isolation of Mitochondria from Soybean Leaves on Discontinuous Percoll Gradients.* Plant Physiology, 1985. **77**(4): p. 1010-1012.

128. Moore, A.L. and J.N. Siedow, *The regulation and nature of the cyanide-resistant alternative oxidase of plant mitochondria.*

Biochimica et Biophysica Acta (BBA) - Bioenergetics, 1991. **1059**(2): p. 121-140.

129. Gualanduzzi, S., et al., *Respiration, hydrogen peroxide levels and antioxidant enzyme activities during cold storage of zucchini squash fruit.* Postharvest Biology and Technology, 2009. **52**(1): p. 16-23.
130. Raison, J.K. and E.A. Chapman, *Membrane Phase Changes in Chilling-Sensitive <I>Vigna radiata</I> and Their Significance to Growth.* Functional Plant Biology, 1976. **3**(3): p. 291-299.
131. Herz, U., et al., *Purification of the NADH:ubiquinone oxidoreductase (complex I) of the respiratory chain from the inner mitochondrial membrane of Solanum tuberosum.* Journal of Biological Chemistry, 1994. **269**(3): p. 2263-2269.
132. Heazlewood, J.L., K.A. Howell, and A.H. Millar, *Mitochondrial complex I from Arabidopsis and rice: orthologs of mammalian and fungal components coupled with plant-specific subunits.* Biochimica et Biophysica Acta (BBA) - Bioenergetics, 2003. **1604**(3): p. 159-169.
133. McKenzie, M., M. Lazarou, and M.T. Ryan, *Chapter 18 Analysis of Respiratory Chain Complex Assembly with Radiolabeled Nuclear-and Mitochondrial-Encoded Subunits*, in *Methods in Enzymology*. 2009, Academic Press. p. 321-339.
134. Chevallet, M., S. Luche, and T. Rabilloud, *Silver staining of proteins in polyacrylamide gels.* Nature Protocols, 2006. **1**(4): p. 1852-1858.
135. Haider, S.R., B.L. Sharp, and H.J. Reid, *A comparison of Tris-glycine and Tris-tricine buffers for the electrophoretic separation of major serum proteins.* Journal of separation science, 2011. **34**(18): p. 2463-7.
136. Melo, A.M.P., M. Duarte, and A. Videira, *Primary structure and characterisation of a 64 kDa NADH dehydrogenase from the inner membrane of Neurospora crassa mitochondria1*. Biochimica et Biophysica Acta (BBA) - Bioenergetics, 1999. **1412**(3): p. 282-287.
137. Duncan, O., M.W. Murcha, and J. Whelan, *Unique components of the plant mitochondrial protein import apparatus.* Biochimica et Biophysica Acta (BBA) - Molecular Cell Research, 2013. **1833**(2): p. 304-313.
138. Rudenberg, H.G. and P.G. Rudenberg, *Chapter 6 - Origin and Background of the Invention of the Electron Microscope: Commentary and Expanded Notes on Memoir of Reinhold Rüdenberg**, in *Advances in Imaging and Electron Physics*. 2010, Elsevier. p. 207-286.
139. De Graef, M., *Introduction to Conventional Transmission Electron Microscopy*. 2003: Cambridge University Press.

140. Williams, D. and C.B. Carter, *The Transmission Electron Microscope*, in *Transmission Electron Microscopy*. 1996, Springer US. p. 3-17.

141. Thorpe, J.R. *Sussex Centre for Advanced Microscopy*. 2015 11/6/2015 [cited 2015 01/08]; Available from: http://www.lifesci.sussex.ac.uk/home/Julian_Thorpe/genem.htm.

142. Williams, D.B., Carter, B.C., *Transmission Electron Microscopy*. 2 ed. A Textbook for Materials Science. 2009: Springer US. 820.

143. Kiernan, J., *Formaldehyde, formalin, paraformaldehyde and glutaraldehyde: What they are and what they do.* Microscopy Today, 2000. **00-1 pp. 8-12 (2000).**

144. Buchanan, B.B., Gruissem, W., Jones, R.L., *Biochemistry & Molecular Biology of Plants*. 1st ed, ed. A.S.o.P. Physiologists. 2002, Rockville, MD American Society of Plant Physiologists

145. Arimura, S.-i., et al., *Frequent fusion and fission of plant mitochondria with unequal nucleoid distribution.* Proceedings of the National Academy of Sciences of the United States of America, 2004. **101**(20): p. 7805-7808.

146. Wilson, S.M. and A. Bacic, *Preparation of plant cells for transmission electron microscopy to optimize immunogold labeling of carbohydrate and protein epitopes.* Nat. Protocols, 2012. **7**(9): p. 1716-1727.

147. Voeltz, G.K., M.M. Rolls, and T.A. Rapoport, *Structural organization of the endoplasmic reticulum.* EMBO reports, 2002. **3**(10): p. 944-950.

148. Saito, G.Y., et al., *Chloroplast Development and Nuclear Gene Expression in Cotyledons of Soybean Seedlings.* New Phytologist, 1990. **114**(4): p. 547-554.

149. Kang, B.H., *Electron microscopy and high-pressure freezing of Arabidopsis.* Methods Cell Biol, 2010. **96**: p. 259-83.

150. Dupree, P. and D.J. Sherrier, *The plant Golgi apparatus.* Biochimica et Biophysica Acta (BBA) - Molecular Cell Research, 1998. **1404**(1–2): p. 259-270.

151. Thorpe, T., *History of Plant Tissue Culture*, in *Plant Cell Culture Protocols*, V.M. Loyola-Vargas and N. Ochoa-Alejo, Editors. 2012, Humana Press. p. 9-27.

152. Krikorian, A.D. and D. Berquam, *Plant cell and tissue cultures: The role of Haberlandt.* The Botanical Review, 1969. **35**(1): p. 59-67.

153. Encina, C.L., Constantin, M., Botella, J., *An Easy and Reliable Method for Establishment and Maintenance of Leaf and Root Cell Cultures of Arabidopsis thaliana.* Plant Molecular Biology

Reporter, 2001. **19**: p. 245-248.

154. Negrutiu, I., F. Beeftink, and M. Jacobs, *Arabidopsis thaliana as a model system in somatic cell genetics I. Cell and tissue culture.* Plant Science Letters, 1975. **5**(5): p. 293-304.

155. Mathur, J., Koncz, C., Szabados, L., *A simple method for isolation, liquid culture, transformation and regeneration of Arabidopsis thaliana protoplasts.* Plant Cell Reports, 1995. **14**: p. 221-226.

156. May, M.J., Leaver, C.J, *Oxidative Stimulation of Glutathione Synthesis in Arabidopsis thaliana Suspension cultures.* Plant Physiology, 1993. **103**: p. 621-627.

157. Murashige, T., Skoog, F., *A revised medium for rapid growth and bioassays with tobacco tissue cultures.* Physiol. Plant., 1962. **15**(473).

158. van Emmerik, W., *Energy metabolism of Petunia hybrida cell suspensions*, in *Biology*. 1994, Vrije Universiteit te Amsterdam: Amsterdam.

159. Bespalhok-Filho J. C., H., K., *Embryogenic callus formation and histological studies from Stevia rebaudiana (Bert.) Bertoni floret explants.* R. Bras. Fisiol. Veg, 1997. **9**(3): p. 185-188.

160. Fernandez-Da Silva, R. and A. Menendez-Yuffa, *Viability in protoplasts and cell suspensions of Coffea arabica cv. Catimor.* Electronic Journal of Biotechnology, 2006. **9**(5): p. 0-0.

161. Mustafa, N.R., et al., *Initiation, growth and cryopreservation of plant cell suspension cultures.* Nature Protocols, 2011. **6**(6): p. 715-742.

162. Rahman, M., S., Miah, M., A., B., Hossain, M., S. Kabit, A., H. Rahman, M., M., *Establishment of Cell Suspension Culture and Plant Regeneration in Abrus precatorius L., a Rare Medicinal Plant*. 2012. Vol. 4. 2012.

163. Iantcheva, A., Vlahova, M., Atanassov, A., Duque, A.S., Araujo, S., Dos Santos, D.F., Fevereiro, P., *Cell suspension cultures*, in *Medicago truncatula handbook*. 2006, Agro Bio Institute: Sofia, Bulgaria.

164. Meurant, G., *Advances in Genetics*. 1987: Elsevier Science.

165. Pola, S., *Leaf Discs as a Source Material for Plant Tissue Culture Studies of Sorghum bicolor (L.) Moench*. 2011. Vol. 3. 2011.

166. Ikeuchi, M., K. Sugimoto, and A. Iwase, *Plant callus: mechanisms of induction and repression.* Plant Cell, 2013. **25**(9): p. 3159-73.

167. Iwase, A., et al., *The AP2/ERF transcription factor WIND1 controls cell dedifferentiation in Arabidopsis.* Curr Biol,

2011. **21**(6): p. 508-14.

168. Murashige, T. and F. Skoog, *A Revised Medium for Rapid Growth and Bio Assays with Tobacco Tissue Cultures.* Physiologia Plantarum, 1962. **15**(3): p. 473-497.

169. Gamborg, O.L., R.A. Miller, and K. Ojima, *Nutrient requirements of suspension cultures of soybean root cells.* Experimental Cell Research, 1968. **50**(1): p. 151-158.

170. Trigiano, R.N. and D.J. Gray, *Plant Tissue Culture Concepts and Laboratory Exercises, Second Edition*. 1999: Taylor & Francis.

171. Skirvin, R.M., et al., *Stability of tissue culture medium pH as a function of autoclaving, time, and cultured plant material.* Plant Cell Rep, 1986. **5**(4): p. 292-4.

172. Chen, C., R. Bates, and J. Carlson, *Effect of environmental and cultural conditions in medium pH and plant growth performance of Douglas-fir (Pseudotsuga menziesii) shoot culture [v1; ref status: approved with reservations 2]*. Vol. 3. 2014.

173. Yesil-Celiktas, O., Gurel, A., Vardar-Sukan, F., *Large scale cultivation of plant cell and tissue culture in bioreactors*, in *Transworld Research Network* 2010: Bornova- Izmir, Turkey. p. 1-54.

174. Su, Y.H., Y.B. Liu, and X.S. Zhang, *Auxin-cytokinin interaction regulates meristem development.* Mol Plant, 2011. **4**(4): p. 616-25.

175. Song, Y., *Insight into the mode of action of 2,4-dichlorophenoxyacetic acid (2,4-D) as an herbicide.* J Integr Plant Biol, 2014. **56**(2): p. 106-13.

176. Coenen, C. and T.L. Lomax, *Auxin—cytokinin interactions in higher plants: old problems and new tools.* Trends in Plant Science, 1997. **2**(9): p. 351-356.

177. Sugiyama, M., *Historical review of research on plant cell dedifferentiation.* Journal of Plant Research, 2015. **128**(3): p. 349-359.

178. Sigma-Aldrich. *Plant Tissue Culture Protocols - Growth Regulators*. 16/05/13]; Available from: http://www.sigmaaldrich.com/life-science/molecular-biology/plant- biotechnology/tissue-culture-protocols/growth-regulators.html.

179. Yasuda, T., Y. Fujii, and T. Yamaguchi, *Embryogenic Callus Induction from Coffea arabica Leaf Explants by Benzyladenine.* Plant and Cell Physiology, 1985. **26**(3): p. 595-597.

180. Sen, M.K., et al., *In vitro callus induction and plantlet regeneration of Achyranthes aspera L., a high value medicinal plant.* Asian Pac J Trop Biomed, 2014. **4**(1): p. 40- 6.

181. Gao, J., et al., *Callus induction and plant regeneration in*

Alternanthera philoxeroides. Mol Biol Rep, 2011. **38**(2): p. 1413-7.

182. Milian, E. and A.A. Kamen, *Current and emerging cell culture manufacturing technologies for influenza vaccines.* Biomed Res Int, 2015. **2015**: p. 504831.

183. Kantardjieff, A. and W. Zhou, *Mammalian cell cultures for biologics manufacturing.* Adv Biochem Eng Biotechnol, 2014. **139**: p. 1-9.

184. Saifullah, K., *Callus Induction and Cell Suspension culture production of Catharanthus roseus for biotransformation studies of (-) Caryophyllene oxide.* Pak. J. Bot., 2011. **43**(1): p. 467-473.

185. Lynn, D.E., *Methods for Maintaining Insect Cell Cultures.* Journal of Insect Science, 2002. **2**: p. 9.

186. Maiorella, B., et al., *Large-Scale Insect Cell-Culture for Recombinant Protein Production.* Nat Biotech, 1988. **6**(12): p. 1406-1410.

187. ten Hoopen, H.J.G., W.M. van Gulik, and J.J. Heijnen, *Continuous culture of suspended plant cells.* In Vitro – Plant, 1992. **28**(3): p. 115-120.

188. Glish, G.L. and R.W. Vachet, *The basics of mass spectrometry in the twenty-first century.* Nat Rev Drug Discov, 2003. **2**(2): p. 140-150.

189. Griffiths, J., *A brief history of mass spectrometry.* Analytical chemistry, 2008. **80**(15): p. 5678-5683.

190. El-Faramawy, A., K.W.M. Siu, and B.A. Thomson, *Efficiency of Nano-Electrospray Ionization.* Journal of the American Society for Mass Spectrometry, 2005. **16**(10): p. 1702-1707.

191. Ho, C.S., et al., *Electrospray Ionisation Mass Spectrometry: Principles and Clinical Applications.* The Clinical Biochemist Reviews, 2003. **24**(1): p. 3-12.

192. McLafferty, F., *Tandem mass spectrometry.* Science, 1981. **214**(4518): p. 280-287.

193. Miladinović, S.a.M., et al., *In-spray supercharging of peptides and proteins in electrospray ionization mass spectrometry.* Analytical chemistry, 2012. **84**(11): p. 4647-4651.

194. Mitchell Wells, J. and S.A. McLuckey, *Collision-Induced Dissociation (CID) of Peptides and Proteins*, in *Methods in Enzymology*. 2005, Academic Press. p. 148-185.

195. Laremore, T.N., et al., *Glycosaminoglycan Characterization by*

Electrospray Ionization Mass Spectrometry Including Fourier Transform Mass Spectrometry. Methods in enzymology, 2010. **478**: p. 79-108.

196. Huynh, M.-L., P. Russell, and B. Walsh, *Tryptic Digestion of In-Gel Proteins for Mass Spectrometry Analysis*, in *Two-Dimensional Electrophoresis Protocols*, R. Tyther and D. Sheehan, Editors. 2009, Humana Press. p. 507-513.

197. Perkins, D.N., et al., *Probability-based protein identification by searching sequence databases using mass spectrometry data.* Electrophoresis, 1999. **20**(18): p. 3551-67.

198. Ishihama, Y., et al., *Exponentially modified protein abundance index (emPAI) for estimation of absolute protein amount in proteomics by the number of sequenced peptides per protein.* Mol Cell Proteomics, 2005. **4**(9): p. 1265-72.

199. Ong, C.-l., et al., *Molecular analysis of type 3 fimbrial genes from Escherichia coli, Klebsiella and Citrobacter species.* BMC Microbiology, 2010. **10**(1): p. 183.

200. Consortium, T.U., *UniProt: a hub for protein information.* Nucleic Acids Research, 2015. **43**(D1): p. D204-D212.

201. Stock, D., A.G. Leslie, and J.E. Walker, *Molecular architecture of the rotary motor in ATP synthase.* Science, 1999. **286**(5445): p. 1700-1705.

202. Cadenas, E. and K.J.A. Davies, *Mitochondrial free radical generation, oxidative stress, and aging1.* Free Radical Biology and Medicine, 2000. **29**(3–4): p. 222-230.

203. Detmer, S.A. and D.C. Chan, *Functions and dysfunctions of mitochondrial dynamics.* Nat Rev Mol Cell Biol, 2007. **8**(11): p. 870-879.

204. Yoshida, M., E. Muneyuki, and T. Hisabori, *ATP synthase — a marvellous rotary engine of the cell.* Nat Rev Mol Cell Biol, 2001. **2**(9): p. 669-677.

205. Kanazawa, H., et al., *Nucleotide sequence of the genes coding for α, β and γ subunits of the proton-translocating ATPase of Escherichia coli.* Biochemical and Biophysical Research Communications, 1981. **103**(2): p. 604-612.

206. Jonckheere, A.I., J.A.M. Smeitink, and R.J.T. Rodenburg, *Mitochondrial ATP synthase: architecture, function and pathology.* Journal of Inherited Metabolic Disease, 2012. **35**(2): p. 211-225.

207. Walker, J.E., et al., *Distantly related sequences in the alpha- and beta-subunits of ATP synthase, myosin, kinases and other ATP-requiring enzymes and a common nucleotide binding fold.* The

EMBO Journal, 1982. **1**(8): p. 945-951.

208. Lapaille, M., et al., *Loss of mitochondrial ATP synthase subunit beta (Atp2) alters mitochondrial and chloroplastic function and morphology in Chlamydomonas.* Biochimica et Biophysica Acta (BBA) - Bioenergetics, 2010. **1797**(8): p. 1533-1539.

209. Gurtubay, J.I., et al., *Triton X-100 solubilization of mitochondrial inner and outer membranes.* J Bioenerg Biomembr, 1980. **12**(1-2): p. 47-70.

210. Koen, A.L. and M. Goodman, *Aconitate hydratase isozymes: subcellular location, tissue distribution and possible subunit structure.* Biochimica et Biophysica Acta (BBA) - Enzymology, 1969. **191**(3): p. 698-701.

211. Ternette, N., et al., *Inhibition of Mitochondrial Aconitase by Succination in Fumarate Hydratase Deficiency.* Cell Reports, 2013. **3**(3): p. 689-700.

212. Eprintsev, A.T., et al., *Expression and properties of the mitochondrial and cytosolic forms of aconitase in maize scutellum.* Journal of Plant Physiology, 2015. **181**: p. 14- 19.

213. Berg JM, T.J., Stryer L., *Chapter 17, The Citric Acid Cycle*, in *Biochemistry*. 2002, W H Freeman: New York.

214. Goda, S.K. and N.P. Minton, *A simple procedure for gel electrophoresis and Northern blotting of RNA.* Nucleic Acids Research, 1995. **23**(16): p. 3357-3358.

215. Schenk, P.M., et al., *Coordinated plant defense responses in Arabidopsis revealed by microarray analysis.* Proceedings of the National Academy of Sciences, 2000. **97**(21): p. 11655-11660.

216. Boutry, M. and N.H. Chua, *A nuclear gene encoding the beta subunit of the mitochondrial ATP synthase in Nicotiana plumbaginifolia.* The EMBO Journal, 1985. **4**(9): p. 2159-2165.

217. Franz, O., I. Bruchhaus, and T. Roeder, *Verification of differential gene transcription using virtual northern blotting.* Nucleic Acids Research, 1999. **27**(11): p. i-iii.

218. Matoba, S., et al., *p53 regulates mitochondrial respiration.* Science, 2006. **312**(5780): p. 1650-3.

219. Ishii, R. and G.H. Schmid, *Consequences of Warburg Effect Conditions on Growth Parameters and CO2-Exchange Rates in Tobacco Mutants.* Plant and Cell Physiology, 1983. **24**(8): p. 1525-1533.

220. Plaxton, W.C., *The Organization and Regulation of Plant Glycolysis.*

Annual Review Plant Physiology and Plant Molecular Biology, 1996. **47**: p. 185-214.

221. Rohan, M., *Herbicides Market worth $30 Billion by 2019*, MarketsandMarkets, Editor. 2015: Dallas, TX.

222. Kraehmer, H., et al., *Herbicides as Weed Control Agents: State of the Art: II. Recent Achievements.* Plant Physiology, 2014. **166**(3): p. 1132-1148.

223. Beckie, H.J., *Herbicide Resistance in Weeds and Crops: Challenges and Opportunities*, in *Recent Advances in Weed Management*, B.S. Chauhan and G. Mahajan, Editors. 2014, Springer New York. p. 347-364.

224. Griffin, K. L., et al. *Plant growth in elevated CO2 alters mitochondrial number and chloroplast fine structure.* PNAS, 2001. **98:** p. 2473–2478.

225. Colaço, R., Moreno, N., Feijo, J. A. *On the fast lane: mitochondria structure, dynamics and function in growing pollen tubes.* Journal of Microscopy. 2012. **247**: p 106-118.

226. Robertson, E.J., Williams, M., Harwood, J.L., Lindsay, G., Leaver, C. J., Leech, R. M. *Mitochondria lncrease Three-Fold and Mitochondrial Proteins and Lipid Change Dramatically in Postmeristematic Cells in Young Wheat Leaves Grown in Elevated CO,*' Plant Physiol. 1995. **108**: p.469-474.

227. Tissue, D. T., Lewis, J. D., Wullschleger, S. D., Amthor, J. S., Griffin, K. L., Anderson, O. R. *Leaf respiration at different canopy positions in sweetgum (Liquidambar styraciflua) grown in ambient and elevated concentrations of carbon dioxide in the field.* Tree Physiology. 2002: **22**. p.1157–1166.

228. Welchen, E., Garcia, L., Mansilla, N., Gonzalez, D. H. *Coordination of plant mitochondrial biogenesis: keeping pace with cellular requirements.* Frontiers in Plant Science. 2013. **4**: 551.